UNIVERSITA' DEGLI STUDI DI PARMA

Dottorato in Ecologia - XXV Ciclo

A MULTIDISCIPLINARY APPROACH TO PHYSICAL-BIOLOGICAL INTERACTIONS IN EARLY LIFE HISTORY OF MARINE POPULATIONS

Ph.D. Thesis
Marcello Schiavina

Advisor: prof. Giulio A. De Leo
Co-advisors: prof. Marino Gatto
prof. Paco Melià
dr. Daniele Bevacqua
Supervisor: prof. Marcello Vichi

"The most important challenge for ecologists remains to understand the linkages between what is going on at the level of the physiology and the behavior of individual organisms and emergent properties such as the productivity and resiliency of ecosystems"

- Simon Levin, 1999

ABSTRACT

Traditionally, the quantitative analysis of ecological processes considered separately the temporal population dynamics, under the assumption of homogenous mixing over space, and the spatial distributions of individuals, as a "snapshot" of the species displacement. However, when dealing with populations distributed along a heterogeneous space with fluxes of individuals among separated groups, it is necessary to couple both the spatial and temporal dimensions. A new paradigm for Movement Ecology has been recently proposed renewing the challenge to investigate the driving forces and the ultimate result of movement integrating biological information about interacting species with the mathematical modelling of the organism's movement. Many models are devoted to the Movement Ecology approach, but the study of species' early life history in marine ecology has found in the individual-based coupled physical-biological models the specific tool to investigate the dispersal and movement of juveniles.

In this thesis some new individual-based coupled physical-biological models for larval dispersal are proposed and analysed. These models are built reproducing the most important biological features of the species considering also the interactions with the external environment. In particular, this work tries to integrate experimental observations and laboratory data to build reliable models through validation and tuning, a not much common practice in this field of modelling.

The first part of the thesis presents two dispersal models coupled with a genetic analysis for two species (the European green crab and the white sea bream) in the Adriatic Sea. These models are used with an explanatory approach generating patterns of larval distribution. Larval retention, spill-over and level of connectivity among different places are evaluated. The model results are compared with the results of the genetic analysis. The consistency between the two approaches points out the role of the ocean currents and temperatures in determining the separation or the homogeneity among the analysed groups.

The second part of the thesis is devoted to the study of the larval migration of the European eel in the North Atlantic Ocean. An individual-based coupled physical-biological model is developed using alternative scenarios to quantitatively compare the outputs with observed field data. This inferential approach allows to characterize the species biological features, namely body growth, mortality and active locomotion, and to investigate, with the most likely scenario, the inter-annual variation (1960-2000) of juveniles arriving on the European shelf. This application is used to generate hypothesis that could explain the recruitment collapse observed during the 1980s.

CONTENTS

PART I

GENERAL INTRODUCTION

State of the art

An introduction to Movement Ecology

The quantitative analysis of ecological processes has mainly followed two path: on one hand, the study of temporal dynamics and population density fluctuations which, for the sake of simplicity, have usually neglected the spatial distribution, considering a particular point or the average over an area (e.g. ordinary differential equation or difference equation models; see Murray 2003, for a review); on the other hand, the analysis of species distribution patterns of animals or plants has usually ignored the temporal dimension by taking a "snapshot" of the population displacement at a given time, or averaged over a period (e.g. GIS-based models; see Goodchild 2003). Moreover, the different research approaches between plant and animal ecology, the first traditionally more focused on distribution of organisms over space, and the second concentrated on population density and fluctuations over time, exacerbated the separation between time-oriented and space-oriented studies. This historical separation is mainly due to the inner complexity of considering both the spatial and temporal dimensions at the same time with an acceptable level of details. Some attempts to couple these two components have been made though (see Okubo and Levin 2001, for a review), but resulting in too simplistic modelling to grasp the details of movement without loosing accuracy of demographic descriptions.

However, for all those cases in which the demographic dynamic of the species is determined by several populations (meta-population) distributed along an heterogeneous space with fluxes of individuals among sub-populations, or characterized by long-migrating phases across several habitats, during one or more stages of the species lifecycle, an approach that couples both spatial and temporal dimensions is necessary. Movement of an individual is, in fact, a change in the spatial location during a lapse of time. In some extent, movement is important to all organisms because all of them have to move in a certain point of their lives, both if they are passively transported either they move actively (e.g. spores, pollen, seeds or propagules transported by wind, water currents or animals; eggs or larvae carried by water currents or, in general, animals moving, swimming or flying). The fate of all single individuals, driven by internal and/or external factors, and thus of the structure and dynamics of populations, communities and ecosystems are strongly affected by movement that determines, in the end, the evolution and diversity of life. Therefore, the overall comprehension of individuals' movement and the interaction with a variable environment is central in the upcoming research in ecology.

There is an increasing production of literature about organismal movement reflecting the crucial role of this process in the ecological dynamics and the consequences on human life. A step forward in the comprehension of movement process and its implication in the ecosystem would help scientists in conservation, restoration and management issues. This means more effective decision processes (e.g. fishery or marine reserve management) or control of diseases and human impacts (e.g. spreading of alien-invasive species or of pests, infections, or toxins). Movement can be considered one of the most captivating research fields of ecology with an increasing interest and nearly 40,000 published articles in last decade (Sci-extended database, Web of Science)[1]. The number of relevant papers increased by an average 5.2% per year, more then twice the rate of increase (2.2%) in total number of papers published by the selected journals. The proportion of papers in the last decade, referring to

---

[1] This number of relevant papers has been assessed following the approach of Holyolak et al. (2008), updating their results by moving the decade window between 2003 and 2012 on the same sample of 496 journals (see Hoylolak et al., 2008 Supplementary information, for more details about journal selection and "relevant paper" definition)

Figure I.1 – ISI Web of Knowledge literature survey on organismal movement (bars) and percentage (points) with respect to the overall publications (numbers in italic) of the selected 496 journals. Journal selection, terms and relevant paper definition as Holyolak et al. (2008, see Supplementary Information)

organismal movement, averaged 9.0% and increased 0.3% per year (a constant increase since 1997, Holyolak et al. 2008). Organismal-movement papers reach a 10.0% prevalence in 2012 (Figure I.1), with a mean number of almost 4000 published papers per year (i.e. +40% with respect to the decade analysed by Holyolak et al. 2008). Despite this huge amount of literature published about organismal movement, few articles have an overall and complete comprehension of causes, mechanisms, cues and interactions between the environment and the individual. Most studies simply measured and described the movement of organisms or related the environmental factors with motion capacity. In 2008, Nathan et al. (2008) pointed out the lack of a common framework and discussed about a Movement Ecology paradigm. Renewing the Aristotle's *De Motu Animalium* (On the Movement of Animals) challenge to explore the movement mechanisms, motivations and interactions with the external world, the authors underlined the importance of a multidisciplinary approach that accounts for all aspect that movement involves. Integrating mathematical modelling with biological information, Movement Ecology should investigate the driving forces and the ultimate results of movement in a new interdisciplinary field. Nathan et al. proposed a general conceptual framework for Movement Ecology. The four components of this framework (i.e. internal state, motion capacity, navigation capacity and external factors, Figure I.2) interacting together, generate the trajectory of a single individual. Internal state, motion and navigation capacities are the three components properly belonging to the organism while the external factors are all biotic and abiotic variables surrounding the individual. The internal state reflects the motivation of an organism to move and it is represented by its physiological and, if any, psycological state addressing the question "why move?". The motion capacity (i.e. "how?") is the ability to produce an active locomotion, or being transported passively, given by a set of morphological traits of the organism. The navigation capacity (i.e. "where and when?") is the capacity to get and process the external information to orient the movement in space and time (*taxis*). Changes in internal state and/or external factors can affect motion and navigation capacities as well as the movement modifies the environment and the individual state and perceptions. Considering all these inteacting components allows an exaustive comprehension of the movement process improving the understanding of its consequencies for ecology and evolution at all levels (i.e. individuals, populations and communities).

Models for spatio-temporal problems in ecology

Modelling a spatio-temporal dynamic, as movement, is not an easy task because it involves several levels of organizations (i.e. individuals, groups, populations, communities, ecosystems) requiring specific tools for the description and analysis of this process. There are various levels of complexity, from a simple descriptive model to a very detailed and complex one, according to the approach and level of details needed. It is possible to classify three different main groups of models on the basis of the mathematical formalism chosen: empirical, diffusion and individual-based models.

Empirical models are the first quantitative approach to a spatio-temporal problem in ecology and they are still used, mainly to quantify seed dispersal (Nathan and Muller-Landau 2000; Nathan 2006), but also to evaluate animals' distributions (Aarts et al. 2008) or pathogens spreading (Leighton et al. 2012). They are simple descriptive models that

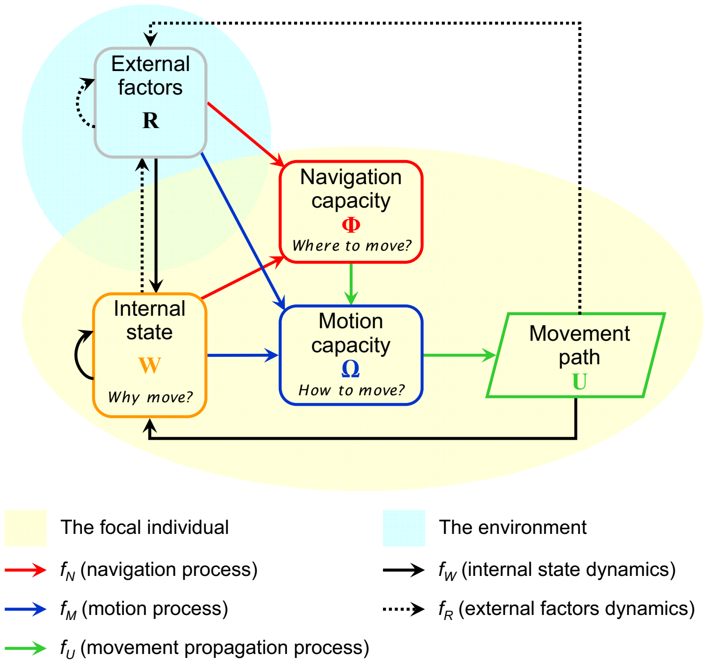

Figure I.2 – The general conceptual framework for Movement Ecology, source Nathan et al. (2008, Figure 2). Arrows represent the interactions among components (i.e. who influences who). See the text for components description.

incorporate environmental relationships, often lacking of mechanistic rules, to evaluate the dispersal. These models describe the phenomenological relationship between the population density and the distance from a focal point in the space (e.g. a nest or an individual source).

Diffusion models have also been used since long in ecology. Initially based on simple reaction-diffusion partial differential equations (PDE) and random walk, these models have a variety of possible approaches. By using discrete or continuous variables, namely population density, space and time, the organismal movement can be successfully described either by continuous reaction-diffusion or networks, cellular automata or map lattice (see Turchin 1998). Although diffusion models are very informative tools to describe spatio-temporal dynamics, it is difficult to incorporate the mathematical formulation for all levels of ecological complexity.

Individual-based models (IBMs), or Lagrangian models, rise in the second half of the last century (Newnham 1964; see Deangelis & Gross

1992 and Deangelis & Mooij 2005 for a review), as soon as adequate computers were available. Early advocates of IBMs claimed that a shift in focus from population to individuals would lead to new fundamental insight for ecology. However, this great expectation wasn't fully honoured, and scientists realized soon that this shift from population to individuals does not automatically mean better general ecological theories. Freedom from constrains of analytical modelling and less mathematical difficulties come at a price: models are able to incorporate any level of ecological complexity, but they are hardly adaptable to different contexts and harder to develop, understand and communicate. Nevertheless, a rising research effort, with a paper increase rate of more than 9% per year in last decade, is devoted to this approach that allows, not to simplify, but to understand the complexity of nature explaining system-level phenomena and deriving general mechanisms of movement up to the population level (Couzin et al. 2005). In marine ecosystems, thanks to the improvements in fish ecology along with the parallel advances in physical oceanography, these models have seen a particular development that boosts incredibly the usefulness of these tools in the Movement Ecology paradigm: the integration of physical-biological interactions (Gallego et al. 2007).

Individual-based Coupled Physical-Biological Models (ICPBMs) in marine ecology

ICPBMs are *de facto* the specific tool for studies of early life history in marine populations (Werner et al. 2001, Miller 2007), following single individuals from the eggs to a focal time of his life (e.g. recruitment, reproduction or death) in an advanced particle-tracking scheme. The first application date back to the late 1980s (Bartsch 1988, Bartsch et al. 1989) and now ICPBMs are increasingly used for understanding the processes that drive the larval dispersal, the connectivity (i.e. the exchange of individuals, gene flow, among geographically separated sub-populations) and the variability of recruitment in marine systems. An individual-level approach is required in order to detect the characteristics of survivors. Individuals that succeed in becoming adults are not a random subset of the offspring but have followed a particular biophysical trajectory (Rice et al. 1987, Meekan & Fortier 1996, Browman et al. 2006, Thorrold et al. 2001). ICPBMs allow generating individuals' biophysical trajectories as a result of several processes, namely spawning, transport and behaviour, growth and mortality, feeding, recruitment and settlement (Figure I.3).

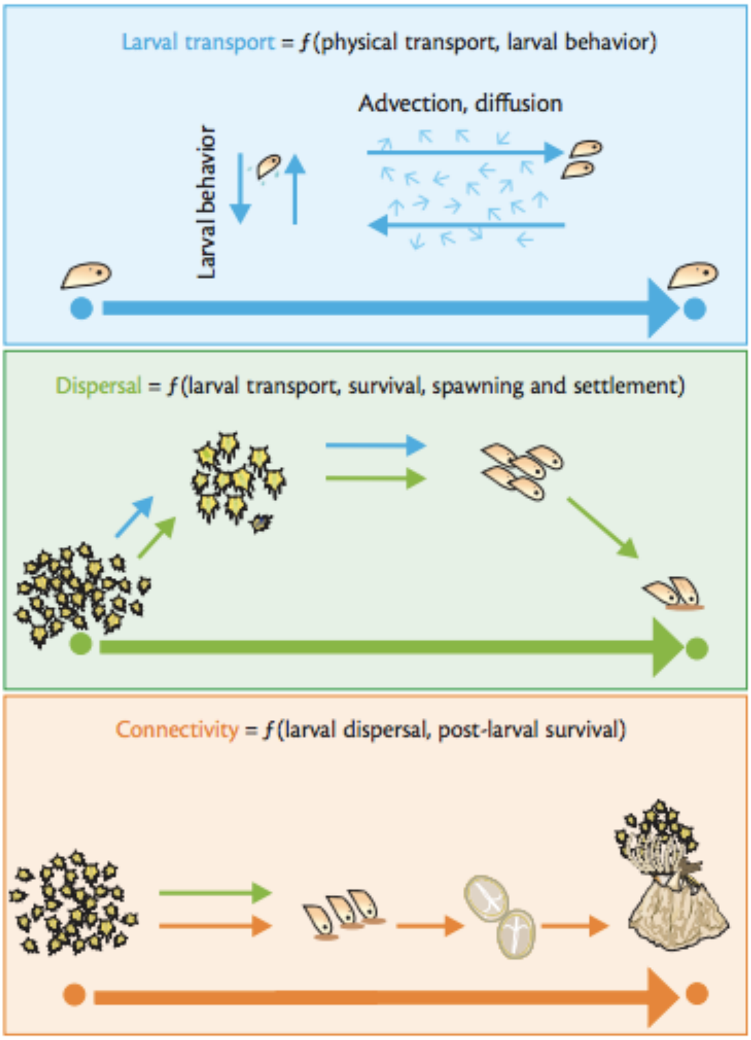

Figure I.3 – Representation of the processes considered in an Individual-based Coupled Physical-Biological Model, source Pineda et al. (2007, Figure 2)

Spawning is the initial condition of a trajectory. It sets the place and time where eggs have to be released, from which the biophysical trajectory begins, and defines the initial conditions of the individual's internal state. In practice, spawning is a set of rules of release and of biological information at birth. The objective of the model can have a particular influence on spawning setting: a connectivity analysis (i.e. the study of connectivity levels and drivers among different sites and their temporal variation) might prefer a uniform distribution of releases, allowing the assessment of connection levels between different points (Lett et al. 2007); the analysis of recruitment patterns and variability should prefer a realistic representation of eggs production (Heath & Gallego 1998). Recently, a new method has been developed to investigate the displacement of spawning: particle backtracking (Christensen et al. 2007, Thygesen 2011, Holliday et al. 2012). This method consists in reverting the ocean flow and back-calculating the origin of larvae found in different places by using ICPBMs with some stochastic expedients.

Transport and behaviour are the main core of ICPBMs determining the movement of particles. There is a basic advection model that uses stored flow field on a grid (the off-line use of hydrodynamic models is usually preferred) interpolated and integrated with a chosen method (e.g. explicit, semi-explicit or implicit) according to the ocean resolution and computational effort at disposal, with several motion components (e.g. horizontal locomotion, vertical migration) and/or stochastic errors. These components are the species-specific rules of motion (Fiksen et al. 2007, Vikebø et al. 2007) and orientation (Leis et al. 2007), based on the interaction between the external factors (e.g. environmental temperature, salinity, enlightenment and/or depth) and the individual's internal state (e.g. length, age, stage).

Biological processes that are usually modelled in the ICPBMs are body growth and mortality. Growth has a central role in early life history of marine species, due to all size-dependent processes (e.g. mortality, motion and navigation capacities). Nevertheless, in many cases it is omitted (Miller 2007), often for a lack of knowledge, by simply considering the age and pelagic larval duration (see chapters 1 and 2) as a deterministic or stochastic process. However, accurate body growth models (see chapters 3 and 4) are increasingly integrated in ICPBMs, in some cases temperature dependent or even energetic models, taking into account feeding processes. As for body growth, mortality is sometimes neglected (see chapters 1 and 2) or implemented with different levels of details, from a fixed off-line cut to on-line size-temperature-dependent models (see chapter 3 and 4) or predator models. Clearly, the omission of body growth or mortality models has strong consequences in the results and objectives setting of the ICPBM under development.

Feeding process is not very commonly considered into ICPBMs because it involves more level of organization, increasing the complexity of the model, and requires modelling prey encounter and capture (Fiksen & MacKenzie 2002, Mariani et al 2007) with expensive laboratory or *in situ* species-specific observations. Nonetheless, coupled NPZ-ICPBMs (Nutrients-Phytoplankton-Zooplankton) have been successfully developed (Hermann et al. 2001), suggesting that a multiple-trophic-level individual-based modelling is possible.

In very few cases ICPBMs incorporate explicitly post-larval stages (Hinckley et al. 1996). Commonly, individuals that reach the nursery ground are usually considered successful arrivals. This could be implemented by defining a buffer around a specific location (see chapters 1 and 2) or by considering particles that cross a placed transect (see chapters 3 and 4). Incorporating rules of settlement (e.g. habitat suitability, settlement mechanisms) and/or density-dependent effects needs specific research studies often lacking (Gallego et al. 2007).

As shown above, the level of details and complexity of the model depends strongly on available knowledge about the species and determines the objectives of the model itself. Miller (2007) sub-divided ICPBMs into three categories according to the application: explanatory, inferential and hypotheses generating. Explanatory ICPBMs (as applied in chapters 1,2 and part of 4) are those used to generate patterns of larval distribution, trying to explain the observed data. Miller (2007) pointed out that the agreement between observed and predicted data does not imply that the mechanisms represented in the model are the real processes operating in the field. Nevertheless, such models are very useful to evaluate larval retention and spill-over and the level of connectivity among different places. Inferential ICPBMs (as applied in chapter 3) quantitatively compares observed and predicted data using alternative scenarios (e.g. parameters set, initial conditions, biological models) determining which is more likely to occur in nature. The last application, hypotheses generating ICPBMs (part of the chapter 4), is the rarest but probably the most useful (Miller 2007). On the basis of simulation results, this application generates hypotheses for general theories (e.g. species behaviour or characteristics, or evolutionary rules of the species) that can be tested within the model (Mullon et al. 2002) or externally (Quinlan et al. 1999).

Consistency of ICPBMs relies on the accuracy of the hydrodynamical model and the adequacy of tracking algorithm; models should be as simple as possible but as complex as necessary (Gallego et al. 2007). Development of accurate ICPBMs is sometimes prevented by the lack of fundamental information on biological processes of mortality, behaviour and energetics. Furthermore, validation is crucial to build reliable models, as for any model, and should be enhanced with rigorous approaches, integrating experimental observations and laboratory data as an integral part of modelling (Hannah 2007).

Aims and outline of the thesis

This thesis is a collection of different case studies each one with its own results and aims, nevertheless they shear the main topic of larval dispersal in aquatic ecosystem, binging together distant branches of science and applying them to realistic ecological problems. The main goal of this thesis is the development and analysis, integrated with genetic studies and field-sampling data, of ICPBMs for three case studies in which the coupled physical-biological approach at the individual level is crucial. The use of these ICPBMs allows to answer some open questions (discussed in the following paragraphs) related to the species investigated.

The thesis is divided into four parts. Part I is this introductory chapter. Part 2 (chapters 1-2) is devoted to the analysis of the level of connectivity in the Adriatic Sea for two aquatic species: chapter 1 presents a coupled oceanographic and genetic study for the European green crab (*Carcinus aestuarii*) investigating the level of connectivity among different sites along the Italian coast; in chapter 2 the same approach is used for the white sea bream larvae (*Diplodus sargus sargus*) to study the level of connectivity among sites inside and outside a Marine Protected Area in Apulia. In Part III (chapters 3-4) the domain is the Atlantic Ocean and the focus is moved to the larval migration of the European eel (*Anguilla anguilla*). A detailed ICPBM has been developed to represent this migration, tuning the model parameters on field data found in literature (chapter 3). Chapter 4 uses this calibrated model simulating the migration over a 40-yrs horizon, analysing the inter-annual variability of juvenile recruitment. Finally, Part IV reports the main conclusions of these works and ideas for future developments.

The European green crab (*Carcinus aestuarii*) in the Adriatic Sea

The European green crab is a common inhabitant of shallow waters of estuaries and lagoon, with an important role in the food webs of these habitats. This benthonic species is native of the Mediterranean basin but,

Figure I.4 – *Carcinus aestuarii* zoeas

as a result of maritime commerce and ballast transport, it has colonized several regions outside its native range, even reaching the Japan (Chen et al. 2004). Mature crabs (about 30mm carapace, Mori et al. 1990) mates in late summer and, following the rainy season, ovigerous females descend to coastal waters where they spawn (from September to December) during new or full moon phases. Pelagic zoeas (Figure I.4) are transported by the marine waters until the metamorphosis into megalopas, when individuals swim back to coasts and settle. Unfortunately, this larval stage has not yet been fully studied and few biological information are available. To move around this problem the biological characteristics needed, namely the pelagic larval duration and the larval behaviour (see chapter 1), were taken from the very similar species *Carcinus maenas*.

In the Adriatic Sea, the European green crab has been found in different sites. It is not clear if the pelagic larval phase makes them a single meta-population, reshuffling each year the genes from all sites, or generates a spatial pattern, constraining the gene flow and separating the populations in different areas. The answer to this question has been investigated following a multidisciplinary approach: the genetic divergence among sites has been assessed through genetic marker analysis to figure out the possible presence of a genetic structure among sites; an ICPBM model has been developed to evaluate the larval retention of each site and to generate a connectivity matrix among sites. The consistency

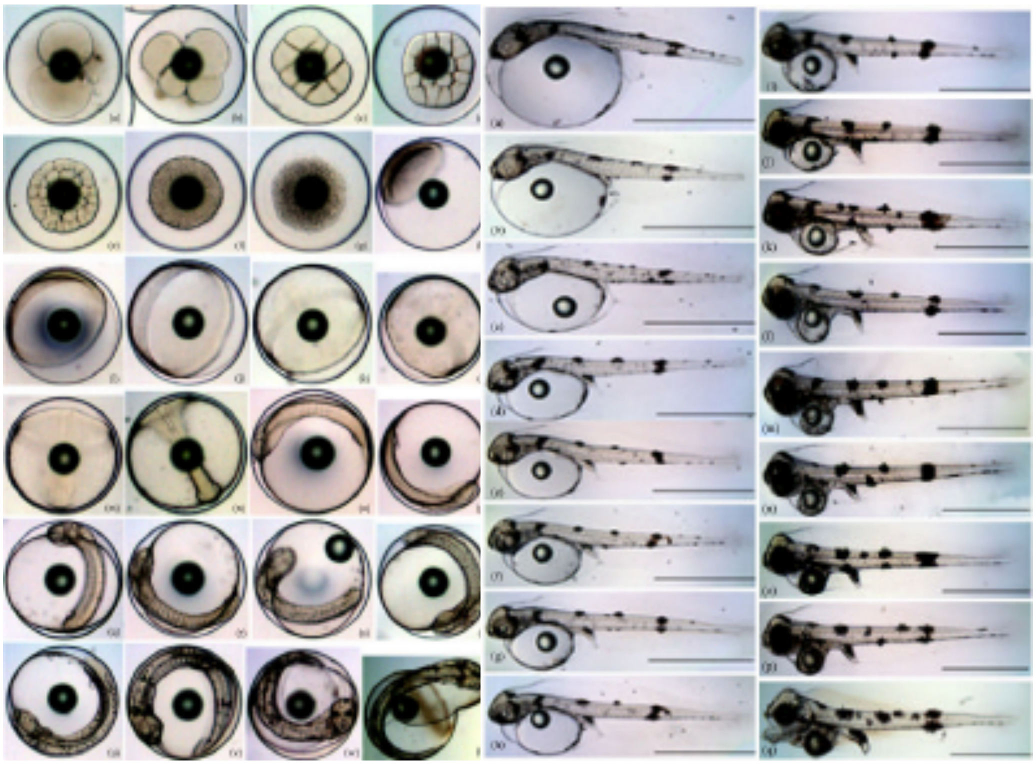

Figure I.5 – *Diplodus sargus sargus* larval development

between the two approaches can reveal the role of the oceanic currents, during the pelagic larval phase, in determining the observed pattern.

The white sea bream (*Diplodus sargus sargus*) and the Torre Guaceto Marine Protected Area

Torre Guaceto (Southwest Adriatic Sea) hosts a well-established Marine Protected Area (TGMPA in the following) with reported positive effect on the local community (Guidetti 2006, 2007, Guidetti et al. 2008). One of the most ecologically important species of this community is the white sea bream *Diplodus sargus sargus*. This species has an important ecological role because it is a major predator of sea urchins, controlling its abundances and, therefore, regulating the benthic community. It is a demersal fish with a wide range of distribution (Eastern Atlantic, Mediterranean and Black sea). Sedentary adults inhabit shallow coastal waters with a mixed rocky and sandy bottom up to 50m depths. Spawning takes place in late spring (Di Franco et al. 2012) and pelagic propagules (Figure I.5) disperse in the ocean for more than two weeks before settlement (Di Franco et al. 2011), with a potential migration of 200km (Di Franco et al. 2012). This potential distance of dispersal characterises the TGMPA also as a source, not just enhancing its own population but also replenishing the surrounding fishing grounds with new settlers. How this dual potential role (i.e. conservation and fishery management) of this MPA is possible is explored in chapter 2. Using genetic markers and individual-based modelling, coupled with early-life-history traits of the species, it has been possible to explore the connectivity dynamics of TGMPA better understanding the dispersal mechanisms (i.e. retention and spill-over) and the genetic consequences of dispersal.

The larval migration of the European eel (*Anguilla anguilla*) in the Atlantic Ocean

The European eel (*Anguilla anguilla*) is a very peculiar catadromous fish characterized by two long migrating phases (i.e. larval and adult migrations) across the Atlantic Ocean. In fact, before dying, mature eels spawn in the Sargasso Sea (panmittic mating), while the adult phase is spent in coastal brackish waters, lagoons and rivers of all Europe (from

Figure I.6 – European eel larvae (leptocephali)

Sweden to Greece) and North Africa (Atlantic Morocco and Mediterranean Africa). There is a rising concern about the fate of European eel whose stock is clearly declining since the late 1970s. In fact, European Commission has recently issued a Regulation (EC 1100/2007) aimed to restore the stock and many management studies have been published (e.g. Bevacqua et al. 2007, 2009, Schiavina et al. under revision). The reasons of this decline are still under investigation but it is not yet clear what produced the reduction of more than 90% of the annual juvenile recruitment (Dekker 2000). Multiple and not mutually exclusive causes are likely to explain the collapse, namely overfishing, habitat disruption (i.e. habitat loss and pollution), alien-parasite spreading, and ocean circulation changes. The latter could have affected migration routes, timing or recruitment success (food availability, increasing mortality due to temperature shifts). However, little is known about the migration of eel larvae (Righton et al. 2012), called leptocephali (Figure I.6). In the last century many studies (e.g. field sampling, otholit macro and micro-structure analyses, modelling and correlation analyses, see chapter 3 for more details) tried to improve our knowledge about leptocephalus stage. In this work it has been developed an ICPBM integrating all the main biological features related to the larval stage of European eel, namely body growth, mortality, and behaviour to analyse this migration process. This model has been tested against field data in order to tune the model parameters by contrasting alternative scenarios. The best scenario has been used to characterize the larval migration, assessing the probability of success, duration and exploring the alternatives of passive drift or active locomotion. With this model it has been possible to evaluate the role of the ocean in the recruitment drop of this species using data about the ocean circulation and water temperature from 1958 to 2000, encompassing the pre- and post-collapse periods.

References

Aarts G, MacKenzie M, McConnel B, Fedak M & Matthiopoulos J (2008). Estimating space-use and habitat preference from wildlife telemetry data. *Ecography* **31**:140-160

Bartsch J (1988). Numerical simulation of the advection of vertically migrating herring larvae in the North Sea. *Meeresforschung* **32**:30–45

Bartsch J, Brander K, Heath M, Munk P, Richardson K & Svendsen E (1989). Modeling the advection of herring larvae in the North Sea. Nature **340**:632–636

Browman HI, St-Pierre JF, Skiftesvik AB & Racca RG (2006). Behaviour of Atlantic cod (*Gadus morhua*) larvae: an attempt to link maternal condition with larval quality. In: Browman HI, Skiftesvik AB (eds) The big fish bang: proceedings of the 26th annual larval fish conference. *Institute of Marine Research*, Bergen, p 71–95

Bevacqua D, Melià P, Crivelli AJ, Gatto M & De Leo GA (2007). Multi-objective assessment of conservation measures for the European eel (*Anguilla anguilla*): an application to the Camargue lagoons. ICES J Mar Sci **64**: 1483-1490

Bevacqua D, Melià P, Crivelli AJ, De Leo GA & Gatto M (2009) Assessing Management Plans for the Recovery of the European Eel: A Need for Multi-Objective Analyses. *Am. Fish. Soc. Symp.* **69**:637–647

Chen RB, Wanatabe S & Yokota M (2004). Feeding habits of an exotic species, the Mediterranean green crab *Carcinus aestuarii*, in Tokyo Bay. *Fish Sci* **70**:430-435

Christensen A, Daewel U, Jensen H, Mosegaard H, St. John M & Schrum C (2007). Hydrodynamic backtracking of fish larvae by individual-based modelling. *Mar. Ecol. Prog. Ser.* **347**:221–232

Couzin ID, Krause J, Franks NR, & Levin SA (2005). Effective leadership and decision-making in animals groups on the move. *Nature* **433**:513-516

Deangelis DL & Gross LJ (1992). Individual-based models and approaches in ecology: populations, communities and ecosystems, Chapman and Hall, London

Deangelis DL & Mooij WM (2005). Individual-based modelling of ecologuical and evolutionary processes. *Annu. Rev. Ecol. Evol. Syst.* **36**:147-168

Dekker W (2000) A Procrustean assessment of the European eel stock.

ICES J *Mar Sci* **57**:938–947

Di Franco A, De Benedetto G., De Rinaldis G, Raventos N, Sahyoun R & Guidetti P (2011). Large scale variability in otolith microstructure and microchemistry: the case study of *Diplodus sargus sargus* in the Mediterranean Sea. *Ital J Zool* **78**:182-192.

Di Franco A, Gillanders BM, De Benedetto G, Pennetta A, De Leo GA, & Guidetti P (2012). Dispersal patterns of coastal fish: implications for designing networks of marine protected areas*. PLoS One* **7**:e31681.

Fiksen Ø, Jørgensen C, Kristiansen T, Vikebø F & Huse G (2007). Linking behavioural ecology and oceanography: larval behaviour determines growth, mortality and dispersal. *Mar. Ecol. Prog. Ser.* **347**:195-205

Fiksen Ø & MacKenzie BR (2002). Process-based models of feeding and prey selection in larval fish. *Mar Ecol Prog Ser* **243**:151–164

Gallego A, North EW & Petitgas P (2007). Introduction: status and future of modelling physical–biological interactions during the early life of fishes. *Mar. Ecol. Prog. Ser.* **347**:121–126

Goodchild ME (2003). Geographic information science and systems for environmental management. *Ann. Rev. Env. Res.* **28**:493-519

Guidetti P (2006). Marine reserves re-establish lost predatory interactions and cause community-wide changes in rocky reefs. *Ecol Appl* **16**:963–976.

Guidetti P (2007). Potential of marine reserves to cause community-wide changes beyond their boundaries. *Conserv Biol* **21**:540-545.

Guidetti P, Milazzo M, Bussotti S, Molinari A, Mureno M, Pais A, Spanò N, et al. (2008). Italian marine reserve effectiveness: does enforcement matter? *Biol Conserv* **141**:699–709.

Hannah CG (2007) Future directions in modelling physical–biological interactions. *Mar. Ecol. Prog. Ser.* **347**:301–306

Heath MR & Gallego A (1998). Biophysical modelling of the early life stages of haddock, *Melanogrammus aeglefinus*, in the North Sea. *Fish. Oceanogr.* **7**:110–125

Hermann AJ, Hinckley S, Megrey BA & Napp JM (2001). Applied and theoretical considerations for structuring spatially explicit individual-based models of marine larval fish that include multiple trophic levels. *ICES J Mar Sci* **58**:1030 –1041

Hinckley S, Hermann AJ & Megrey BA (1996). Development of a spatially explicit, individual-based model of marine fish early life history. *Mar Ecol Prog Ser* **139**:47–68

Holliday D, Beckley LE, Millar N, Olivar MP, Slawinski D, Feng M & Thompson PA (2012). Larval fish assemblages and particle back-tracking define latitudinal and cross-shelf variability in an eastern Indian Ocean boundary current. *Mar. Ecol. Prog. Ser.* **460**:127-144

Holyoak M, Casagrandi R, Nathan R, Revilla E & Spiegel O (2008) Trends and missing parts in the study of movement ecology. *PNAS* **105**:19060–19065

Leighton PA, Koffi JK, Pelcat YP, Lindsay LR & Ogden NH (2012). Predicting the speed of tick invasion: en empirical model of range expansion for the Lyme disease vector *Ixidez scapularis* in Canada. *J Appl Ecol* **49**:457-464

Leis JM (2007). Behaviour as input for modelling dispersal of fish larvae: behaviour, biogeography, hydrodynamics, ontogeny, physiology and phylogeny meet hydrography. *Mar. Ecol. Prog. Ser.* **347**:185-193

Lett C, Veitch J, van der Lingen CD & Hutchings L (2007). Assessment of an environmental barrier to transport of ichthyoplankton from the southern to the northern Benguela ecosystems. *Mar. Ecol. Prog. Ser.* **347**:247–259

Mariani P, MacKenzie BR, Visser AW & Botte V (2007). Individual-based simulations of larval fish feeding in turbulent environments. *Mar. Ecol. Prog. Ser.* **347**:155-169

Meekan MG & Fortier L (1996). Selection for fast growth during the larval life of Atlantic cod *Gadus morhua* on the Scotian Shelf. *Mar. Ecol. Prog. Ser.* **137**:25–37

Miller TJ (2007) Contribution of individual-based coupled physical–biological models to understanding recruitment in marine fish populations. *Mar Ecol Prog Ser* **347**:127–138

Mori M, Manconi R. & Fanciulli G. (1990). Notes on the reproductive biology of *Carcinus aestuarii* Nardo (Crustacea, Decapoda) from the lagoon of San Teodoro (Island of Sardinia, Italy). *Riv. Idrobiol.* **29:**763–774.

Mullon C, Cury P & Penven P (2002). Evolutionary individual- based model for the recruitment of anchovy (*Engraulis capensis*) in the southern Benguela. *Can. J. Fish. Aquat. Sci.* **59**:910–922

Murray (2003). Mathematical Biology I: An introduction. Springer, New York

Nathan R, MG Wayne, Revilla E, Holyoak M, Kadmon R, Saltz D & Smouse PE (2008) A movement ecology paradigm for unifying organismal movement research. *PNAS* **105**:19052–19059

Nathan R & Muller-Landau HC (2000). Spatial patterns of seed dispersal, their determinants and consequences for recruitment. *Trends Ecol. Evol.* **15**:278-285

Nathan R (2006). Long-distance dispersal of plants. *Science* **313**:786-788

Newnham RM (1964). The development of a stand model for Douglas-fir. PhD Thesis, *Univ. Br. Columbia*. Vancouver.

Okubo A & Levin SA (2001). Diffusion and ecological problems: modern perspectives. Springer, New York

Pineda J, Hare JA & Sponaugle S (2007). Larval transport and dispersal in the coastal ocean and consequences for population connectivity. *Oceanogr.* **20**:22-39.

Quinlan JA, Blanton BO, Miller TJ & Werner FE (1999). From spawning grounds to the estuary: using linked individual-based and hydrodynamic models to interpret patterns and processes in the oceanic phase of Atlantic menhaden *Brevoortia tyrannus* life history. *Fish. Oceanogr.* **8**(Suppl 2): 224–246

Rice J, Crowder L & Holey M (1987). Exploration of mechanisms regulating larval survival in Lake Michigan bloater: a recruitment analysis based on characteristics of individual larvae. *Trans. Am. Fish. Soc.* **116**:703–718

Righton D, Aarestrup K, Jellyman D, Sébert P, van den Thillart G & Tsukamoto K (2012) The *Anguilla* spp. migration problem: 40 million years of evolution and two millennia of speculation*. J Fish Biol* **81**:365–386

Schiavina M, Bevacqua D, Melià P, Crivelli AJ, Gatto M & De Leo GA (under revision). Eel Management Software, a user-friendly tool for the management of European eel fishery and conservation. *Env. Model. Soft.*

Thorrold S, Latkoczy C, Swart P & Jones C (2001). Natal homing in a marine fish metapopulation. *Science* **291**:297–299

Thygesen UH (2011). How to reverse time in stochastic particle tracking model. *J. Mar. Sys.* **88**:159-168

Turchin P (1998). Quantitative analysis of movement. Sinauer Associates, Sunderland

Vikebø F, Jørgensen C, Kristiansen T & Fiksen Ø (2007). Drift, growth and survival of larval Northeast Atlantic cod with simple rules of behaviour. *Mar. Ecol. Prog. Ser.* **347**:207–219

Werner FE, Quinlan JA, Lough RG & Lynch DR (2001). Spatially-explicit individual based modeling of marine populations: a review of the advances in the 1990s. *Sarsia* **86**:411–421

PART II

COUPLING OCEANOGRAPHY AND GENETICS TO ASSESS THE CONNECTIVITY OF EUROPEAN GREEN CRAB POPULATIONS IN THE ADRIATIC SEA

Abstract

Identifying the spatio-temporal scale of connectivity among populations is crucial to understand the factors driving population dynamics, dispersal patterns and gene flow in marine species. Coupled physical biological models are increasingly used to investigate larval dispersal and contrast alternative hypotheses by simulation. We coupled individual-based Lagrangian simulations incorporating early-life-history traits with a genetic marker analysis to investigate larval dispersal patterns of the European green crab (*Carcinus aestuarii*) in the Adriatic Sea and study the connectivity among seven locations during three years (2006-2008). The coupled physical biological model explicitly allowed for pelagic larval duration, diel vertical migration and synchronization between reproduction and moon phases and provided an assessment of oceanographic connectivity. Genetic analyses, based on eleven polymorphic microsatellite loci, tested for genetic divergence among populations using pairwise F_{ST} and AMOVA. We eventually compared connectivity matrices resulting from the two approaches to point out the role of Adriatic Sea currents in determining retention and spill-over patterns and their consequences on the genetic structure of the local European green crab populations. Results revealed the existence of weak but significant differentiation patterns, with three significantly

differentiated groups of samples reflecting an oceanographic subdivision of the Adriatic Sea into three sub-basins.

Introduction

Many marine species are characterized by large population sizes, high fecundity and external fertilization with a broad, mainly passive, pelagic larval phase followed by a local and less mobile benthic stage. The consequences of this particular behaviour are the extensive gene flow during larval stage, with an expected low genetic divergence, and the possible local adaptation in the adult phase (Ward et al. 1994). In this scenario, increasing the larval dispersal radius influences the geographic genetic structure reducing the genetic distance between populations (Hellberg et al. 2002; Palumbi 2003). Thus, identifying the spatio-temporal scale of connectivity among populations is crucial to understand the factors driving population dynamics, dispersal patterns and gene flow in marine species (Cowen et al. 2006). The study of connectivity in marine systems can be challenging because many biological and environmental factors affect the dispersal patterns (Pringle & Wares 2007) and the generally large population sizes leads to low statistical power to detect population and spatial structures (Selkoe et al. 2008). Individual–based coupled physical-biological models (ICPBMs) are increasingly used to investigate mechanisms of larval dispersal and to contrast alternative hypotheses by simulation (Gallego et al. 2007), moreover integrating the outputs of CPBMs with population genetic models can provide new insights of both verifying model predictions (Galindo et al. 2010) and boosting inference of genetic analyses (Selkoe et al. 2008). In this work, we investigated larval dispersal patterns of the European Green Crab (*Carcinus aestuarii*) in the Adriatic Sea by coupling Lagrangian simulations (incorporating early-life-history traits) with a genetic marker analysis and comparing the connectivity matrices resulting from the two approaches. The aim of the work was to study the role of Adriatic Sea currents in determining retention and spill-over patterns and their consequences on the genetic structure of the local European green crab populations.

Materials and methods

Genetic analyses were conducted on samples, collected in 2006, 2007 and 2008 from six sites along the Italian Adriatic coast (Marano, Venezia, Goro, Ravenna, Foggia, and Lecce), with an additional sample from the Ionian Sea (Taranto). Total genomic DNA was extracted using a salting-out protocol (Patwary et al. 1994) and individuals (N=381) were genotyped at eleven polymorphic microsatellite loci measuring the population differentiation due to genetic structure through the Wright's fixation index (F_{ST}) based on the variance of allele frequencies between populations. Population pairwise F_{ST} were determined with the permutation-based statistical inference procedures implemented in GENETIX software (Belkir et al. 2005), using 10000 permutations for all comparisons. Genetic divergence between populations was analysed also using the analysis of molecular variance approach (AMOVA; Excoffier & Lischer 2010), a statistical model for the molecular variation in a single species, to define groups of lagoon populations, which are geographically and genetically homogeneous and maximally differentiated from each other.

Lagrangian simulations were based on circulation fields produced by the Adriatic Forecasting System[2]. The dataset includes daily average fields of current velocity, water temperature and salinity, generated by the Adriatic Sea Regional Model (AREG; Oddo et al. 2006; Guarnieri et al. 2008), an implementation of the Princeton Ocean Model (Blumberg & Mellor 1987) for the Adriatic basin that extends south of the Otranto channel into the Ionian Sea down to the 39°N parallel (Figure 1.1 shows a snapshot of the current and temperature fields). The AREG model is nested into the general circulation model of the Mediterranean Sea, which provides the initial and lateral boundary conditions for current velocity, temperature and salinity (Pinardi et al. 2003). AREG has been implemented on a regular horizontal grid with a resolution of 1/45° (about 2.2 km), with 31 vertical sigma layers. Model bathymetry is based on US navy data with a horizontal resolution of 1/60°, with the coastline set at the 10-m isobath.

Lagrangian particles were released from each of the 7 sites at which genetic samples had been collected and over the same 3-year period (2006 to 2008). Particle release was designed to fit the available knowledge regarding the spawning season of C. aestuarii (from September to December, in correspondence with neap tides; Marta-Almeida et al. 2006). At each spawning event, 2000 particles, each one representing an individual zoea, were released according to a three-dimensional Gaussian distribution within a 1-km radius from each site. Particle trajectories were stepped forward using a 4th-order Runge-Kutta

---

[2] http://gnoo.bo.ingv.it/afs

method with a 6-minute time step and followed until the end of their pelagic phase, i.e. when they develop into megalopae and colonize estuaries. Figure 1.2 shows the location of the releasing site and an example of the model outputs. For each release site, self-retention and connectivity with the other sites were calculated as the percentage of larvae whose final position fell within a 10-km radius buffer from the release or destination site, respectively. The size of the buffer accounts for the swimming and navigation ability of megalopae, which are known to follow the freshwater lure and use selective tidal stream transport to reach suitable settlement areas (Queiroga 1998).

Green crab zoeae perform a diel vertical migration (Queiroga et

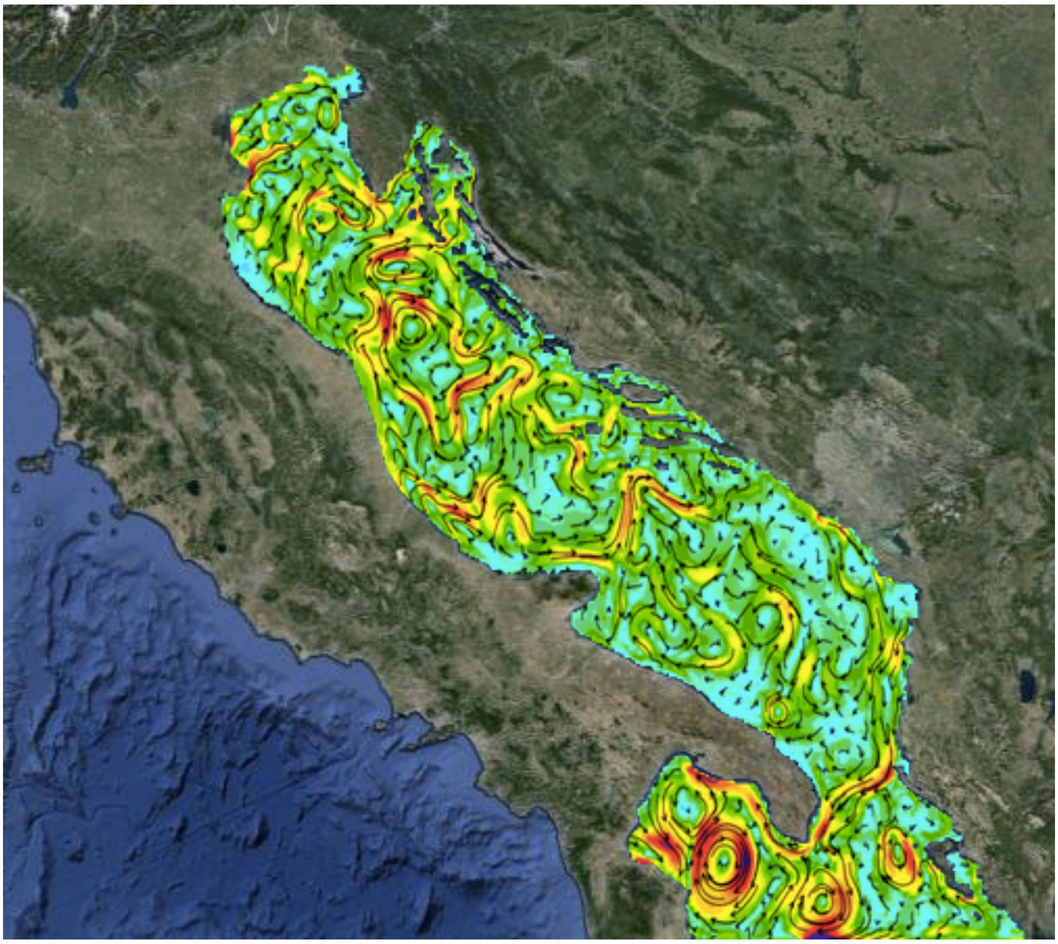

Figure 1.1 - An example of the Adriatic Forecasting System output. Figure shows a “snapshot” of the circulation field (black arrows) and the temperature field (colours) for the surface level in a given time

al.1997); we integrated this active behaviour in our Lagrangian model by combining two modelling approaches described in Marta-Almeida et al. (2006). We subdivided the water column into 6 equally spaced layers between 0 and 60 m (or down to the bottom when the depth was <60 m). Every morning at 6:00, each Lagrangian particle was assigned to a diurnal layer, which was randomly determined according to the probability distribution proposed by Marta-Almeida et al. (2006). Then, particles were let swim from their current position towards the destination layer at a constant speed of 1 cm s–1 (Chia et al. 1984). Once they reached the target layer, they were allowed to move randomly within the layer (within a depth range of ±0.5 m). Every evening at 18:00, particles were assigned to a nocturnal layer (according to the relevant probability distribution), let swim downwards (similarly to the upwards migration) and remain in the layer until next morning.

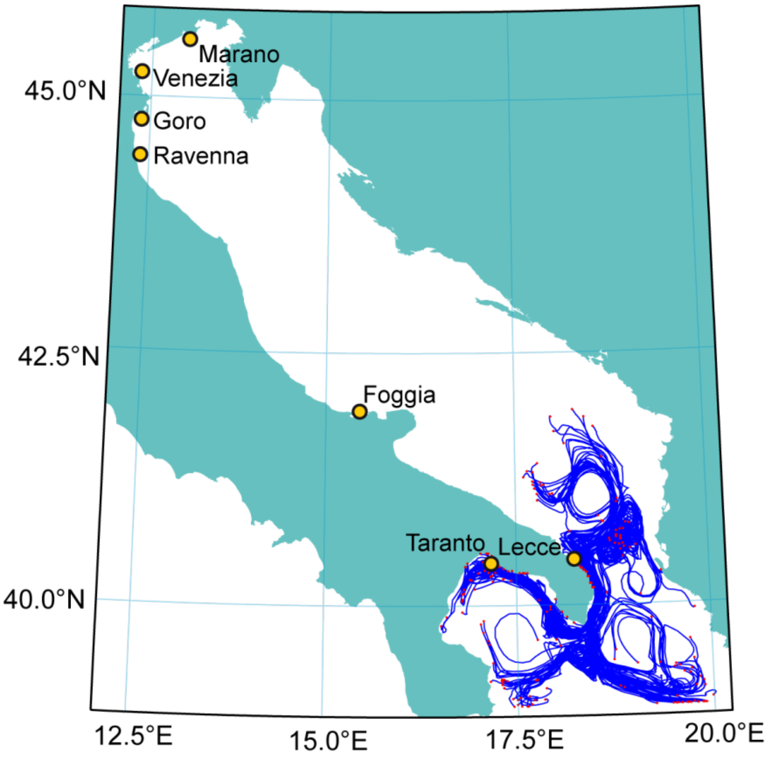

Figure 1.2 – Examples of Lagrangian model output: particles trajectories in blue and ending positions marked as red dots. Yellow circles represents the releasing locations and the sapling sites the European green crab.

We expressed pelagic larval duration and survival of zoeae as functions of water temperature on the basis of the relationships derived by deRivera et al. (2007) for the green crab Carcinus maenas, whose vital traits are very similar to those of C. aestuarii (Klassen & Locke 2007; Behrens Yamada & Hauck 2001). deRivera et al. (2007) linked the duration of the zoea stage to water temperature T through a logarithmic function $\tau = 130.46 - 36.93 \ln T$. To account for the variability of the temperature to which Lagrangian particles are subject during the simulations (which would determine a different pelagic larval duration at each time step), we introduced a dummy metric D (ranging between 0 and 1) representing the development of each zoea (with $D = 0$ at birth and $D = 1$ at full development into megalopa). We then expressed the progress of larval development through time as $dD/dt = \delta$, where $\delta = 1/\tau$ (with τ given by the above cited relationship with temperature). By integrating D throughout the simulation, the end of the zoea stage can be easily determined when the condition $D = 1$ is satisfied. Survival σ over the whole duration of the zoea stage was expressed by deRivera et al. (2007) as a polynomial function of water temperature T, namely $\sigma = -0.004T^2 + 0.14T - 0.74$. We derived from this function the instantaneous rate of natural mortality μ, calculated as $\mu = -\ln(\sigma)/\tau$ (where σ and τ are both functions of water temperature) and were therefore able to describe the variation in mortality rate across the journey of larvae experiencing different temperature patterns. Temperatures below 6.5°C or above 28.5°C (for which σ becomes <0) were considered to be lethal, while mortality rate attains its lowest value (0.025 day^{-1}) at an intermediate temperature of 13.9°C.

Results

Genetic data showed the existence of weak but significant genetic differentiation between samples (overall $F_{ST} = 0.002$; 95% CI = 0.000–0.004, $p<0.01$). Pairwise F_{ST} ranged from -0.001 to 0.005 and five values significant at the 5% level were found suggesting some genetic structure among samples (Table 1.1). Accordingly, AMOVA analysis identified 3 significantly differentiated groups of samples inside the Adriatic ($F_{ST} = 0.002$, $p<0.01$), the first including Marano, Venezia, Goro and Ravenna samples, the second including the Foggia sample and the third one represented by Lecce and Taranto samples.

	Marano	*Venezia*	*Goro*	*Ravenna*	*Foggia*	*Lecce*	*Taranto*
Marano	-						
Venezia	0.002	-					
Goro	0.002	0.001	-				
Ravenna	0.002	0.001	-0.001	-			
Foggia	**0.004***	0.000	0.000	0.002	-		
Lecce	**0.003***	0.003	0.002	0.001	**0.003***	-	
Taranto	**0.003***	0.003	0.002	0.003	**0.005***	0.000	-

Table 1.1 - *Carcinus aestuarii* pairwise F_{ST} . Estimates of pairwise genetic differentiation (F_{ST} values) among 7 populations. Asterisk: significant values, uncorrected $p < 0.05$.

	Marano	*Venezia*	*Goro*	*Ravenna*	*Foggia*	*Lecce*	*Taranto*
Marano	**31.19%**						
Venezia	**0.05%**	**1.87%**					
Goro	**0.14%**	**0.94%**	**48.87%**				
Ravenna	**0.03%**	**0.11%**	**1.78%**	**2.29%**			
Foggia	0.00%	0.00%	0.00%	**0.00%**	**0.15%**		
Lecce	0.00%	0.00%	0.00%	0.00%	**0.09%**	**38.50%**	
Taranto	0.00%	0.00%	0.00%	0.00%	0.00%	**0.06%**	**6.59%**

Table 1.2 - *Carcinus aestuarii* connectivity matrix in the Adriatic Sea resulting from Lagrangian simulations. Bold values represent a connection level different from zero.

	Marano	*Venezia*	*Goro*	*Ravenna*	*Foggia*	*Lecce*	*Taranto*
Marano	31.19%	0.04%	0.14%	0.03%	0.00%	0.00%	0.00%
Venezia	0.01%	1.87%	0.94%	0.11%	0.00%	0.00%	0.00%
Goro	0.00%	0.00%	48.87%	1.64%	0.00%	0.00%	0.00%
Ravenna	0.00%	0.00%	0.13%	2.29%	0.00%	0.00%	0.00%
Foggia	0.00%	0.00%	0.00%	0.00%	0.15%	0.09%	0.00%
Lecce	0.00%	0.00%	0.00%	0.00%	0.00%	38.50%	0.06%
Taranto	0.00%	0.00%	0.00%	0.00%	0.00%	0.00%	6.59%

Table 1.3 - *Carcinus aestuarii* directed connectivity matrix in the Adriatic Sea resulting from Lagrangian simulations. Rows are the origin sites and column the destinations. Connectivity levels greater than zero are highlighted in a gray scale from low levels (light gray) to high levels (dark gray)

Table 1.2 and Table 1.3 show the connectivity matrices obtained with the ICPBM for the 3 years analysed. European green crab dispersal is characterized by an almost mono-directional flow from the north towards the south (Table 1.3). In accordance with the results of the genetic analysis, Lagrangian simulations confirm the existence of a connection among the four northern sites, which, in contrast, are almost isolated from the others, except for a very low flux (<0.01%) of individuals from

Marano	*Marano*	*Venezia*	*Goro*	*Ravenna*	*Foggia*	*Lecce*	*Taranto*
September	28.90%	0.04%	0.00%	0.00%	0.00%	0.00%	0.00%
October	41.63%	0.02%	0.05%	3.33E-05	0.00%	0.00%	0.00%
November	33.22%	0.10%	0.23%	0.07%	0.00%	0.00%	0.00%
December	21.02%	0.00%	0.28%	0.06%	0.00%	0.00%	0.00%
Venezia	*Marano*	*Venezia*	*Goro*	*Ravenna*	*Foggia*	*Lecce*	*Taranto*
September	0.03%	5.07%	0.04%	0.00%	0.00%	0.00%	0.00%
October	0.01%	1.41%	0.96%	0.13%	0.00%	0.00%	0.00%
November	0.00%	0.99%	0.70%	0.11%	0.00%	0.00%	0.00%
December	0.01%	0.02%	2.06%	0.21%	0.00%	0.00%	0.00%
Goro	*Marano*	*Venezia*	*Goro*	*Ravenna*	*Foggia*	*Lecce*	*Taranto*
September	0.00%	0.00%	35.01%	2.47%	0.00%	0.00%	0.00%
October	0.00%	0.00%	34.04%	2.08%	0.00%	0.00%	0.00%
November	0.00%	0.00%	54.83%	1.87%	0.00%	0.00%	0.00%
December	0.00%	0.00%	71.61%	0.15%	0.00%	0.00%	0.00%
Ravenna	*Marano*	*Venezia*	*Goro*	*Ravenna*	*Foggia*	*Lecce*	*Taranto*
September	0.00%	0.00%	0.00%	2.77%	0.00%	0.00%	0.00%
October	0.00%	0.00%	0.01%	1.62%	0.00%	0.00%	0.00%
November	0.00%	0.00%	0.15%	2.70%	0.00%	0.00%	0.00%
December	0.00%	0.00%	0.38%	2.07%	0.00%	0.00%	0.00%
Foggia	*Marano*	*Venezia*	*Goro*	*Ravenna*	*Foggia*	*Lecce*	*Taranto*
September	0.00%	0.00%	0.00%	0.00%	0.58%	0.00%	0.00%
October	0.00%	0.00%	0.00%	0.00%	0.01%	0.01%	0.00%
November	0.00%	0.00%	0.00%	0.00%	0.00%	0.01%	0.00%
December	0.00%	0.00%	0.00%	0.00%	0.00%	0.36%	0.00%
Lecce	*Marano*	*Venezia*	*Goro*	*Ravenna*	*Foggia*	*Lecce*	*Taranto*
September	0.00%	0.00%	0.00%	0.00%	0.00%	31.15%	0.03%
October	0.00%	0.00%	0.00%	0.00%	0.00%	38.69%	0.12%
November	0.00%	0.00%	0.00%	0.00%	0.00%	43.86%	0.02%
December	0.00%	0.00%	0.00%	0.00%	0.00%	40.31%	0.06%
Taranto	*Marano*	*Venezia*	*Goro*	*Ravenna*	*Foggia*	*Lecce*	*Taranto*
September	0.00%	0.00%	0.00%	0.00%	0.00%	0.00%	4.32%
October	0.00%	0.00%	0.00%	0.00%	0.00%	0.00%	13.58%
November	0.00%	0.00%	0.00%	0.00%	0.00%	0.00%	3.30%
December	0.00%	0.00%	0.00%	0.00%	0.00%	0.00%	5.15%

Table 1.4 - *Carcinus aestuarii* connectivity matrices per site in the Adriatic Sea resulting from Lagrangian simulations averaged over the releasing month. Connectivity levels greater than zero are highlighted in a gray scale from low levels (light gray) to high levels (dark gray)

Ravenna to Foggia (Table 1.4). The southernmost location along the Adriatic coast (Lecce) is characterized by only an occasional input (>0.01%) from Foggia (Table 1.4) shown in Figure 1.3, that determines alone their connectivity level (0.09%). This confirms the observed genetic separation between these two populations. Noticeably, larvae released from Lecce are also able to reach Taranto with a low (0.06%) but constant flux of individuals (Table 1.4) that, for this reason can be considered more significant than the occasional connection between Foggia and Lecce.

Figure 1.3-1.4 point out how variations of the currents can determine the connections or the separation between sites in different years and

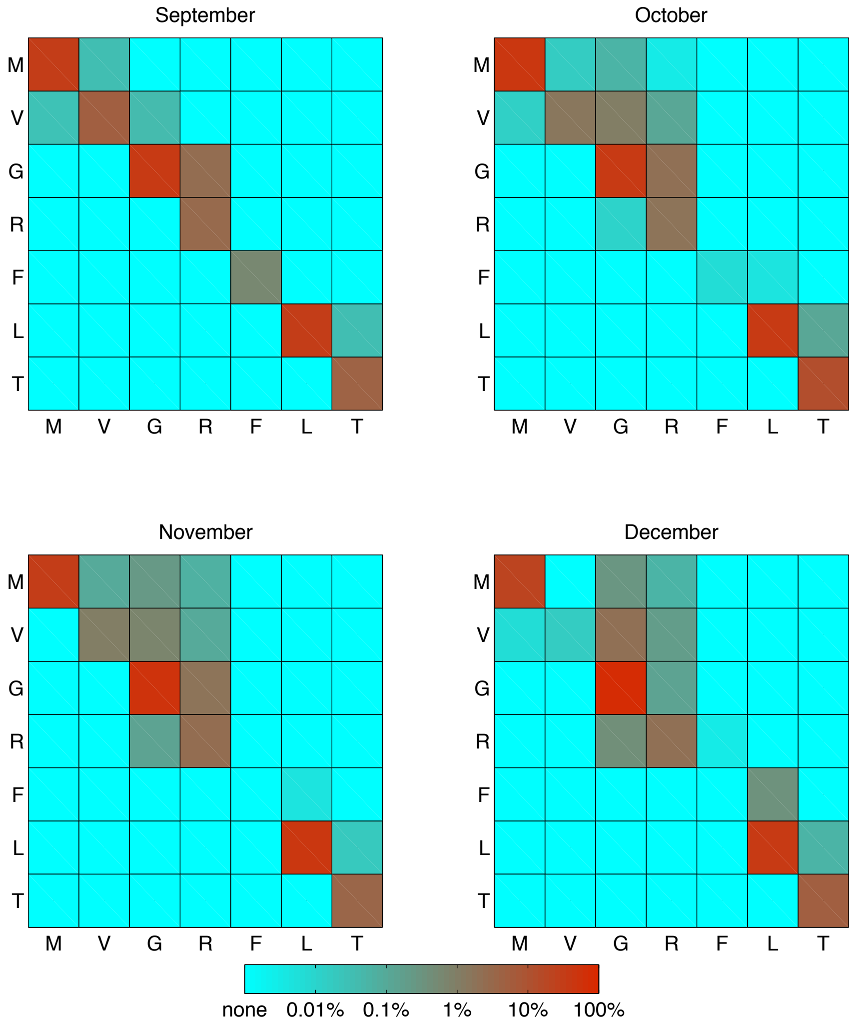

Figure 1.3 - *Carcinus aestuarii* connectivity matrices per month in the Adriatic Sea resulting from Lagrangian simulations. Rows are the origin site while column are the destination. The color represents the percentage of larvae released in one origin and ending in the destination site.

periods, showing the usual trajectories generated from Foggia (Figure 1.4a), that are able to reach the Dalmatian coast against the occasional connection with Lecce (Figure 1.4b). Similarly Figure 1.4c shows the unique event where no larvae from Lecce reached Taranto, trapped in local gyres and drifted towards the Albanian coast, while typically remain closer to the coast until Taranto (Figure 1.4d).

Discussion

A coupled oceanographic-genetic analysis allowed us to derive potential dispersal patterns of *C. aestuarii* in the Adriatic Sea and, at the same time, to elucidate the genetic consequences of larval dispersal.

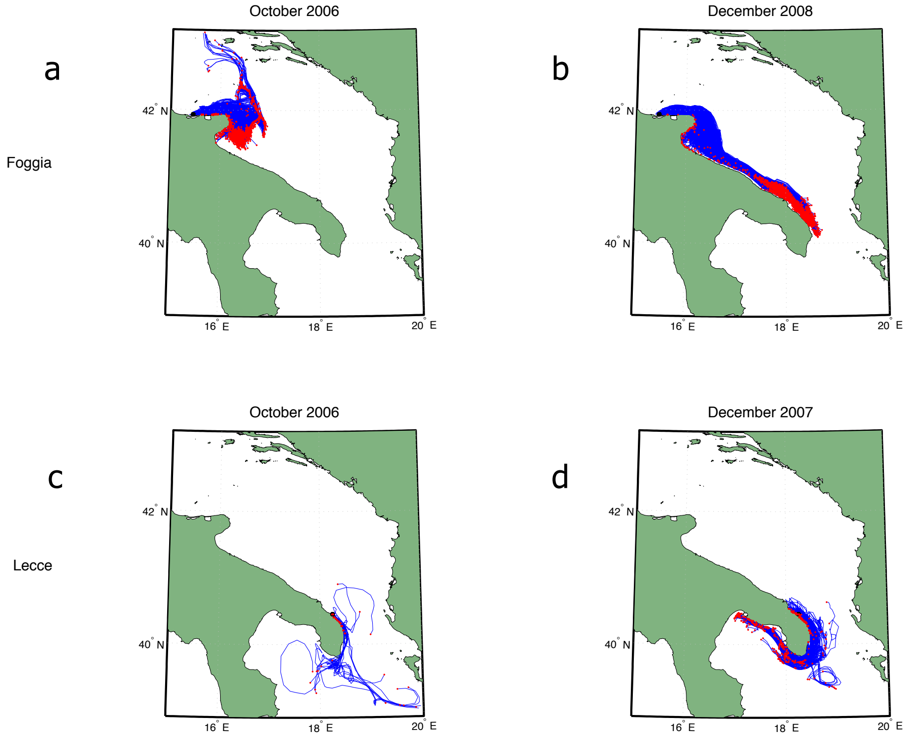

Figure 1.4 – Lagrangian model outputs for two sites in two different releasing events. a) shows the trajectories generated from Foggia in October 2006; b) shows the trajectories generated from Foggia in December 2008; c) shows the trajectories generated from Lecce in October 2006; d) shows the trajectories generated from Lecce in December 2007

Genetic analyses revealed the existence of weak but significant differentiation, apparently reflecting an oceanographic subdivision of the Adriatic Sea in three sub-basins. Lagrangian simulations confirm the same geographic subdivision pointing out that the ocean current is probably the main driver of the genetic differentiation of European green crab populations in the Adriatic basin. When dealing with such subtle genetic differences the challenge is to discriminate between minor but real population structure and artefacts due to noise related to sampling errors (Wirth & Bernatchez 2001). On the other hand the Lagrangian simulations are not exempt of criticism especially when dealing with coastal circulation where the resolution of the ocean model do not incorporate the complexity of the shelf structure. The turbulence generated by the irregular shape of the coast and the sea bottom, as well as the tidal currents, could have a strong effect on the larval dispersal, while the ocean circulation models, mainly focused on the meso-scale patterns, usually uses an approximation of the coastal line (in our case represented by the 10-m isobath) reducing the reliability of retention values. The joint consideration of the two approaches is important to gain confidence on processes driving connectivity among sites and to provide the basis to forecast the effects of present-day climate change.

References

Belkir K, Borsa P, Goudet J, Bonhomme F (2005) GENETIX v. 4.05, logiciel sous Windows pour la génétique des populations. Laboratoire Génome et Populations. CNRS UPR 9060, Université Montpellier II

Blumberg AF & Mellor GL (1987). A description of a three-dimensional coastal ocean circulation model, in: Three-dimensional coastal ocean models, edited by: Heaps NS, Washington, DC, *American Geophysical Union*, 208 pp.

Chia FS, Buckland-Nicks J, Young CM (1984). Locomotion of marine invertebrate larvae: a review. *Can J Zool* **62**:1205–1222

Cowen RK, Paris CB & Srinivasan A (2006). Scaling of connectivity in marine populations. Science **311**:522–527

DeRivera CE, Hitchcock NG, Teck SJ, Steves BP, Hines AH & Ruiz GM (2007). Larval development rate predicts range expansion of an introduced crab. *Mar. Biol.* **150**:1275–1288

Excoffier L & Lischer HEL (2010). Arlequin suite ver 3.5: A new series of programs to perform population genetics analyses under Linux and Windows. *Mol. Ecol. Resour.* **10**: 564-567

Galindo HM, Pfeiffer-Herbert AS, McManus M A, Chao Y, Chai F & Palumbi SR (2010). Seascape genetics along a steep cline: using genetic patterns to test predictions of marine larval dispersal*. Mol. Ecol.* **19**:3692– 3707

Gallego A, North EW & Petitgas P (2007). Introduction: status and future of modelling physical–biological interactions during the early life of fishes. *Mar. Ecol. Prog. Ser.* **347**:121–126

Guarnieri A, Oddo P, Pastore M & Pinardi N (2008). The Adriatic Basin Forecasting System: new model and System development. Coastal to Global Operational Oceanography: Achievements and Challenges, edited by: Dahlin H, Fleming NC & Petersson SE, *Proceeding of 5th EuroGOOS Conference*, Exeter, 20–22

Hellberg ME, Burton RS, Neigel JE & Palumbi SR (2002). Genetic assessment of connectivity among marine populations. *Bull. Mar. Sci.* **70**:273-290.

Klassen G & Locke A (2007). A Biological Synopsis of the European Green Crab, *Carcinus maenas*. Canadian Manuscript report of Fisheries and Aquatic Sciences 2818. Fisheries and Oceans Canada Gulf Fisheries Centre Moncton, New Brunswick

Marta-Almeida M, Dubert J, Peliz A & Queiroga H (2006). Influence of vertical migration pattern on retention of crab larvae in a seasonal upwelling system. *Mar. Ecol. Prog. Ser*. **307**:1–19

Oddo P, Pinardi N, Zavatarelli M & Colucelli A (2006). The Adriatic Basin forecasting system. *Acta Adriat.* **47**:169–184

Palumbi SR (2003). Population genetics, demographic connectivity, and the design of marine reserves. *Ecol. Appl.* **13**:S146-S158.

Patwary MU, Kenchington EL., Bird CJ & Zouros E (1994). The use of random amplified polymorphic DNA (RAPD) markers in genetic studies of the sea scallop Placopecten magellanicus (Gmelin, 1791). *J. Shellfish Res.* **13**: 547-553

Pinardi N, Allen I, Demirov E, De Mey P, Korres G, Lascaratos A, Le Traon PY, Maillard C, Manzella G, & Tziavos C (2003). The Mediterranean ocean forecasting system: first phase of implementation (1998–2001). *Ann Geophys* **21**:3–20.

Pringle JM & Wares JP (2007). Going against the flow: maintenance of alongshore variation in allele frequency in a coastal ocean. *Mar. Ecol. Prog. Ser*. **335**:69-84

Queiroga HJ, Costlow JD, & Moreira MH (1997). Vertical migration of the crab *Carcinus maenas* first zoea: implications for tidal stream transport. *Mar. Ecol. Prog. Ser*. **149**: 121–132.

Queiroga H (1998) Vertical migration and selective tidal stream transport in the megalopa of the crab *Carcinus maenas*. *Hydrobiologia* **375/376**: 137–149.

Selkoe KA, Henzler CM, Gaines SD, (2008). Seascape genetics and the spatial ecology of marine populations. *Fish. Fish.* **9**:363-377

Ward RD, Woodwark M & Skibinski DOF (1994). A comparison of genetic diversity levels in marine, freshwater, and anadromous fishes. *J Fish Biol.* **44**:213-232

Wirth T & Bernatchez L (2001). Genetic evidence against panmixia in the European eel. *Nature* **409**:1037–1040

UNDERSTANDING THE EFFECTIVENESS OF MARINE PROTECTED AREAS USING GENETIC CONNECTIVITY PATTERNS AND LAGRANGIAN SIMULATIONS

Abstract

Determining genetic connectivity is fundamental for the design of marine protected areas (MPAs) as it contributes to understanding whether larval retention/export occurs within MPAs and toward outside areas. In the present study, we explored the connectivity dynamics among the MPA of Torre Guaceto (TGMPA) and neighbouring non-protected areas in the South-western Adriatic Sea, using the white sea bream *Diplodus sargus* as model species. A multi-disciplinary approach was used combining genetic data and Lagrangian simulations. Microsatellite markers revealed a high similarity in genetic diversity and genetic composition, suggesting the existence of a single white sea bream population in the study area. The lack of genetic sub-structuring was consistent over time in the temporally replicated samples from 2009 and 2010. The overall genetic homogeneity observed indicates that the TGMPA is not isolated and that there is genetic connectivity among locations across a scale of at least ~200 km. A high degree of connectivity between the TGMPA and neighbouring areas is in agreement with Lagrangian simulations, which indicated that white sea bream larvae can be transported over large distances up to about 300 km. Trajectories released from the TGMPA confirmed the existence of transport outside of the TGMPA boundaries, showing that larvae are in part retained within the TGMPA and in part travel south towards non-protected areas. Our findings highlight the potential benefits of effectively enforced MPAs for neighbouring or relatively distant non-protected fishing areas and the potential connection with other MPAs at regional scale.

Introduction

Determining genetic connectivity and the relative influence of physical and biotic factors is particularly important for the design of marine protected areas (MPAs) (Palumbi 2003). MPAs have been advocated worldwide as a powerful conservation and fishery management tool that can safeguard from populations of species to ecosystems and also benefit fisheries by means of density-dependent spill-over of adults and enhanced larval dispersal into fishing areas (Roberts et al. 2001; Halpern and Warner 2002; Lubchenco et al. 2003; Hilborn 2004; Claudet et al. 2008; White et al. 2008; Lester et al. 2009; Molloy et al. 2009; Palumbi et al. 2009; Edgar 2011). Therefore, it is fundamental for MPA design to understand contemporary larval transport in and out of the marine protected areas, whether larval retention/export occurs within MPAs and from MPAs to non-protected fished areas, and whether and at what extent MPA-networks may exchange recruits (Palumbi 2003). However, due to a poor understanding of the interactions between dispersal and oceanic features, the measurement of connectivity and consequently the design of MPAs and their networks remain an extremely difficult challenge. In this sense, population genetic data have the potential to estimate the rate of exchange among populations and provide an indirect measure of connectivity (Waples and Gaggiotti 2006), which can facilitate the set-up of the appropriate spatial scale at which effective single MPAs and/or MPA networks should be designed.

In the present study, we explored the connectivity dynamics of a Mediterranean MPA, Torre Guaceto in the South-western Adriatic Sea (TGMPA), using the white sea bream *Diplodus sargus sargus* as model species. This is a benthopelagic (demersal) species inhabiting shallow coastal rocky bottoms interspersed with sand down to depths of about 50 m in the Eastern Atlantic, Mediterranean and Black Seas (Harmelin-Vivien et al. 1995). Adults are relatively sedentary and produce larvae that develop in pelagic waters for a period of 16-28 days until settlement (Vigliola 1998; Di Franco and Guidetti 2011; Di Franco et al. 2011). A larval dispersal of at least 200 km has been recently suggested on the basis of otolith microchemistry, while post-settlement dispersal was highly variable, with some individuals not dispersing at all and other individuals dispersing over about 30 km (Di Franco et al. 2012). Despite this high larval dispersal, weak but significant genetic differences have been detected at a scale ranging from less than 100 km (González-Wangüemert et al. 2012) to several hundreds of kilometres (Lenfant and Planes 1996). This species was selected because of its ecologic importance, being the major predator of sea urchins and therefore playing a major role in controlling their abundance and effects on benthic communities (Sala and Zabala 1996; Sala et al. 1998; Guidetti 2006; Guidetti and Sala 2007). The species also has important socio-economic value and supports local artisanal and recreational fisheries (Guidetti 2006).

The TGMPA is effectively enforced and a number of studies have reported a long-term positive effect of the TGMPA including higher density and size of many coastal fish compared to adjacent fished areas and community-wide effects of protection (Guidetti 2006; Guidetti 2007; Guidetti et al. 2008). On the basis of this evidence, we conjectured that the TGMPA is also an important source of propagules (eggs and larvae) significantly enhancing recruitment in outside fishing areas. In order to explore this hypothesis, we employed a multi-disciplinary approach combining genetic analyses using microsatellite loci and Lagrangian simulations of dispersal based on an oceanographic model of the region and fed with data on early-life-history traits of the species (e.g. spawning date, pelagic larval duration). The combined strategy allowed us to estimate dispersal in the white sea bream, but at the same time, also to elucidate the genetic consequences of dispersal. The seminal paper of Waples (1998) argued that the single most effective strategy for dealing with the relatively weak genetic signal for high gene flow marine species is to replicate samples over time. Patterns of genetic differentiation that are temporally-consistent are unlikely to be caused by sampling artefacts. Similarly, it is important to assess temporal variation in ocean currents in terms of speed and direction, as it can greatly influence recruitment and gene flow among populations (Schunter et al. 2011). In order to account for temporal heterogeneity, both sampling campaigns and simulation studies were temporally replicated during two consecutive years (2009 and 2010). Aside from assessing the effectiveness of the MPA of Torre Guaceto, whether larvae are retained and/or exported outside the reserve boundaries, the information obtained on the patterns of spatial connectivity of the white sea bream in our study area using genetic markers and modelling will provide a better understanding of the dual potential role of MPAs as conservation and fishery management tools.

Material and Methods

Study area

The marine protected area of Torre Guaceto (TGMPA) was formally established in 1991 and has been effectively enforced since 2000-2001. The TGMPA covers 2,227 ha along ~8 km of coastline and is subdivided into three zones: (1) a no-take/no-access reserve (Zone A, 179 ha); (2) a general reserve zone with recreational use only (i.e. swimming) (Zone B, 163 ha) and (3) a partial reserve, formally a buffer zone (Zone C, 1885 ha). In Zone C, artisanal (professional) fishing is allowed but limited, while recreational fishing is allowed but severely restricted and spearfishing is totally banned.

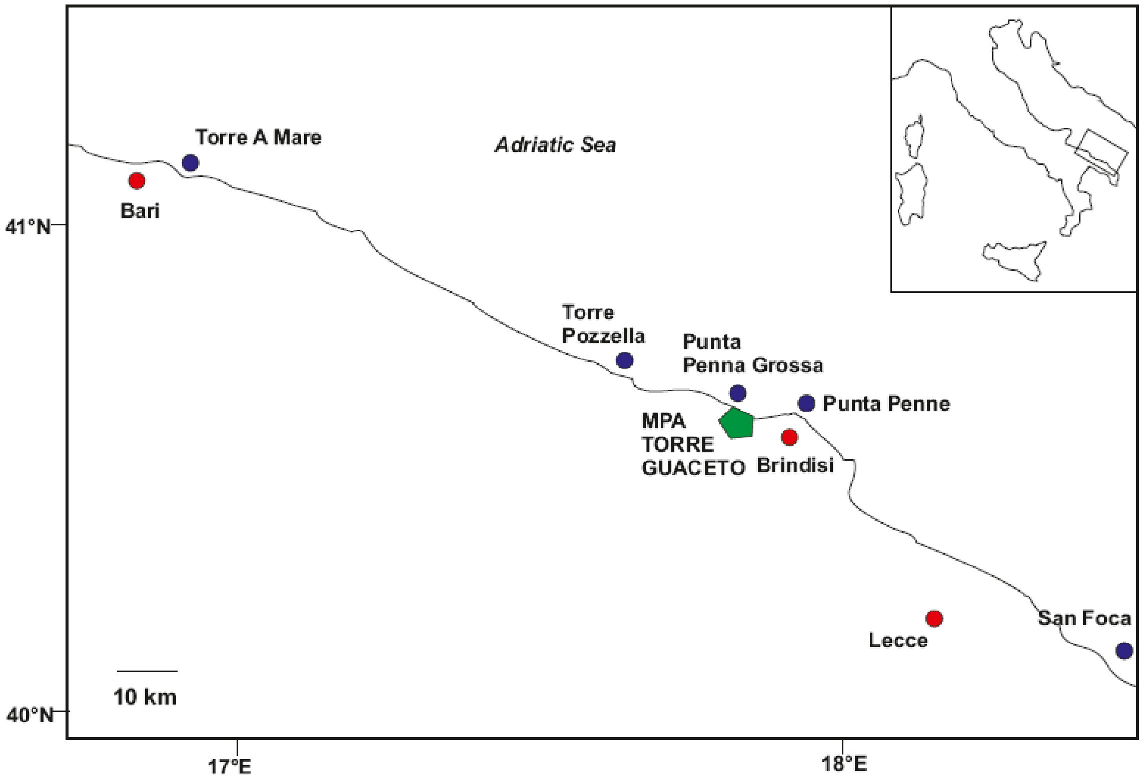

Figure 2.1 - Sampling locations of white sea bream.

Genetic Samples

A total of 298 settlers of *D. sargus sargus* were caught using hand-nets at five separate geographic locations along 200 km of the Apulian Coast in the South Adriatic Sea (Figure 2.1). One location was inside the TGMPA and four locations were outside (two northward and two southward) in surrounding non-protected areas up to 100 km from the TGMPA. The details of the locations are as follows: (1) Punta Penna Grossa inside the TGMPA (40°43'N, 17°46'E), (2) Torre Pozzella situated 20 km north of the TGMPA (40°49'N, 17°30'E), (3) Torre a Mare situated 100 km north of the TGMPA and south of Bari (41°5'N, 17°E), (4) Punta Penne situated 10 km south of the TGMPA and north of Brindisi (40°41'N, 17°56'E), and (5) San Foca situated 90 km south of the TGMPA (40°18'N, 18°25'E). Settlers were collected at all five locations during May 2009 (N= 168) and May 2010 (N= 130) as detailed in Table 2.1.

Additionally, a total of 84 adults were collected at the TGMPA during 2010. Individuals were aged using otolithometry and each fish was assigned to a single cohort or year-class. Each pair of sagittal otoliths were extracted from all studied individuals, cleaned and stored to dry. From each pair, one otolith was randomly selected and then treated to obtain thin sections. First, the sagitta was ground starting from the posterior using a metallographic grinding paper disc to the edge of the core, until all increment along the counting path were readable. Then the ground surface was polished with alumina (0.5 and 0.05 µm). In a second phase, the remaining half-otolith was glued to a glass slide using crystal bond and, again ground and polished from the rostrum towards the core until a section around the core was obtained, thin enough (1mm or less) to be observed under stereomicroscope. The number of annual rings on otoliths was read using a software image analysis system equipped with video-camera, able to get and display large HD images on a wide screen (see Panfili et al. 2002 for generalities on ageing fish using otoliths). A sub-sample of 54 adults corresponding to four cohorts (2005, 2006, 2007 and 2008) was selected for the genetic analysis.

Location	**Year**	**N**	H_o	H_e	**TNA**	**MNA**	**AR**
Settlers							
North 2 - Torre a Mare	2009	32	0.659 (0.318)	0.696 (0.325)	139	11.58	6.50
	2010	26	0.611 (0.323)	0.651 (0.338)	104	8.67	5.79
North 1 - Torre Pozzella	2009	24	0.617 (0.297)	0.677 (0.302)	103	8.58	5.89
	2010	28	0.669 (0.281)	0.680 (0.285)	118	9.83	5.95
TGMPA - Punta Penna G	2009	48	0.678 (0.296)	0.721 (0.294)	155	12.92	6.52
	2010	27	0.607 (0.302)	0.671 (0.296)	110	9.17	6.08
South 1 - Punta Penne	2009	24	0.692 (0.296)	0.706 (0.308)	123	10.25	6.48
	2010	12	0.625 (0.355)	0.637 (0.338)	79	6.59	5.78
South 2 - San Foca	2009	40	0.643 (0.354)	0.669 (0.350)	139	11.58	6.13
	2010	37	0.639 (0.289)	0.676 (0.296)	118	9.83	5.96
Adults							
TGMPA - Punta Penna G	2010	54	0.687 (0.325)	0.696 (0.307)	162	13.50	5.78

Table 2.1 - Summary of diversity indices for all white sea bream samples including number of individuals (N), observed (Ho) and expected heterozygosity (He), total (TNA) and mean number of alleles (MNA) and allelic richness (AR). Standard deviation in parentheses

Microsatellite Analysis

Minute sections of the caudal fin were digested in a lysis buffer containing 100 μl TE Buffer, 7 μl 1 M DTT (dithiothreitol) solution pH 5.2 (diluted in 0.08M NaAC) and 2 μl proteinase K solution (20 mg/ml) for at least 8 hours at 56°C. After incubation at 96°C for 10 min, samples were centrifuged at 13,000 rpm for 11 min and the supernatant was stored at -20°C.

Genotypes were examined at a total of 12 microsatellite loci originally developed for the gilthead sea bream *Sparus aurata* (Franch et al. 2006; Moritz et al. 2010) that positively amplified in *D. sargus sargus*. PCR products were obtained in a GeneAmp PCR System 2700 Thermocycler (Applied Biosystems) using the QIAGEN Multiplex PCR Kit. PCR reactions consisted of 2 μl template DNA, 5 μl QIAGEN Multiplex PCR Master Mix, 0.2 μl 10 μM forward and reverse primers and water up to 10 μl. PCR conditions were as follows: 15 min at 95^{o}C, 35 cycles of 30 sec at 94^{o}C, 90 sec at 57^{o}C and 1 min at 72^{o}C and final elongation for 30 min at 60^{o}C. PCR products were visualized on 1.8% agarose gels and screened for microsatellite polymorphism using an ABI 3130 AVANT automatic capillary sequencer (Applied Biosystems).

Genetic Data Analysis

Within-sample genetic diversity was assessed by observed (Ho) and expected (He) heterozygosities per locus and mean and total number of alleles using GENETIX version 4.05 (Belkhir et al. 2005) and allelic richness (AR) using FSTAT version 2.3.9.2 (Goudet 2002). Diversity values across samples were compared with one-way ANOVA using STATISTICA version 10 (StatSoft). Deviations from Hardy-Weinberg equilibrium (HWE) and linkage disequilibrium were tested using GENEPOP version 3.4 (Raymond and Rousset 1995). Significance levels for multiple comparisons were adjusted using the sequential Bonferroni technique (Rice 1989). Presence of null alleles was tested using the program MICRO-CHECKER version 2.2.3 (Van oosterhout et al. 2004).

Prior to the population structure analysis, the statistical power of the markers employed was assessed with POWSIM (Ryman and Palm 2006). We tested a range of predefined levels of expected divergence (F_{ST}= 0.001, 0.005, 0.01, 0.05, 0.1). Differences in allele and genotype frequencies among samples were assessed using Fisher's exact test as implemented in GENEPOP. Significance levels for multiple simultaneous comparisons were adjusted using Bonferroni as described above. Population structure was explored by calculating pairwise F_{ST} between samples in ARLEQUIN 3.5.1.2 (Excoffier et al. 2005) and conducting a multivariate ordination based on F_{ST} values by Multi-dimensional Scaling (MDS) using STATISTICA. A hierarchical AMOVA was also conducted on ARLEQUIN, partitioning genetic differentiation among locations (FCT, geographical) and among samples within locations (FSC, temporal). Isolation-by-Distance (IBD) and Isolation-by-Time (IBT) were tested using a Mantel test implemented in GENETIX, by correlating linearized genetic distance ($F_{ST}/(1- F_{ST})$) versus coastal distance (between locations) and temporal distance (measured as number of years between cohorts), respectively.

Population sub-structuring was also explored with the software STRUCTURE (Pritchard et al. 2000), a model based clustering algorithm that infers the most likely number of groups in the data. The software organizes individuals into a predefined number of clusters (K) with a given likelihood, which might represent putative populations. The analysis was performed for 1<K<5, with five replicates per K and using the admixture model. A burn-in length of 104 iterations followed by 106 additional Markov Chain Monte Carlo (MCMC) iterations was performed. The most likely K was determined using the criterion of Evanno et al. (2005).

Circulation data and Lagrangian simulation design

Lagrangian simulations were performed using daily mean circulation fields produced by the Adriatic Forecasting System (AFS, http://gnoo.bo.ingv.it/afs). Current velocity, water temperature and salinity fields produced by the AFS are based on the AREG model (Adriatic Regional Model; Oddo et al. 2005; 2006), an implementation of the Princeton Ocean Model for the Adriatic Sea nested into the general circulation model of the Mediterranean Sea. The AREG model domain encompasses the whole Adriatic basin and extends south of the Otranto Channel into the Northern Ionian Sea. The model grid has a horizontal resolution of 1/45° (about 2.2 km) and a vertical resolution of 31 layers of variable depth (sigma layers) following the sea bottom.

In order to assess potential dispersal patterns in the study area, particles were released at three out of the five sampling locations: the TGMPA (Punta Penna Grossa) and the two most extreme locations, the northernmost location (Torre a Mare) and the southernmost location (San Foca). Simulations were started at four dates (9 May and 15 May 2009; 19 May and 25 May 2010), encompassing the spawning period reconstructed on the basis of the settlement peaks for 2009 and 2010 following Di Franco et al. (2012). In each simulation, a total of 100 particles, each corresponding to a single larva, were released according to a Gaussian distribution (with mean corresponding to the coordinates of the location and variance set to encompass 99% of the larvae within a radius of 5 km). Particles were tracked for 17 days, which is the average pelagic larval duration (PLD) estimated from otolith data (Di Franco et al. 2011). Each simulation was conducted at two different fixed depths (1 and 10 m) in order to cover the range in which larvae of white sea bream are more frequently located in the water column (Olivar and Sabatés 1997). The total number of simulations was 24 (3 locations x 4 dates x 2 depths).

Larval trajectories were stepped forward using an explicit 4th order Runge-Kutta integration procedure with a 6-minute time step. At each step t, the horizontal components of the velocity field $v_x(p,t)$, $v_y(p,t)$ at the current position (p_x, p_y, p_z) of each particle p were calculated by means of a quadri-linear interpolation in time (between two daily average circulation datasets) and space (among the surrounding nodes of the AREG grid). For each of the 24 simulations, larval retention and spill-over were calculated as the percentage of larvae with final position located within and outside the 5 km-radius-release area after 17 days, respectively. Note that, like for other regional circulation models, the horizontal resolution of the AREG model does not allow a precise simulation of hydrodynamic processes very close to the coast, so that near-shore currents should be considered less definite.

Results

Genetic diversity

Similar values were observed for all diversity indices in all samples (Table 2.1). All comparisons across 2009 and 2010 settlers using one-way ANOVA were statistically not significant ($p > 0.05$). Also, no differences were found when re-examining the data by comparing pooled 2009 settlers (Ho= 0.660±0.308; He= 0.707±0.318), pooled 2010 settlers (Ho= 0.631±0.288; He= 0.689±0.317) and adults (Ho= 0.687±0.325; He= 0.696±0.307), with all differences being statistically not significant ($p > 0.05$).

Following Bonferroni correction, only 3 out of 56 tests departed significantly from HWE (locus Ad05 at Torre a Mare-2009 and TGMPA-2010 and locus Ad26 at Torre Pozzella-2010). The software MICRO-CHECKER showed no evidence for scoring errors due to stuttering or large allele dropout. No linkage disequilibrium was observed between any pair of loci after Bonferroni correction. Simulations using our empirical microsatellite data in POWSIM, taking into account the sample size of each population, and a wide range of predefined F_{ST} values showed that our markers have enough statistical power to detect F_{ST} values ranging from 0.001 to 0.1 (p= 1.000).

Genetic differentiation among settlers

When investigating the genetic structure among samples of settlers, all pairwise F_{ST} comparisons were not significant ($p > 0.05$), with an average pairwise F_{ST} value of 0.0077. A higher genetic similarity was found among 2009 samples (F_{ST}= 0.0016) than among 2010 samples (F_{ST}= 0.0081).

Comparison of allele frequencies among 2009 samples showed no significant differences at any locus or across all loci (p= 0.202). When comparing 2010 samples, significant differences were found at locus CId11, due to a higher frequency of allele *200 (0.26) at Torre Pozzella in comparison with the rest of samples (0.02-0.12), but not at the rest of loci or across all loci (p= 0.088).

Hierarchical AMOVA was first conducted separately for the 2009 and 2010 samples testing different geographic groupings. Genetic variance did not partition significantly among groups when considering three geographic areas, (1) TGMPA, (2) North (Torre Pozzella and Torre a Mare) and (3) South (Punta Penne and San Foca) for neither the 2009 (FCT= 0.00067; p= 0.455) nor the 2010 samples (FCT= 0.00049; p= 0.859). Similarly, genetic differentiation did not partition significantly when the three geographic groupings considered were (1) TGMPA plus adjacent areas (TGMPA, Torre Pozzella and Punta Penne), (2) North (Torre a Mare) and (3) South (San Foca), FCT= 0.00022 (p= 0.491) for 2009 and FCT= 0.00046 (p= 0.782) for 2010. When including all 2009 and 2010 samples in the AMOVA, genetic variance did not partition significantly among temporal samples (2009 vs. 2010; FCT= 0.00023; p= 0.500). In accordance with the AMOVA results, an MDS plotting the first and second coordinates obtained from pairwise genetic distances showed all samples mixed together (Figure 2.2a), fitting no apparent geographical or temporal pattern as samples did not cluster according to location or sampling year.

A Mantel test showed no correlation between genetic and waterway distances (2009: r= 0.449; p= 0.199/2010: r= 0.262; p= 0.463), which suggests no Isolation-by-Distance (IBD) pattern. No correlation was found between genetic and temporal distance (r= 0.158; p= 0.301) when considering all 2009 and 2010 samples, which suggests no Isolation-by-Time (IBT) pattern.

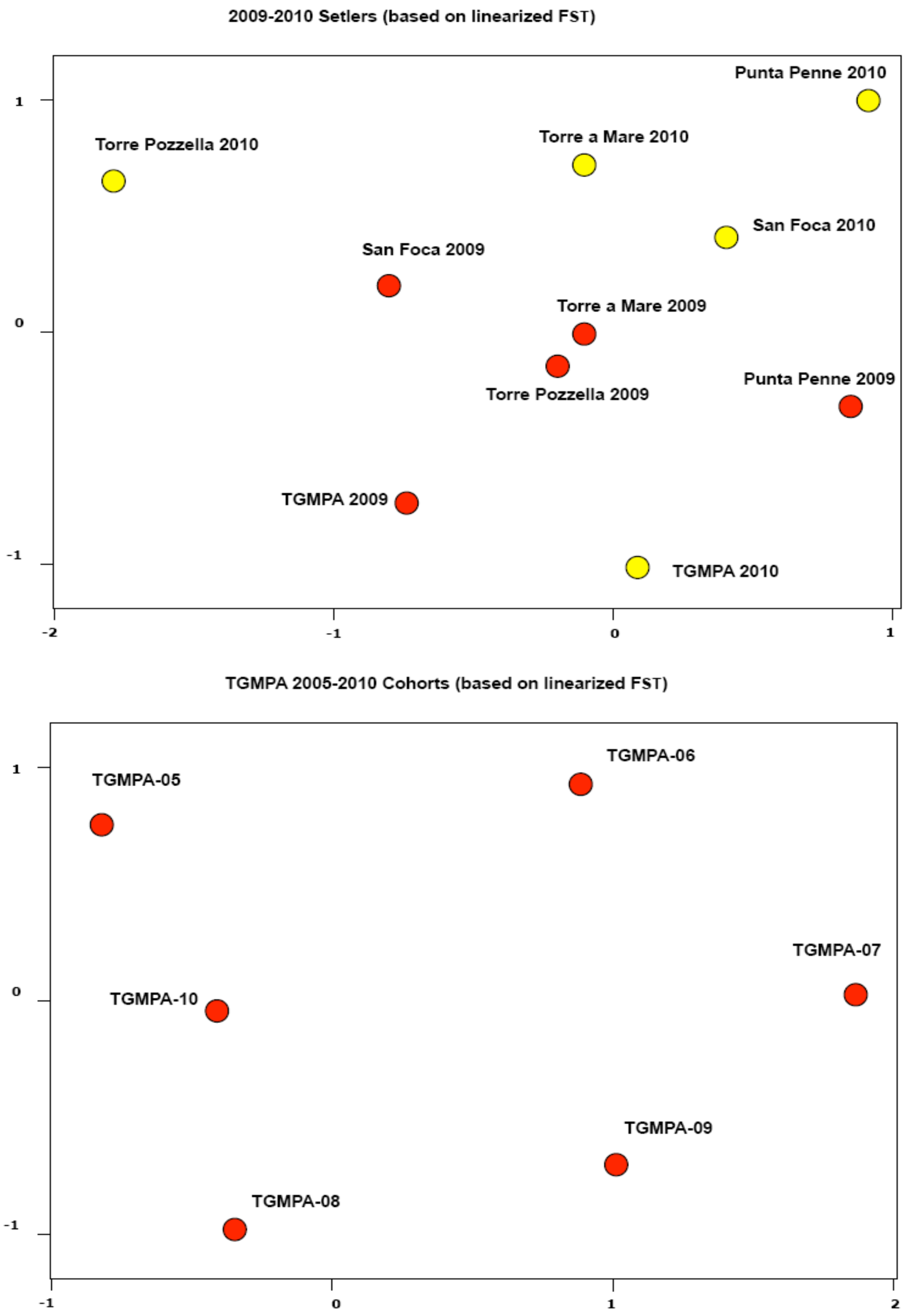

2009-2010 Setlers (based on linearized FST)

TGMPA 2005-2010 Cohorts (based on linearized FST)

Figure 2.2 - Plots from Multi-Dimensional Scaling analysis based on linearized genetic distance considering (a) all 2009 and 2010 settlers (labelled as in Table 1) and (b) all cohorts within the TGMPA (2004-2010).

Finally, the software STRUCTURE inferred one single population as the most likely for both 2009 samples (K=1: log-likelihood= -6871.2) and 2010 samples (K=1: log- likelihood= -4421.3).

Genetic differentiation between settlers and adults

Genetic structure was further explored by comparing the genetic composition of settlers and adults collected within the TGMPA. No differences in allelic frequencies were found when considering all samples separately (p= 0.087) or when comparing pooled settlers vs. adults (p= 0.078). Pairwise F_{ST} values were all non-significant ($p > 0.05$).

In order to test IBT over a longer time scale than the 2-year period tested with settlers (2009 and 2010), adults were split according to year-class into 4 cohorts (2005-2008). A Mantel test showed no correlation between genetic and temporal distance (2005-2008: r= 0.078; p= 0.833). Similarly, when adding to the analysis the two samples of settlers obtained in the TGMPA corresponding to the 2009 and 2010 cohorts, no IBT pattern was observed (2005-2010: r= 0.097; p= 0.731). Accordingly, an MDS considering all cohorts showed no clustering of samples following a temporal pattern (Figure 2.2b).

Lagrangian simulations

The 24 simulations obtained agree in showing a high larval dispersal. Simulations at depth 10 m were consistent and showed travel distances ranging from 0 to 300 km (Figure 2.3). Simulations at depth 1 m were more variable and the maximum distance travelled varied from 20 to over 300 km (Figure 2.4). While travel distances varied depending on starting date and depth, a general trend was observed in which particles flowed from north to south, transported by the Western Adriatic Coastal Current. None of the simulations suggested movement of particles from south to north. The general pattern observed was temporally stable and no major discrepancies were observed when comparing the 2009 and 2010.

Table 2.2 summarizes the percentage of larval retention and spill-over at each location. Simulations started at the TGMPA showed that some larvae stay within the TGMPA but there is also export outside the boundaries of the TGMPA to the locations situated south of the TGMPA, with some larvae surpassing the strait of Otranto and entering the Ionian Sea. Considering the 8 simulations carried out for the TGMPA (4 dates and 2 depths), on average 12.75% of the larvae produced within the TGMPA recruited inside the TGMPA boundaries. Simulations started at the northernmost location (Torre a Mare) showed that propagules can disperse all throughout the study area, including not only the northern locations but also the TGMPA and southern locations. Larval retention at Torre a Mare was virtually zero and >99% of the larvae were transported downstream. Simulations started at the southernmost location (San Foca) showed that particles in part stay locally and in part enter the Ionian Sea, flowing into the Gulf of Taranto. Larval retention was highly variable depending on both date and simulation depth, with an average larval retention of 21.3% considering the 8 simulations conducted at San Foca. No eastward dispersal toward the Balkan Peninsula or East Mediterranean was observed at any simulation.

	Torre a Mare				**TGMPA**				**San Foca**			
	1m		**10m**		**1m**		**10m**		**1m**		**10m**	
Date	**IN**	**OUT**	**IN**	**OUT**	**IN**	**OUT**	**IN**	**OUT**	**IN**	**OUT**	**IN**	**OUT**
9/5/ 2009	0	100	0	100	9	91	0	100	19	81	0	1
15/5/2009	0	100	1	99	43	57	1	99	100	0	6	94
19/5/2010	0	100	0	100	40	60	0	100	11	89	13	87
25/5/2010	0	100	1	99	8	92	1	99	10	90	12	88
Mean	0	100	0.5	99.5	25	75	0.5	99.5	35	65	8	92
SD	0	0	0.6	0.6	19.1	19.1	0.6	0.6	43.5	43.5	6	6

Table 2.2 - Percentage of larval retention and spill-over at each location (Torre a Mare, TGMPA and San Foca) estimated from Lagrangian simulations started at four dates (9 and 15 May 2009; 19 and 25 May 2010) and two simulation depths (1m and 10 m). Larvae with final position located within the 5 km-radius-release area after 17 days are considered to recruit locally (IN). Larval spill-over considers those larvae with final position outside the release area (OUT). SD= std dev.

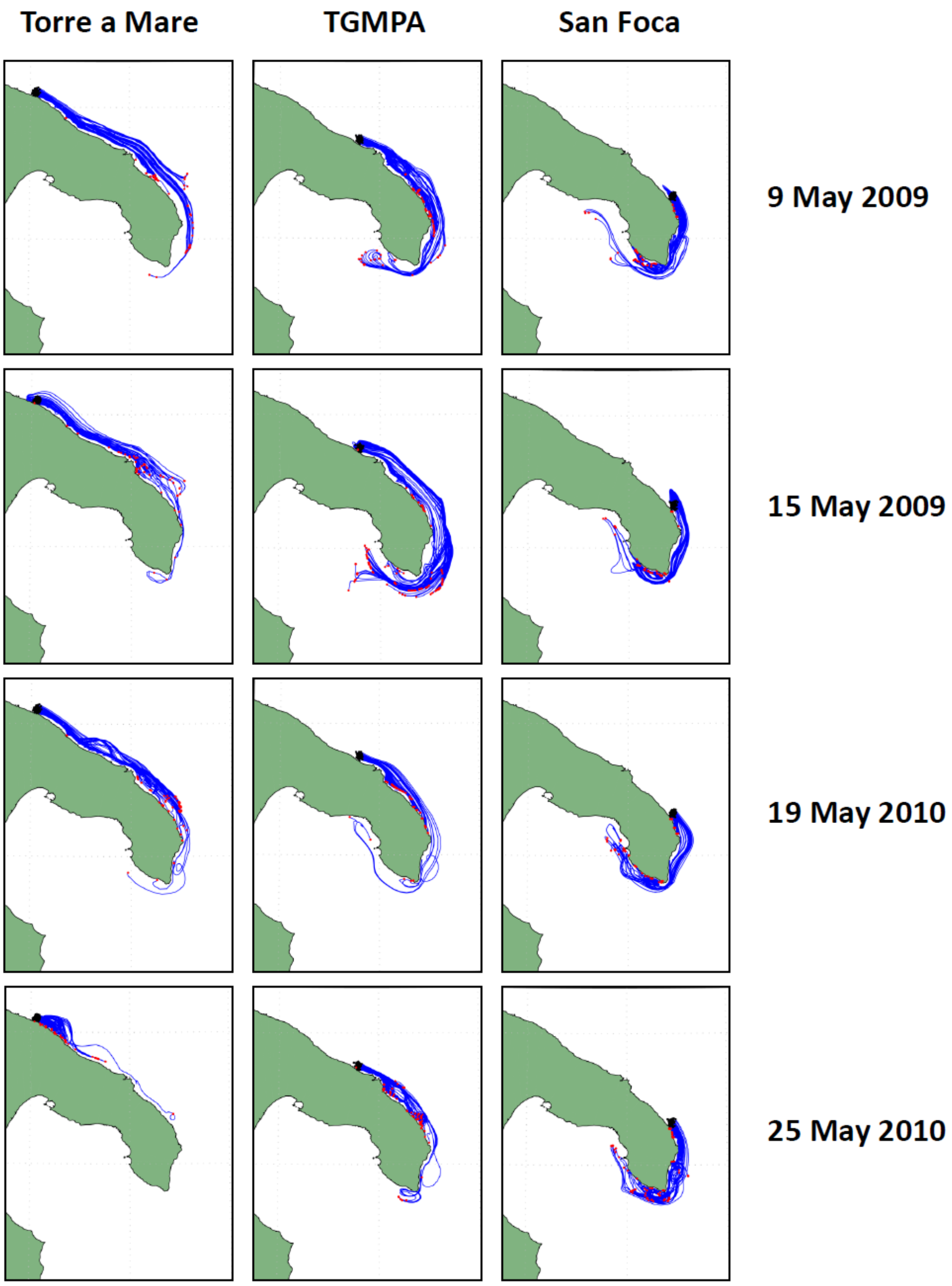

Figure 2.3 - Lagrangian simulations at 10 m simulation depth released at Torre a Mare, TGMPA and San Foca on (a) 9 May 2009, (b) 15 May 2009, (c) 19 May 2010 and (d) 25 May 2010. Black and red dots indicate the release point and final position of each larval trajectory after 17 days.

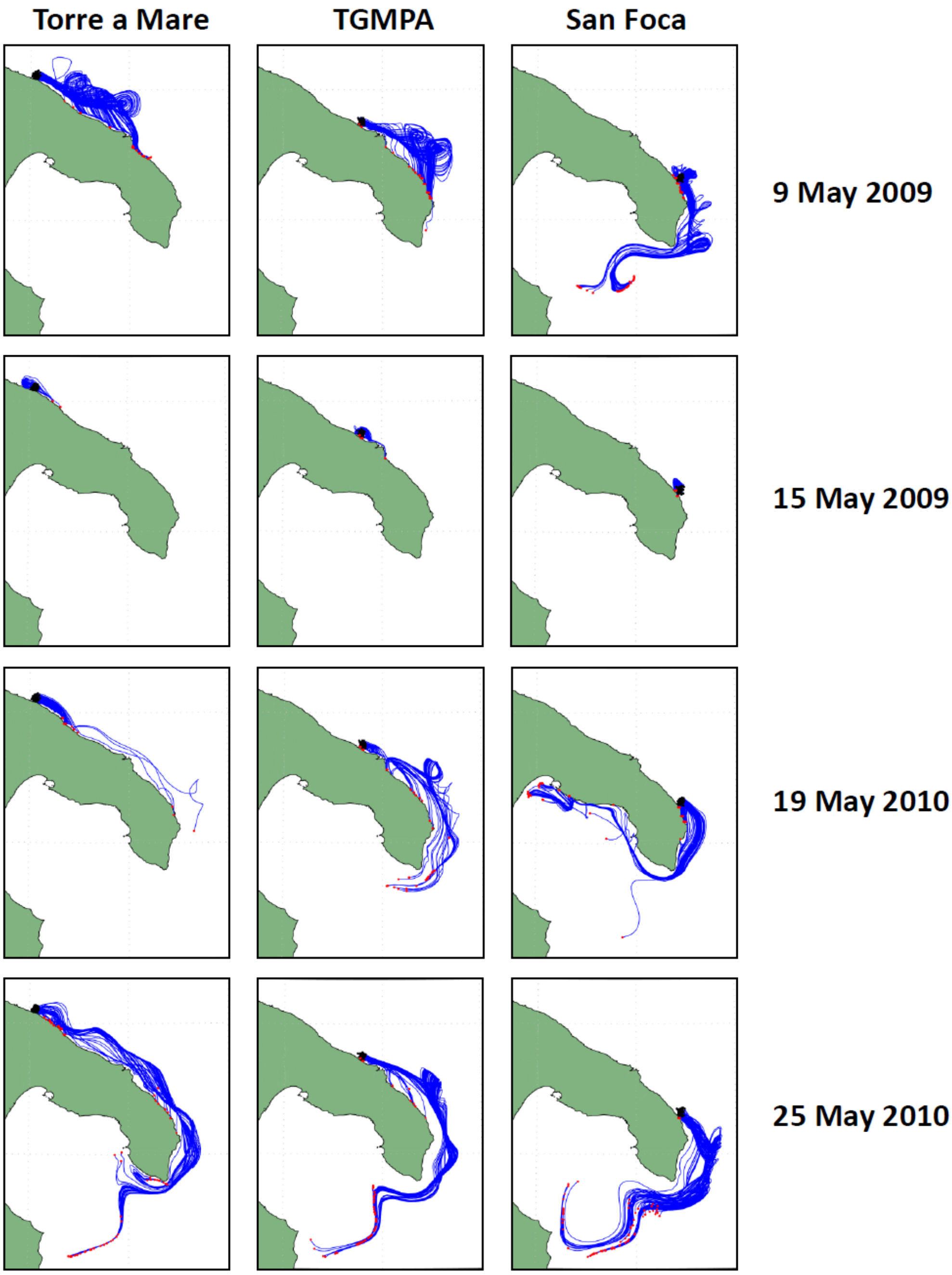

Figure 2.4 - Lagrangian simulations at 1 m simulation depth released at Torre a Mare, TGMPA and San Foca on (a) 9 May 2009, (b) 15 May 2009, (c) 19 May 2010 and (d) 25 May 2010. Black and red dots indicate the release point and final position of each larval trajectory after 17 days.

Discussion

Spatio-temporal stable genetic structure

Quantification of spatio-temporal genetic variation in white sea bream *Diplodus sargus sargus* sampled along 200 km of the southern Apulian Adriatic revealed no inter-location genetic heterogeneity. The high similarity found in genetic diversity and genetic composition suggests the existence of a single white sea bream population in the study area. The lack of genetic sub-structuring was consistent over time, with the same pattern observed in the temporally replicated samples from 2009 and 2010. Furthermore, no differences were found when comparing settlers and adults or Isolation-by-Time (IBT) pattern detected across all cohorts considered (2005-2010). Collectively, these results point out the temporal stability of the pattern of genetic homogeneity found.

Other population genetic studies on white sea bream have revealed different patterns of sub-structuring in populations of the Mediterranean Sea. Limited geographic differentiation was found among populations separated by several hundred kilometres (e.g., Gulf of Lyon - Ligurian Sea; Lenfant and Planes 1996) although larger differences were observed between Murcia and Gulf of Lyon (González-Wangüemert et al. 2004). Similarly, a recent study on genetic connectivity of white seam bream along the Sicilian coast showed genetic differences between locations situated 70 km apart but no differences between populations >200 km apart (González-Wangüemert et al. 2012). A similar lack of spatial differentiation was found between Mediterranean and Atlantic populations (Bargelloni et al. 2005), although recent studies have reported a genetically differentiated population in Azores (González-Wangüemert et al. 2010, 2011). This limited level of geographic sub-structuring contrasts with temporal studies showing significant differences within a single population among cohorts. In a *D. sargus* population of Banyuls-sur-Mer (West Mediterranean), Lenfant and Planes (2002) reported significant divergences at 17 allozyme loci between cohorts over a long time scale (up to 10 years) despite very low F_{ST} values. González-Wangüemert et al. (2007) observed significant genetic heterogeneity among year-classes in two out of five populations from the Spanish Mediterranean coast analysed for temporal changes, Guardamar (F_{ST}= 0.012) and Cape of Palos (F_{ST}= 0.008).

Lenfant and Planes (2002) attributed the pattern of temporal genetic variation found to a large variance in reproductive success of parents. Hedgecock (1994) proposed that in marine species with external fertilization random events determine the successful adults in each spawning event, in which many individuals fail to contribute to recruitment and the progeny of a small fraction of individuals replaces the entire population. This results in a reduction of the effective population size of cohorts and in consequent changes in allele frequencies over time due to random genetic drift, leading to temporal variation in the genetic composition of recruits (Hedgecock 1994; David et al. 1997; Pujolar et al. 2006, 2011). The observation in our study of a temporally stable genetic structure over a long time scale is suggestive of an effective population size large enough to withstand the effects of genetic drift. The homogeneity found suggests little influence of cohort size, as cohorts with reduced size could produce temporal differences between cohorts that were not observed in our study.

High connectivity between the TGMPA and neighboring areas

Population genetics and modelling outputs agree in indicating a high degree of connectivity between the TGMPA and neighbouring northern and southern areas up to 100 km away from the TGMPA.

The existence of transport in and out of the TGMPA is suggested by genetic patterns in terms of overall genetic homogeneity within the studied area. Comparison of samples obtained inside and outside of the TGMPA showed no differences in genetic diversity or genetic composition, which indicates that the TGMPA is not isolated and that there is genetic connectivity among locations. If the TGMPA were entirely closed, genetic differences would be expected to arise, which disagrees with the homogeneity found in our study. The results of Lagrangian simulations further confirm the existence of transport outside of the TGMPA boundaries. Simulated trajectories showed that larvae originating in the TGMPA could either remain within the TGMPA boundaries or travel southwards. Depending on the depth at which particles dispersed, larvae could travel up to 300 km. At both simulation depths (1m and 10m), larvae could reach the southernmost point in our study (San Foca), at about 100 km from the TGMPA. This is in agreement with the recent study of Di Franco et al. (2012), conducted in the same area and spatial scale of our study, which showed on the basis of otolith microchemistry that larval dispersal occurred at least up to the scale examined of 100-200 km.

As for the locations south of the TGMPA, further indication of connectivity comes from census data carried out during summer 2009 (Di Franco et al. submitted). Visual census experiments showed high densities of both adults and settlers within the TGMPA, while southern locations showed similar high densities of settlers but low densities of adults. The suggested spatial decoupling of adults/settlers densities within the TGMPA and at locations south of the TGMPA could indicate that most settlers found at southern locations are not local but the progeny of adults reproducing within the TGMPA and exported southwards by the currents. This scenario, in which the TGMPA contributes to effectively replenishing down-current locations, is consistent with the simulated movement of particles and the homogeneity found at the genetic level.

While the dispersal pattern generated by the Lagrangian simulations could explain the genetic homogeneity observed between the TGMPA and southern locations (Punta Penne and San Foca), the similarity between the TGMPA and northern locations (Torre a Mare and Torre Pozzella) cannot be explained by larval dispersal under the simulated oceanographic regime. Simulated trajectories did not suggest larval export from the TGMPA to the north, since all particles released from the TGMPA either stayed within the protected are or moved southward but no northward particle flow was evident. This seems to suggest gene flow from northern locations toward the TGMPA, which is consistent with the general north-south flow of currents in the region and with simulated trajectories showing that particles released at Torre a Mare are all virtually exported downstream (<1% larval retention). Importantly, simulations also show that larvae released at Torre a Mare can actually reach the TGMPA. Despite the temporal stability of the simulated trajectories in 2009 and 2010, further simulations should be conducted to confirm the observed pattern and to rule out near-shore currents or rare meteorological events that could result in a northbound movement of particles.

Alternatively, the high genetic connectivity between the TGMPA and neighbouring areas could be explained by exchange of juveniles and adults. However, otolith microchemistry analysis showed that, while larvae could travel distances over 200 km, movements of juveniles were more restricted and occurred within a scale of about 30 km (Di Franco et al. 2012). On average, approximately 50% of juveniles did not disperse, 35% recruited to locations 20 km away, and the remaining 15% moved up to

30 km between settlement and recruitment. While this could explain the genetic homogeneity observed between the TGMPA and the nearby locations of Torre Pozzella (20 km north of the TGMPA) and Punta Penne (10 km south of the TGMPA), it seems unlikely that movements of juveniles and adults could explain the similarity between the TGMPA and the northernmost (Torre a Mare) and southernmost (San Foca) locations at about 100 km from the TGMPA. Nevertheless, in a recent tagging-recapture experiment conducted in the south coast of Portugal, two *D. sargus* individuals tagged with acoustic tags were recovered at 12 km and 90 km from the tagging site (Abecasis et al. 2009), suggesting that juveniles moving from nursery to adult habitats can cover quite large distances.

Effectiveness of the TGMPA

In the case of marine species with a dispersive larval stage, like the white sea bream, MPAs can be effective in protecting the target species if they are designed so that to guarantee a significant level of self-recruitment and/or connectivity among MPAs at the spatial scales within MPA networks. In this sense, Lagrangian simulations show that the particles released from the TGMPA in part stay within the TGMPA (on average 12.75%), which suggests that some of the larvae produced in the TGMPA recruit inside the TGMPA boundaries. This is in agreement with the long-term positive "reserve effect" of Torre Guaceto observed at population and community levels (Guidetti 2006; Guidetti et al. 2008), with higher densities of many fish species, including white sea bream, in the TGMPA compared with the surrounding areas.

The benefits of MPAs can also extend beyond their boundaries, and in addition to protecting biodiversity inside the MPA (reviewed in Lester et al. 2009), MPAs can supply local fisheries through spill-over of juveniles and adults into neighbouring fishing grounds (Bohnsack 1998; McClanahan and Mangi 2000; Roberts et al. 2001; Russ et al. 2004). Moreover, MPAs can supplement recruitment of nearby fisheries in outside areas by exporting eggs and larvae produced in the MPA (Stoner and Ray 1996; Roberts 1997; Beukers-Stewart et al. 2005; Cudney-Bueno et al. 2009; Pelc et al. 2009). In our case study of the white sea bream in the TGMPA, the high connectivity suggested by the overall genetic homogeneity, together with the simulated patterns of larval export, point to a positive effect that goes well beyond the limits of the TGMPA. In particular, our data suggest that the TGMPA can supply local fisheries south of the TGMPA, which is corroborated by the concurrent observation of high larval densities but low adult densities in census experiments (Di Franco et al. submitted).

The positive effect of enforcement at Torre Guaceto could extend well beyond our study area and outside the Adriatic Sea, as suggested by Lagrangian simulations showing larval export toward the Ionian Sea. The lack of barriers to gene flow between South Adriatic - Ionian Sea has been demonstrated in many marine species including the sand smelt *Atherina boyeri* (Congiu et al. 2002), the European sprat *Sprattus sprattus* (Debes et al. 2008), the sea urchin *Paracentrotus lividus* (Maltagliati et al. 2010) and the green crab *Carcinus aestuarii* (Marino et al. 2011). Importantly, Lagrangian simulations show that the TGMPA could potentially export larvae to its closest MPA southward, Porto Cesareo in the Gulf of Taranto (North Ionian Sea), despite a separation of about 250 km. This holds true for the simulated trajectories released from the TGMPA, and especially for those released from the San Foca area south of the TGMPA. This aspect is particularly interesting taking into account that a new MPA has been recently proposed in the area of Tricase-Otranto, 50 km south of San Foca. A new MPA in this area could serve as stepping-stone between the Torre Guaceto and Porto Cesareo MPAs, enhancing the potential connectivity between basins suggested by Lagrangian simulations, and ultimately resulting in the implementation of an effective network of MPAs with the potential to meet both conservation and fisheries needs.

Although the benefits of MPAs can be context-dependent (e.g. benefits can be markedly localized depending on the direction of the larval dispersal and enhance only locations down-current of marine protected areas), collectively our findings highlight the potential benefits of protecting fish populations within MPAs and show that a recruitment enhancement can be manifested in neighbouring or relatively distant geographic areas, including non-protected fishing areas and potentially other MPAs.

References

Abecassis D, Bentes L & Erziki K (2009). Home range, residency and movements of *Diplodus sargus* and *Diplodus vulgaris* in a coastal lagoon: connectivity between nursery and adult habitats. *Estuarine, Coastal and Shelf Science* **85**:525-529.

Babbucci M, Buccoli S, Cau A, Cannas R, Goni R, Diaz D, Marcato S, Zane L & Patarnello T (2010). Population structure, demographic history, and selective processes: Contrasting evidences from mitochondrial and nuclear markers in the European spiny lobster *Palinurus elephas*. *Molecular Phylogenetics and Evolution* **56**:1040-1050.

Bargelloni L, Alarcon JA, Alvarez MC, Penzo E, Magoulas A, Palma J & Patarnello T (2005). The Atlantic-Mediterranean transition: discordant genetic patterns in two seabream species, *Diplodus puntazzo* and *Diplodus sargus*. *Molecular Phylogenetics and Evolution* **36**:523-535.

Belkhir K, Borsa P, Goudet J & Bonhomme F (2005). GENETIX 4.05: Logiciel sous Windows pour la genetique des populations. Laboratoire Genome and Population, CNRS-UPR, Universite de Montpellier II, Montpellier.

Behrens Yamada S & Hauck L (2001). Field identification of the European green crab species: Carcinus maenas and Carcinus aestuarii. J. Shellfish Res **20**:905-912.

Bernardi G, Findley L & Rocha-Olivares A (2003). Vicariance and dispersal across Baja California in disjunct marine fish populations. *Evolution* **57**:1599-1609.

Beukers-Stewart BD, Vause BJ, Mosley MWJ, Rossetti HL & Brand AR (2005). Benefits of closed area protection for a population of scallops. *Marine Ecology Progress Series* **298**:189-204.

Bohnsack JA (1998). Application of marine reserves to reef fisheries management. *Australian Journal of Ecology* **23**:298-304.

Claudet J, Osenberg CW, Benedetti-Cecchi L, Domenici P, Garcia-Charton JA, Pérez-Ruzafa A, Badalamenti F, et al. (2008). Marine reserves: size and age do matter. *Ecology Letters* **11**:481-489.

Congiu L, Rossi R & Colombo G (2002). Population analysis of the sand smelt *Atherina boyeri* from Italian coastal lagoons by random amplified polymorphic DNA. *Marine Ecology Progress Series* **229**:279-289.

Cudney-Bueno R, Lavin MF, Marinone S, Raimondi PT & Shaw WW (2009).

Rapid effects of marine reserves via larval dispersal. *PLoS One* **4**:e4140.

David P, Perdie MA, Pernot AF & Jarne P (1997). Fine grained spatial and temporal population genetic structure in the marine bivalve *Spisula ovalis*. *Evolution* **51**:1318–1322.

Deves PV, Zachos FE & Hanel R (2008). Mitochondrial phylogeography of the European sprat *Sprattus sprattus* reveals isolated climatically vulnerable populations in the Mediterranean Sea and range expansion in the northeast Atlantic. *Molecular Ecology* **17**:3873-3888.

Di Franco A & Guidetti P (2011). Patterns of variability of early-life traits of fishes depend on spatial scale of analysis. *Biology Letters* **7**:454-456.

Di Franco A, De Benedetto G., De Rinaldis G, Raventos N, Sahyoun R & Guidetti P (2011). Large scale variability in otolith microstructure and microchemistry: the case study of *Diplodus sargus sargus* in the Mediterranean Sea. *Italian Journal of Zoology* **78**:182-192.

Di Franco A, Gillanders BM, De Benedetto G, Pennetta A, De Leo GA, & Guidetti P (2012). Dispersal patterns of coastal fish: implications for designing networks of marine protected areas*. PLoS One* **7**:e31681.

Doherty P, Planes S & Mather P (1995). Gene flow and larval duration in seven species of fish from the Great Barrier Reef. *Ecology* **76**:2373-2391.

Edgar GJ 2011. Does the global network of marine protected areas provide an adequate safety net for marine biodiversity? *Aquatic Conservation Marine and Freshwater Ecosystems* **21**:313-316.

Evanno G, Regnaut S & Goudet J (2005). Detecting the number of clusters of individuals using the software STRUCTURE: a simulation study. *Molecular Ecology* **14**:2611-2620.

Excoffier L, Laval G & Schneider S (2005). Arlequin ver. 3.0: An integrated software package for population genetics data analysis. *Evolutionary Bioinformatics Online* **1**:47-50.

Franch R, Louro B, Tsalavuota M, Chatzipilis D, Tsigenopoulos CS, Sarropoulou E, Antonello J, et al. (2006). A genetic linkage map of the hermaphrodite teleost fish *Sparus aurata*. *Genetics* **174**:851-861.

Galarza JA, Carreras-Carbonell J, McPherson E, Pascual M, Roques S, Turner GF & Rico C (2009). The influence of oceanographic fronts and early-life-history traits on connectivity among littoral fish species. *Proceedings of the National Academy of Sciences of the USA* **106**:1473-1478.

González-Wangüemert M, Pérez-Ruzafa A, Cánovas F, Marcos C & García-Charton JA (2004). Genetic differentiation of *Diplodus sargus* populations in Southwest Mediterranean. *Biological Journal of the Linnean Society* **82**:249-261.

González-Wangüemert M, Pérez-Ruzafa A, Cánovas F, García-Charton JA & Marcos C (2007). Temporal genetic variation in populations of *Diplodus sargus* from the SW Mediterranean Sea. *Marine Ecology Progress Series* **334**:237-244.

González-Wangüemert M, Cánovas F, Pérez-Ruzafa A, Marcos C & Alexandrino P (2010). Connectivity patterns inferred from the genetic structure of white seabream (*Diplodus sargus*). *Journal of Experimental Marine Biology and Ecology* **383**:23-31.

González-Wangüemert M, Froufe E, Pérez-Ruzafa A & Alexandrino P (2011). Phylogeographical history of the white seabream *Diplodus sargus*: implications for insularity. *Marine Biology Research* **7**:250-260

González-Wangüemert M, Fernández TV, Pérez-Ruzafa A, Giacalone M, D'Anna G & Badalamenti F (2012). Genetic considerations on the introduction of farmed fish in marine protected areas: the case of study of white seabream restocking in the Gulf of Castellammare (Southern Tyrrhenian Sea). *Journal of Sea Research* **68**:41-48.

Goudet J (2002). FSTAT, a program to estimate and test gene diversities and fixation indices. Available from: http://www2.unil.ch/opgen/softwares/fstat.htm.

Guidetti P (2006). Marine reserves re-establish lost predatory interactions and cause community-wide changes in rocky reefs. *Ecological Applications* **16**:963–976.

Guidetti P (2007). Potential of marine reserves to cause community-wide changes beyond their boundaries. *Conservation Biology* **21**:540-545.

Guidetti P & Sala E (2007). Community-wide effects of marine reserves in the Mediterranean Sea. Marine Ecology Progress Series 335:43-56.

Guidetti P, Milazzo M, Bussotti S, Molinari A, Mureno M, Pais A, Spanò N, et al. (2008). Italian marine reserve effectiveness: does enforcement matter? *Biological Conservation* **141**:699–709.

Halpern BS & Warner RR (2002). Marine reserves have rapid and lasting effects. *Ecology Letters* **5**:361-366.

Harmelin-Vivien ML, Harmelin JG & Leboulleux V (1995). Microhabitat requirements for settlement of juvenile sparid fishes on Mediterranean rocky fishes. *Hydrobiologia* **300**-301:309-320.

Hedgecock D (1994). Does variance in reproductive success limit effective population sizes of marine organisms? In A. Beaumont, ed. Genetics and Evolution of Aquatic Organisms. Chapman and Hall, London.

Hilborn R (2004). When can marine reserves improve fisheries management? *Ocean and Coastal Management* **47**:197-205.

Knutsen H, Jorde PE, André C & Stenseth NC (2003). Fine-scaled geographical population structuring in a highly mobile marine species: the Atlantic cod. *Molecular Ecology* **12**:385-394.

Lenfant P & Planes S (1996). Genetic differentiation of white sea bream within the Gulf of Lyon and the Ligurian Sea (Mediterranean Sea). *Journal of Fish Biology* **49**:613-621.

Lenfant P & Planes S (2002). Temporal genetic changes between cohorts in a natural population of a marine fish, *Diplodus sargus*. *Biological Journal of the Linnean Society* **76**:9-20.

Lester SE, Halpern BS, Grorud-Colvert K, Lubchenco J, Ruttenberg BI, Gaines SD, Airamé S & Warner RR (2009). Biological effects within no-take marine reserves: a global synthesis. *Marine Ecology Progress Series* **384**:33-46.

Lubchenco J, Palumbi SR, Gaines SD & Adelman S (2003). Plugging a hole in the ocean: the emerging science of marine reserves. *Ecological Applications* **13**:S3-S7.

McClanahan TR & Mangi S (2000). Spill-over of exploitable fishes from a marine park and its effect on the adjacent fishery. *Ecological Applications* **10**:1792-1805.

Maltagliati F, Di Giuseppe G, Barbieri M, Castelli A & Dini F (2010). Phylogeography and genetic structure of the edible sea urchin *Paracentrotus lividus* inferred from the mitochondrial cytochrome b gene. *Biological Journal of the Linnean Society* **100**:910-923.

Marino IAM, Pujolar JM & Zane L (2011). Reconciling deep calibration and demographic history: Bayesian inference of post glacial colonization patterns in *Carcinus aestuarii* and *C. maenas*. *PLoS One* **6**:e28567.

Massault C, Franch R, De Koning DJ, Bovenhuis H, Pellizzari C, Patarnello T & Bargelloni L (2010). Quantitative trait loci for resistance to fish pasteurellosis in gilthead sea bream *Sparus aurata*. *Animal Genetics* **41**:191-203.

Molloy PP, McLean IB & Coté IM (2009). Effects of marine reserve age on fish populations: a global meta-analysis. *Journal of Applied Ecology* **46**:743-751.

Oddo P, Pinardi N & Zavatarelli M (2005). A numerical study of the interannual variability of the Adriatic Sea (2000-2002). *Science of the Total Environment* **353**:39-56.

Oddo P, Pinardi N, Zavatarelli M & Colucelli A (2006). The Adriatic Basin forecasting system. *Acta Adriatica* **47**:169-184.

Olivar MP & Sabatés A (1997). Vertical distribution of fish larvae in the north-west Mediterranean Sea in spring. *Marine Biology* **129**:289-300.

Palero F, Abello P, McPherson E, Gristina M & Pascual M (2008). Phylogeography of the European spiny lobster (*Palinurus elephas*): influence of current oceanographical features and historical processes. *Molecular Phylogenetics and Evolution* **48**:708-717.

Palumbi SR (2003). Population genetics, demographic connectivity & the design of marine reserves. *Ecological Applications* **13**:S146-S158.

Palumbi SR, Sandifer PA, Allan JD, Beck MW, Fautin DG, Fogarty MJ, Halpern BS, et al. (2009). Managing for ocean biodiversity to sustain marine ecosystem services*. Frontiers in Ecology and Environment* **7**:204-211.

Panfili J, de Pontual H, Troadec JP & Wright PJ (2002). Manual of Fish Sclerochronology. IFREMER/IRD, Brest.

Pelc RA, Baskett ML, Tanci T, Gaines SD & Warner RR (2009). Quantifying larval export from South African marine reserves. *Marine Ecology Progress Series* **394**:65-78.

Pritchard JK, Stephens M & Donelly P (2000). Inference of population structure using multilocus genotype data. *Genetics* **155**:945-959.

Pujolar JM, Maes GE & Volckaert FAM (2006). Genetic patchiness among recruits in the European eel, *Anguilla anguilla*. *Marine Ecology Progress Series* **307**:209-217.

Pujolar JM, Bevacqua D, Andrello M, Capoccioni F, Ciccotti E, De Leo GA & Zane L (2011). Genetic patchiness in European eel adults as evidenced by molecular genetics and population dynamics modelling. *Molecular Phylogenetics and Evolution* **58**:198-206.

Purcell J, Cowen R, Hughes C & Williams D (2006). Weak genetic structure indicates strong dispersal limits. A tale of two coral reef fish. *Proceedings of the Royal Society of London Series B* **273**:1483-1490.

Raymond M & Rousset F (1995). GENEPOP: a population genetics software for exact tests and ecumenicism. *Journal of Heredity* **86**:248-249.

Rice WR (1989). Analyzing tables and statistical tests. *Evolution* **43**:223-

225.

Riginos C & Victor BC (2001). Larval spatial distributions and other early life-history characteristics predict genetic differentiation in eastern Pacific blennioid fishes. *Proceedings of the Royal Society of London Series B* **268**:1931-1936.

Roberts CM (1997). Connectivity and management of Caribbean coral reefs. *Science* **278**:1454-1457.

Roberts CM, Bohnsack JA, Gell F, Hawkins JP & Goodridge R (2001). Effects of marine reserves on adjacent fisheries. *Science* **294**:1920-1923.

Russ GR, Alcala AC, Maypa AP, Calumpong HP & White AT (2004). Marine reserve benefits local fisheries. *Ecological Applications* **14**:597-606.

Ryman N & Palm S (2006). POWSIM: a computer program for assessing statistical power when testing genetic differentiation. *Molecular Ecology Notes* **6**:600-602.

Sala E & Zabala M (1996). Fish predation and the structure of the sea urchin *Paracentrotus lividus* in the North West Mediterranean. *Marine Ecology Progress Series* **140**:71-81.

Sala E, Boudouresque CF & Harmelin-Vivien M (1998). Fishing trophic cascades, and the structure of algal assemblages: evaluation of an old but untested paradigm. *Oikos* **82**:425-439.

Schunter C, Carreras-Carbonell J, McPherson E, Tintoré J, Vidal-Vijande E, Pascual A, Guidetti P & Pascual M (2011). Matching genetics with oceanography: directional gene flow in a Mediterranean fish species. *Molecular Ecology* **20**:5167-5181.

Selkoe KA, Watson JR, White C, Horin TB, Iacchei M, Mitarai S, Siegel DA, Gaines SD & Toonen RJ (2010). Taking the chaos out of genetic patchiness: seascape genetics reveals ecological and oceanographic drivers of genetic patterns in three temperate reef species. *Molecular Ecology* **19**:3708-3726.

Shulman MJ & Bermingham E (1995). Early life histories, ocean currents, and the population genetics of Caribbean reef fishes. *Evolution* **49**:897-910.

Stoner AW & Ray M (1996). Queen conch, *Strombus gigas*, in fished and unfished locations of the Bahamas: Effects of a marine fishery reserve on adults, juveniles, and larval production. *Fisheries Bulletin* **94**:551-565.

Van oosterhout C, Hutchinson WF, Wills DPM & Shipley P (2004). MICRO-

CHECKER: software for identifying and correcting genotyping errors in microsatellite data. *Molecular Ecology* **4**:535-538.

Vigliola L (1998). Contrôle et régulation du recruitment des sparidae (Poissons, Téléostéens) en Méditerranée: importance des processus pré- et post-installation benthique. PhD thesis, University Aix-Marseille II.

Waples RS (1998). Separating the wheat from the chaff: patterns of genetic differentiation in high gene flow species. *Journal of Heredity* **89**:438-450.

Waples RS & Gaggiotti O (2006). What is a population? An empirical evaluation of some genetic methods for identifying the number of gene pools and their degree of connectivity. *Molecular Ecology* **15**:1419-1439.

White C, Kendall BE, Gaines S, Siegel DA & Costello C (2008). Marine reserve effects on fishery profit. *Ecological Applications* **11**:370-379.

White C, Selkoe KA, Watson J, Siegel DA, Zacherl DC & Toonen RJ (2010). Ocean current help explain population genetic structure. *Proceedings of the Royal Society of London Series B* **277**:1685-1694.

PART III

INTEGRATING FIELD DATA INTO INDIVIDUAL-BASED MODELS FOR THE MIGRATION OF EUROPEAN EEL LARVAE

Abstract

Lagrangian simulations based on coupled physical-biological models can help casting light on the mechanisms that affect fish recruitment, if the key biological and environmental drivers are accurately described. Alternative hypotheses on vital traits for which experimental measures are difficult to obtain, such as mortality and/or movement patterns, can be contrasted by comparing simulation outputs with experimental data that can be collected in the field, such as body size distribution at selected transects. We use this approach to study the oceanic migration of European eel larvae. Despite considerable research effort (involving both field surveys and simulation studies), it is still uncertain whether this is a purely passive process or the result of the interaction between transport by currents and an active larval movement. On the basis of current knowledge on the species and predictions of metabolic ecology, we propose a parameterized model providing a simple, yet biologically reasonable description of the key life history traits (body growth, mortality and movement) of eel larvae. We contrast alternative model settings and propose a method to identify the most plausible one by comparing simulation results against experimental data. The best performing scenario includes active larval propulsion proportional to body size. The corresponding migration duration is about 3 years. Our modelling study succeeds in assimilating experimental data within a conceptual framework

consistent with that sketched out, almost one century ago, by Danish biologist Johannes Schmidt.

Introduction

Investigating the mechanisms that determine the variability of fish recruitment is crucial to understand the response of fish populations to anthropogenic pressures on marine ecosystems (Gallego et al. 2007, Miller 2007, Halpern et al. 2008, Cowen & Sponaugle 2009). This is especially true for catadromous eels (genus *Anguilla*), characterized by a complex life cycle encompassing two trans-oceanic migrations. In particular, the European eel (*Anguilla anguilla*) has experienced a dramatic abundance decline in the last decades and its recruitment has decreased by about 95% from the levels recorded between 1960–1979 (Kettle et al. 2011). Consequently, the species has recently been listed in the IUCN Red List as critically endangered.

The European eel is a panmictic species reproducing in the Sargasso Sea (Andrello et al. 2011, Als et al. 2011). From this area, eel larvae (leptocephali) migrate towards Europe and North Africa. After metamorphosing into glass eels, they recruit to continental waters, where they live during their growing phase (yellow eel). After reaching sexual maturation size, adult eels undergo a second metamorphosis into silver eels and migrate back to the spawning area, where they die after reproduction (Tesch 2003). A number of factors, including changes in the oceanic environment, might have negatively affected survival and reproductive success of *A. anguilla* (Kettle et al. 2011). Sustainable management strategies for this species should therefore take into account the whole scope of its peculiar life cycle, encompassing both the continental and the oceanic environment (Bevacqua et al. 2009). Studying how the ocean circulation affects recruitment patterns is critical to (i) fill one of the main knowledge gaps about eel life history and (ii) assess the actual role of oceanic conditions in the eel decline (Bonhommeau et al. 2008).

Individual-based coupled physical-biological models provide a useful tool to investigate fish recruitment and to contrast alternative hypotheses by simulation (Miller 2007). The oceanic migration of eel leptocephali has received considerable attention in the last century but, despite considerable progress has been made towards an understanding of the biology (including physiology, ecology and behaviour) of eel larvae, many fundamental questions about their mysterious journey still remain unanswered (Righton et al. 2012). After some earlier attempts to estimate the duration of American and European eel migration on the basis of oceanic surface current data (Harden Jones 1968, Power & McCleave 1983), Kettle & Haines (2006) were first in using an ocean circulation model to simulate the migration of European eel larvae as a passive drift of particles. Then, Bonhommeau et al. (2009a, b) integrated some biological features within a physical circulation model, accounting for diel vertical migration and mortality of leptocephali. Although recent modelling studies represent a clear improvement compared with previous ones, many important biological features of the travelling particles must be incorporated to make simulations more realistic.

An accurate description of the major biological processes and their dependence upon exogenous (such as temperature or salinity) and endogenous factors (such as body size or developmental stage) is fundamental to develop reliable models (Gallego et al. 2007), as inappropriate settings may strongly affect model predictions (Fiksen et al. 2007, Bonhommeau et al. 2010). The calibration and validation of the proposed model against experimental data is recognised as an equivalently important point (Hannah 2007). Nevertheless, even if field data were gathered during several oceanic surveys conducted in the past century, and were thus available to previous researchers, none of the modelling attempts performed to date has quantitatively assessed the performances of candidate models against empirical evidence.

Here we assess the performances of different simulation scenarios in reproducing the body size distribution of European eel larvae collected at two reference transects during the early 1980s by McCleave & Kleckner (1987) and a collection of historical data from the Iberian Basin (McCleave et al. 1998). To this end, we propose an individual-based coupled physical-biological model incorporating simple, yet biologically reasonable descriptions of body growth, mortality and movement. Our aim is to contrast alternative hypotheses about the development and action of key vital traits by comparing simulation outputs against experimental data.

Materials and methods

Ocean model

We simulated the journey of European eel leptocephali as particles in the Atlantic Ocean by using the global ocean re-analysis developed by Masina et al. (2004). Monthly mean current velocity, water temperature and salinity were obtained by data assimilation via a variational optimal interpolation scheme applied to an eddy-permitting version of the Modular Ocean Model, which covers a near-global domain (78°S–78°N) between 1958–2000. Model resolution is constant in longitude and equal to 1/2°, while it varies in latitude from 1/3° between 10°S and 10°N to 1/2° at the northern boundary of the domain. Note that, although eddy-resolving, higher resolution (1/10° or finer) ocean circulation models are currently available, their use is limited to hindcast experiments (i.e. to generating circulation fields by forcing the ocean with historical atmospheric re-analyses, without assimilation of oceanic data) or to short-term forecasting applications. In contrast, the model used in this study is the result of a global ocean re-analysis, obtained by constraining the ocean circulation model through the assimilation of historical ocean observations (see Masina et al. 2004 for a detailed description of the assimilation procedure and the relevant results). Using assimilated models can greatly improve the realism of coupled physical-biological models (Blanke et al. 2012). On one hand, they provide a more realistic reproduction of the 3-D thermal and dynamical state of the ocean within the considered region. On the other hand, they also improve the description of the temporal variability of the upper ocean at inter-annual and decadal time scales. Among assimilated models, the re-analysis used in this work is one of the best products currently available, as it has gone through an extensive validation procedure. At present, the production of global ocean reanalyses at 1/4° horizontal resolution is under way, and some products at that resolution already exist, but they do not cover the period (early 1980s) for which field data on eel leptocephali are available.

Lagrangian simulation design

In each simulation, a total of one million Lagrangian particles per year, each particle representing a single larva, were released over a 3-year period (1982–1984) and tracked for the subsequent 4 years. This time horizon was chosen to allow for the comparison of the simulations with experimental data gathered in that same period (see section *Experimental data to be compared with simulation outputs*). Releases were performed daily within a time window encompassing the most accredited spawning season (March to May: Schmidt 1923; McCleave & Kleckner 1987; McCleave 2008). More precisely, the probability distribution of births over time was assumed to be Gaussian (with mean set to the 1st of April and

SD = 20 days). The initial geographic position of larvae was randomly drawn from a trivariate Gaussian distribution centred within the polygon identified by McCleave et al. (1987) and manually tuned to match available knowledge (Schoth & Tesch 1982, McCleave & Cleckner 1987 and references therein) about the distribution of leptocephali below 10 mm in length (latitude: 26.5 ± 1.2°N; longitude: 62 ± 4°W; depth: –175 ± 35 m). The drift velocity of each particle was determined through linear interpolation of mean velocity fields in space and time. Trajectories were calculated using an explicit Euler method with a 3-hour time step. The arrival line (where successful larvae were counted) was set to the 15°W meridian, further east than done in previous studies (Kettle & Haines 2006, Bonhommeau et al. 2009a, b). This allowed us to extend Lagrangian simulations to the easternmost longitude at which circulation fields are not affected by the continental slope.

Biological features

Body growth

Body size is a major driver of nearly all biological rates and times (Peters 1983, Brown et al. 2004). Evidence of its role in regulating vital traits of the European eel has been accumulated in recent years (e.g. sex differentiation, Melià et al. 2006b; sexual maturation, Bevacqua et al. 2006; natural mortality, Bevacqua et al. 2011). Identifying a realistic body growth model is therefore important to obtaining reliable estimates of vital traits affecting migration success, such as mortality and movement (on both the horizontal and vertical direction). Back in 1923, Schmidt proposed a body growth curve for *A. anguilla* larvae (Figure 3.1) through an eye fit of average body length data in different months, as resulting from arranging the samples he collected across the Atlantic ocean between 1905 and 1921 (Schmidt 1923). His data were split into putative age groups spanning about 2 years from egg hatching in the Sargasso Sea to the recruitment of full-grown leptocephali to European coasts. Since only body size of larvae was known to the researcher but not their age, Schmidt arranged data in a Cartesian plane suitable to propose a somehow arbitrary growth curve. In fact, Schmidt's arrangement of data was questioned by Boëtius and Harding (1985a), who claimed that data from I-group leptocephali (between 40-50 mm long), which they called “tramps”, cannot be used to assess body growth because larvae of that group can be found over most of the northern Atlantic at any time of the year. Therefore, they put forth the idea that leptocephali may begin metamorphosing into glass eels within 12–15 months only. This hypothesis was supported also by the analysis of daily growth increments in otoliths (Castonguay 1987, Lecomte-Finiger 1992, Wang and Tzeng 2000), but strongly criticized by McCleave (2008) and Zenimoto et al. (2011). As no irrefutable evidence has been brought up to now in favour of either hypothesis, we considered a set of 4 candidate growth curves consistent with both interpretations (Figure 3.2). We fitted Schmidt's (1923) data (as reported in Figure 8 of his paper) under the hypothesis of a 2.5-yr long larval phase with a power function, as suggested by our visual inspection of the data, and with a von Bertalanffy curve, a common choice for modelling body growth in fish. These two body growth models are indicated as PF-slow and VB-slow, respectively, in Figure 3.2a. To contrast Schmidt's interpretation of data with that by Boëtius and Harding, we fitted both functions also against a rearranged dataset from which I-group leptocephali (grey circles in Figure 3.2a) were removed. Under the hypothesis that the larval phase lasts only 1.5 yr, we assigned the largest larvae collected between February and June (black circles in Figure 3.2a) to the second age class (and not to the third, as done by Schmidt). These

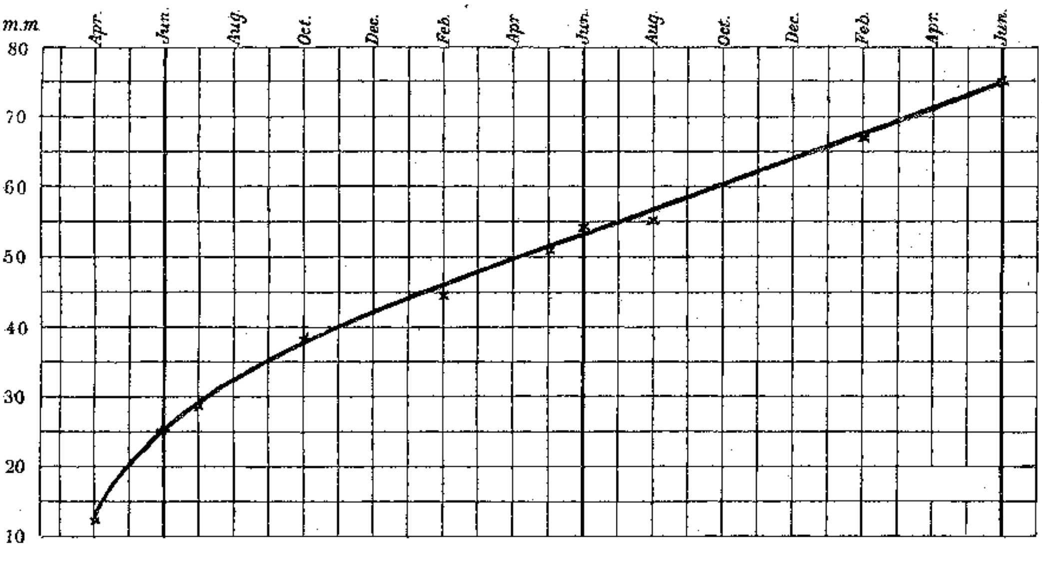

Figure 3.1 – Body growth curve for *Anguilla anguilla* larvae proposed by Schmidt (1923, Figure 8)

two models are graphically represented in Figure 3.2b and indicated as PF-fast and VB-fast, respectively. In conclusion, four body growth models, differing with respect to the functional form and the supposed duration of the larval phase, were fitted to the original Schmidt's (1923) data or to a subset of it (*sensu* Boëtius and Harding 1985a). All curves showed good fitting performances (R^2 between 0.95 and 0.99).

To account for inter-individual body growth variation (typical of fish species characterized by high body growth plasticity, such as *A. anguilla*; Tesch 2003), we used an individual-based body growth model. In particular, we used an assignment-at-birth scheme (Kirkpatrick 1984) similar to that used to describe body growth in the continental phase of European and New Zealand eels (De Leo & Gatto 1995, Hoyle & Jellyman 2002). The realized body length $l(x)$ of an individual at age x was expressed as the product between the expected length predicted by the relevant deterministic model $L(x)$ and a random factor assigned at birth, say g. In accordance with data from glass eels recruited in the Mediterranean Sea (Melià et al. 2006a), we assumed that the natural logarithm of g follows a Gaussian distribution with mean zero and standard deviation $\sigma = 0.056$.

Mortality

So far, the only assessment of natural mortality during the oceanic migration of European eel larvae is that obtained by Bonhommeau et al. (2009b). In the absence of any experimental data on larval survival, however, their estimate relies on model simulations driven under the hypothesis that the global eel stock was stationary during the period considered in the study (1960–2004). As remarked in the Introduction though, it is just in that time window that the European eel stock underwent its dramatic decline. To avoid this stringent hypothesis, we followed the approach of Bevacqua et al. (2011), who relied on the metabolic theory of ecology (Brown et al. 2004). Bevacqua et al. (2011) linked eel mortality μ in the continental phase to water temperature T (through a Boltzmann-Arrhenius factor) and body mass M (through an allometric function):

$$\mu = a \exp(-E/kT)\, M^b \qquad (1)$$

While scaling parameters like b (allometric exponent) and E (activation energy) can be supposed to hold over the whole life cycle of the species, the proportionality coefficient a is affected by factors that cannot be

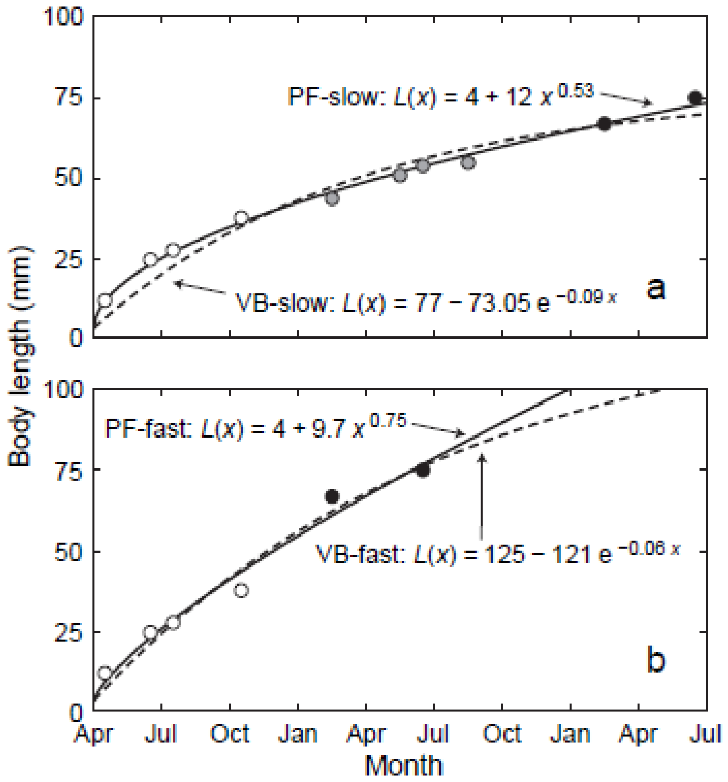

Figure 3.2 - Body growth sub-models for European eel leptocephali. (a) Power function (PF-slow) and von Bertalanffy (VB-slow) curves fitted to the original body length data compiled by Schmidt (1923, his Figure 8; circles with different shadings indicate putative age groups). (b) Power function (PF-fast) and von Bertalanffy (VB-fast) curves fitted to Schmidt's data filtered according to the reanalysis by Boëtius and Harding (1985), i.e. removing I-group leptocephali (grey circles in panel a) and subtracting one year from the age of the largest leptocephali (black circles in panel a)

extrapolated from the continental to the larval oceanic life stage. In the continental phase, the natural logarithm of *a* is reported to range between 48.5 and 50.8 depending upon eel gender and stock density (Bevacqua et al. 2011). For the oceanic phase, after performing some explorative simulations to identify a plausible range of survival probabilities, we tested a set of tentative values for a (ln*a* between 46 and 48) and assessed the sensitivity of the results to this parameter. In fact, for values of ln*a* greater than 48 (like those obtained by Bevacqua et al. 2011) migration success was null (no larvae, out of the 3 million released, survived the migration), while $\ln a = 46$ was the minimum value compatible with computational intensity.

Estimating mortality rate through the model described above requires knowing the body mass of larvae, and not only body length. Unfortunately, no data on the body mass of European eel larvae are available in the literature, thus hindering the estimation of a specific morphometric relationship. For this reason, we linked body mass M (in g) with body length L (in mm) by using the allometric function proposed by Melià et al. (2006a) for undifferentiated yellow eels, i.e. $M = 2.24\times10^{-7} L^{3.37}$. Although the validity of extrapolating a morphometric relationship from a life history stage to a very different one may be questionable (due to the different body mass composition and body shape between the two stages), body mass predicted by this function seems reasonable within the body length range spanned by European eel leptocephali and a comparison with published data on leptocephali of other eel species suggests that the margin for error is acceptable.

Movement

Information about the interplay between navigation capacity and motion ability in generating movement paths (*sensu* Nathan et al. 2008) is available only for a small number of species (Holyoak et al. 2008). As for the motion capacity of adult European eels, we know they can cover the distance between Europe and the Sargasso Sea with a remarkable swimming efficiency and at low energy costs (van Ginneken et al. 2005). Little is known about the swimming performances of eel larvae, and nothing on the species-specific movement of *Anguilla anguilla* larvae. However, Wuenschel & Able (2008) assessed the swimming speed of *Anguilla rostrata* glass eels and *Conger oceanicus* metamorphosing leptocephali, showing that the sustained swimming speed of both species ranges between 5.8–9.3 cm/s, corresponding to ca. 0.9–1.1 body lengths per second (BL s^{-1}). In our simulations, we have compared the results derived under the hypothesis of a purely passive drift with those obtained with increasing levels of larval propulsion. We assumed swimming speed to be proportional to body length (Peters 1983) within a plausible speed range from 0 (passive drift) to 4 BL s^{-1}. Of course, if leptocephali swam continuously at their maximum speed, they would probably not be able to feed properly. For this reason, the swimming speeds considered in our scenario should be considered as average values.

In contrast with Bonhommeau et al. (2009a, b), who hypothesized that eel larvae can regulate their depth to match the maximum current velocity, we did not consider a vertical rheotaxis. In fact, although larvae may perceive local gradients, it is quite unlikely that they can react to current profiles over the whole water column. However, we assumed that leptocephali have a horizontally rheotactic behaviour. The ability of fishes to use their mechanosensory lateral line system to mediate rheotaxis (Montgomery et al. 1997) has been evidenced in several lab studies (e.g. Olszewski et al. 2012), and the results of a recent study on green sturgeons (Kelly & Klimley 2012) suggest that fish can orient their swimming with respect to the current direction even in the open sea. Therefore, active swimming simulations were performed by adding a size-specific individual propulsion to the modulus of the drift velocity.

Besides horizontal movement, eel larvae exhibit also a diel vertical migration (Castonguay & McCleave 1987), possibly driven by a negative phototaxis and/or an entrained circadian rhythm (Yamada et al. 2009) most likely determined by their anti-predator behaviour. Previous Lagrangian simulations by Bonhommeau et al. (2009a, b) and Zenimoto et al. (2011) approximated this behaviour by letting eel larvae switch between two fixed depths (50 at night-time and 300 m at daytime). However, younger larvae collected at daytime between the Sargasso Sea and the Gulf Stream, i.e. at the beginning of their migration, were found at a shallower depth than older eel larvae caught on the continental shelf west of France and the British Isles, i.e. at the end of the migration (Tesch 1980, Castonguay & McCleave 1987). In the absence of any information about the vertical distribution of leptocephali during the rest of their journey across the ocean, we found reasonable to assume that daytime depth increases with body length.

Although previous studies did not consider inter-individual variation in the vertical distribution of leptocephali, the analysis of oceanic circulation fields reveals that changes in current direction and intensity may take place also within relatively small depth ranges. As these changes may have a strong influence on the migration paths of different individuals, we incorporated an individual-based stochastic component into diel vertical migration. At night-time (from 21:00 to 6:00), the vertical position of each larva was drawn randomly at every time step from a Gaussian distribution whose parameters (mean ± SD = 60 ± 25 m) were kept constant during the journey. In contrast, during daytime (from 9:00 to 18:00) larvae were randomly distributed around a mean depth increasing linearly with body length from 73.5 m at *L* = 5 mm to 470 m at *L* = 80 mm, with a constant SD of 25 m. To account for the time required to shift from one depth to the other and vice versa, we considered two intermediate steps (from 6:00 to 9:00 and from 18:00 to 21:00, respectively) in which the vertical position of the larvae was randomly distributed around the average of night-time and daytime mean depths.

Experimental data to be compared with simulation outputs

To provide a comparison with the earliest and latest phases of the migration, we chose datasets from both the western and eastern side of the ocean. Unfortunately, we could not find a suitable dataset relevant to the central part of the eel migration. For the West side, we used data from two cruises conducted in summer and autumn 1984 between the Sargasso Sea and the Florida Current (McCleave & Kleckner 1987). The two samples are referred to as Florida/Summer and Florida/Autumn in the following. For the East side, we used the data reported in McCleave et al. (1998), which summarize the collection of historical data compiled by Boëtius & Harding (1985b) and data collected in summer 1984 in the Iberian Basin (Bast & Strehlow 1990). These data consist of mean body length and standard deviation for 3° latitude by 4° longitude cells spanning between 32–65°N in latitude and between 3–35°W in longitude. To derive a sample to be compared with our simulation results, in this case we proceeded as follows. For each cell, we drew a congruous (i.e. proportional to the abundance of the experimental sample) random sample from a normal distribution with the same mean and SD, thus obtaining a statistically equivalent length distribution. After repeating the draw for each cell adjacent to the 15°W meridian, we merged the synthetic distributions of all cells to derive a synthetic body length distribution along our arrival line. Reference body length distributions at the three transects are shown in Figure 3.3.

Identifying the best simulation scenarios

Tracking Lagrangian particles over the spatial and temporal domain covered by our simulations is computationally intensive, and a rigorous calibration of all sub-models would not be feasible. Hence, we identified a set of plausible values for the most critical parameters of the models described in the previous sections and assessed the realism of different

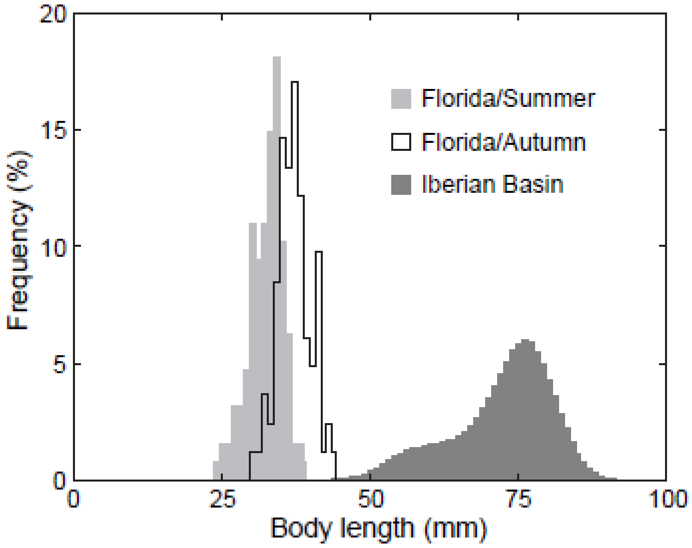

Figure 3.3 - Body length distribution of European eel leptocephali at three reference transects: Florida/Summer, Florida/Autumn, and Iberian Basin. Data for the two transects off Florida are from Fig. 4C of McCleave *et al.* (1998), while those for the Iberian Basin are derived from Fig. 2 of the same paper through the procedure described in the main text

simulation scenarios by comparing the results of the relevant simulations with experimental data. Scenarios, defined as the combination of settings for each of the three sub-models (body growth, mortality and locomotion) are summarized in Table 3.1. The combination of different parameter settings for the three sub-models originates 4 × 5 × 5 = 100 simulation scenarios.

The performances of each scenario were evaluated taking into account the ability of the model to reproduce observed body size patterns of leptocephali. First, we intercepted Lagrangian particles along the reference transects described in the previous section over the relevant time horizon (i.e. during the period in which the transects were actually sampled in the field). Second, we assessed the predictive ability of each scenario along each transect through two discrepancy indicators: the absolute percent error on median, e_{median}, and the absolute percent error on interquartile range, e_{iqr}, defined as

$$e_{median} = \left| median(L) - median(\hat{L}) \right| / median(L) \qquad (2)$$

$$e_{iqr} = \left| iqr(L) - iqr(\hat{L}) \right| / iqr(L) \qquad (3)$$

where median(L) and median($\hat{L}$) are observed and simulated median body lengths, and iqr(L) and iqr($\hat{L}$) the observed and simulated interquartile ranges of body length, respectively. After calculating e_{median} and e_{iqr} for each of the three transects, we calculated the overall discrepancy of each scenario with respect to median and interquartile range as the following Euclidean norms (subscripts FS, FA, IB indicate the relevant reference transects):

$$d_{median} = \sqrt{e^2_{median,FS} + e^2_{median,FA} + e^2_{median,IB}} \qquad (4)$$

$$d_{iqr} = \sqrt{e^2_{iqr,FS} + e^2_{iqr,FA} + e^2_{iqr,IB}} \qquad (5)$$

Therefore, the two indicators d_{median} and d_{iqr} summarize the discrepancy between observations and simulations as refers to 1) central tendency, 2) inter-individual variability and 3) spatial variability of body size distribution. Finally, to identify the best scenario we looked, in a multi-criteria perspective, for that realizing the best trade-off between minimizing the two indicators d_{median} and d_{iqr}.

body growth sub-model (see Figure 3.2)	
PF-slow	power function fitted to Schmidt's (1923) original data
VB-slow	von Bertalanffy curve fitted to the same data as PF-slow
PF-fast	power function fitted to Schmidt's (1923) data by removing I-group leptocephali as suggested by Boëtius and Harding (1985a)
VB-fast	von Bertalanffy curve fitted to the same data as PF-fast
mortality sub-model	
very low mortality	$\ln a = 46.0$
low mortality	$\ln a = 46.5$
medium mortality	$\ln a = 47.0$
high mortality	$\ln a = 47.5$
very high mortality	$\ln a = 48.0$
locomotion sub-model	
passive drift	0 BL s^{-1}
low speed	0.5 BL s^{-1}
moderate speed	1 BL s^{-1}
high speed	2 BL s^{-1}
very high speed	4 BL s^{-1}

Table 3.1 - Summary of the settings for the different simulation scenarios. A scenario is defined by a combination of 3 settings, one for each sub-model. In text and figures, scenarios are identified through a short description of the relevant sub-models: for instance, "PF-slow growth with medium mortality and moderate speed" indicates a model including a power function describing body growth, fitted on Schmidt's (1923) original data, an intermediate mortality rate ($\ln a = 47.0$ in Eq. 1) and an active locomotion at a swimming speed of 1 BL s^{-1}.

Results

Lagrangian simulations

For each simulation scenario, we calculated the statistics of interest for migration duration, migration success and latitudinal distribution across the 15°W meridian, assumed to be the arrival. We also derived the body length structure at the three reference transects. Depending on the scenario (see again Table 3.1), the average duration migration from the Sargasso Sea to the 15°W meridian was comprised between 21 months (PF-fast growth, very high mortality and very high speed) and 41 months (VB-slow growth, all mortality rates, passive drift). Migration success ranged between 0.001% (very high mortality) and 7% (very low mortality) for active locomotion scenarios, while in passive drift scenarios at very high mortality no eel larvae reached the arrival line. Mean latitude of arrivals varied between 38–39°N (very high speed) and 52–54°N (passive drift). Median body length ranged between 24 mm (VB-slow growth, very high mortality and moderate speed) and 36 mm (PF/VB-fast growth and very high speed) at the FS transect, between 35 mm (VB-slow growth) and 46 mm (VB-fast growth, very high mortality and low speed) at the FA transect and between 68 mm (PF-slow growth, moderate to high speed) and >100 mm (PF-fast growth) at the IB transect (15°W).

Comparison with experimental data

Figure 3.4 shows the performances of the 100 scenarios as synthesized by the two indicators d_{median} (which measures the error on central tendency of body size distributions) and d_{iqr} (measuring the error on inter-individuals variability). Note that lower values of d_{median} and d_{iqr} indicate better performances: therefore, the symbols in the left-bottom corner of Figure 3.4a represent the best performing scenarios. Slow body growth curves (both PF and VB) perform better (in terms of median body size at the reference transects) than those derived by removing I-group leptocephali, as suggested by Boëtius and Harding (fast body growth). Also, the power function model (PF-slow growth) matches observed inter-individual body size variation better than the corresponding von Bertalanffy curve (VB-slow growth), and the relevant scenarios are therefore characterized by a lower d_{iqr}. As for locomotion, the closer look offered by Figure 3.4b reveals that the scenarios considering active

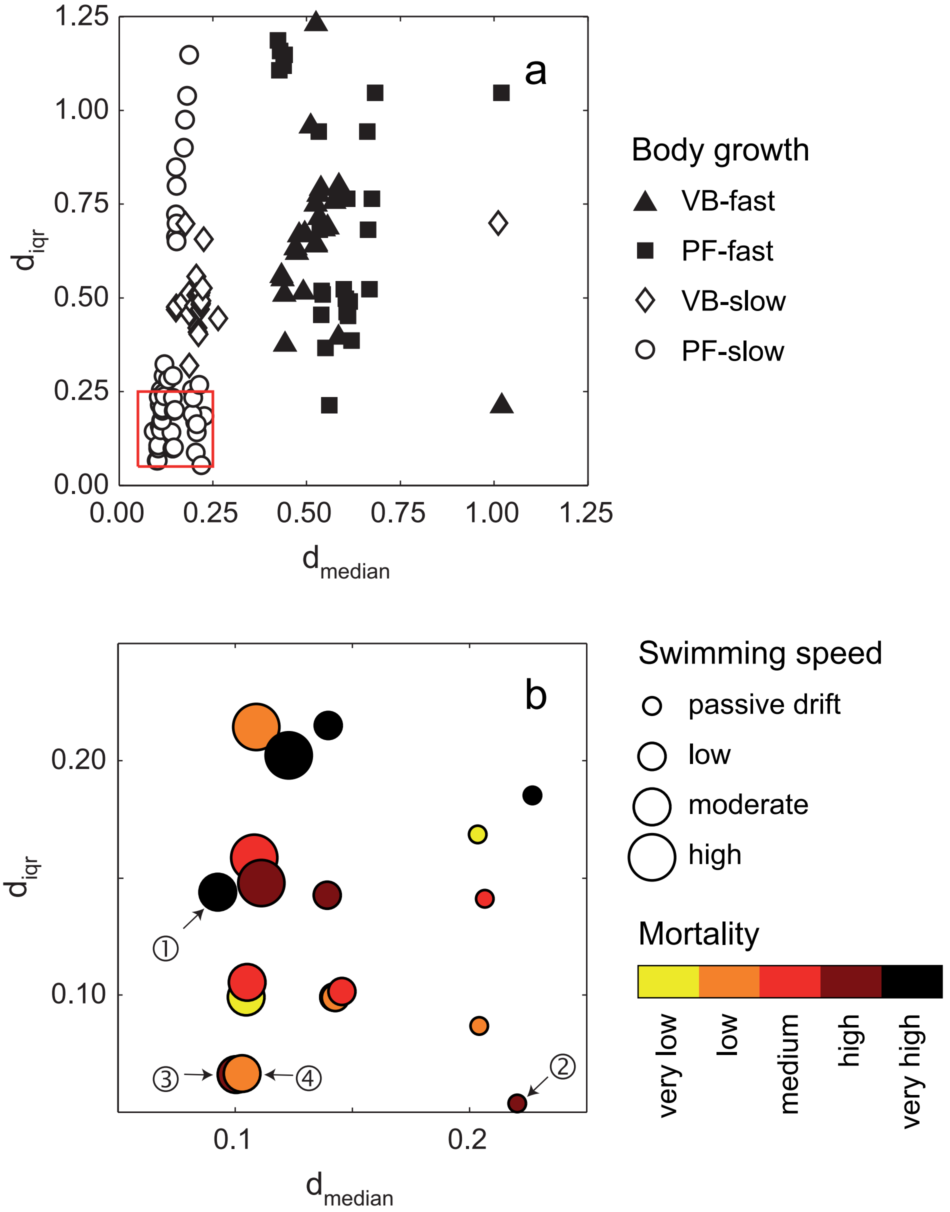

Figure 3.4 - Fitting performances of 100 simulation scenarios (see Table 3.1) reproducing the oceanic migration of European eel leptocephali. d_{median} and d_{iqr} measure the discrepancy between observed and simulated median and interquartile range of body length, respectively (see text for details). Lower values of d_{median} and d_{iqr} indicate increasing performances. Scenarios (identified by symbols) are classified by (a) the settings of body growth sub-models, and (b) mortality and locomotion sub-models. Panel (b) shows only the most performing scenarios (red box in panel a), all sharing the same body growth function (PF-slow growth). The specific parameter settings of the 4 most interesting scenarios, indicated as ①, ②, ③ and ④ in panel (b), are described in the main text

swimming at low to high speed perform better than those considering a passive drift or an active movement at high speed. The very high speed setting (4 BL s^{-1}) for the locomotion sub-model is not listed in the legend of Figure 3.4b, because none of the relevant scenarios is comprised among the best performing ones. As somehow expected, the value attributed to mortality rate does not influence much the realized body size distribution at the selected transects, while it does affect migration success and duration, as we discuss below.

All best performing simulation scenarios share the same body growth curve (PF-slow growth). The scenario that best reproduces median body size at the reference transects, i.e. minimizes d_{median}, is indicated as ① in Figure 3.4 and has a very high mortality rate and active locomotion at moderate speed (1 BL s^{-1}). On the other hand, the scenario that best matches the observed dispersion around the central tendency, i.e. minimizes d_{iqr}, is indicated as ② and has a high mortality rate and passive transport. However, there are two scenarios (③ and ④), both characterized by an active locomotion at moderate speed but slightly different mortalities (high and low, respectively), which provide a good trade-off between the two objectives of minimizing the performance indicators. Compared to ①, scenarios ③ and ④ guarantee a remarkable decrease in d_{iqr} that offsets a modest increase in d_{median}; at the same time, they guarantee a remarkable decrease in d_{iqr} that offsets a modest increase in d_{median}; at the same time, they guarantee a considerable decrease in d_{median} compared to ②, while determining an acceptable increase in d_{iqr}. As the performances of ③ are slightly better than those of ④ with respect to both indicators, we consider ③ as the reference scenario and analyse it in more detail in the following.

The ecologically important characteristics of our reference scenario – characterized by Schmidt's body growth curve (PF-slow), high mortality rate and moderate swimming speed– are summarized in Figures 3.5–3.7. Figure 3.5 shows the simulated frequency distribution of migration duration and the latitudinal distribution of successful larvae. Migration duration has a peak at ca. 26 months, with an average of about 30 months from the Sargasso Sea to the arrival line. The latitudinal distribution of arrivals has a main peak in front of the Bay of Biscay (between ca. 45–50°N) and a secondary one off Moroccan coasts (at about 35°N). Figure 3.6 compares the spatial distribution of all released larvae (Figure 3.6a) with the starting location of only those successfully

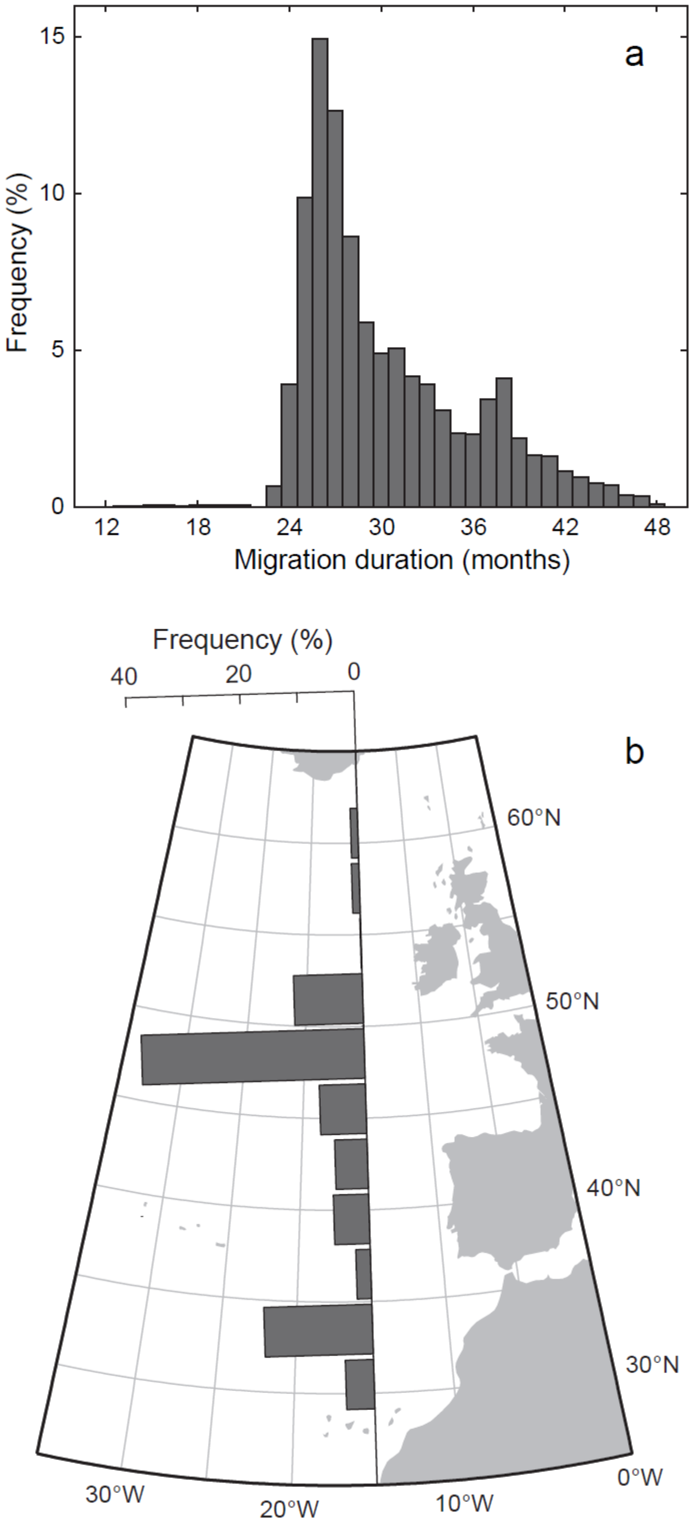

Figure 3.5 - Frequency distribution of (a) migration duration and (b) latitude of European eel leptocephali successfully reaching the 15°W meridian within 4 years, as obtained by simulation under reference scenario (indicated as ③ in Figure 3.4, see text for details)

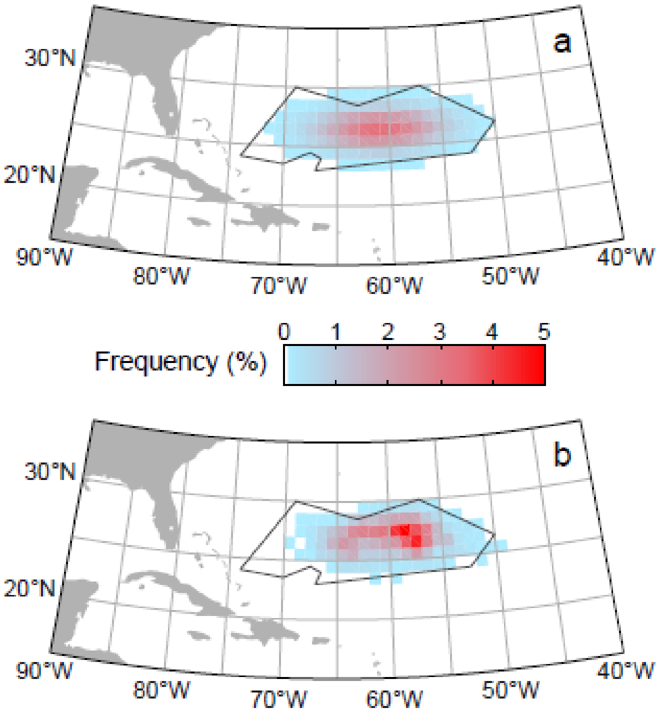

Figure 3.6 - Comparison between the spatial distribution of starting locations (a) for all Lagrangian particles released within the polygon identified by McCleave et al. (1987) and (b) for the subset of particles that successfully crossed the 15°W meridian within 4 years under reference scenario ③ (see text for details)

arriving at the 15°W meridian within 4 years (Figure 3.6b). The figure shows that the majority of successful larvae began their journey from a quite restricted zone within the McCleave polygon, namely the region comprised between 50–65°W and 25–30°N. Finally, Figure 3.7 shows the simulated occurrence limits of leptocephali of different body size, which can be compared with those derived by Schmidt (1923, his Figure 4) on the basis of field samples.

Discussion

Identifying the simulation scenario that best reproduces experimental body length distributions at the different transects does not prove *per se* that the biological mechanisms as included in the model are correct. However, it corroborates the underlying hypotheses against alternative

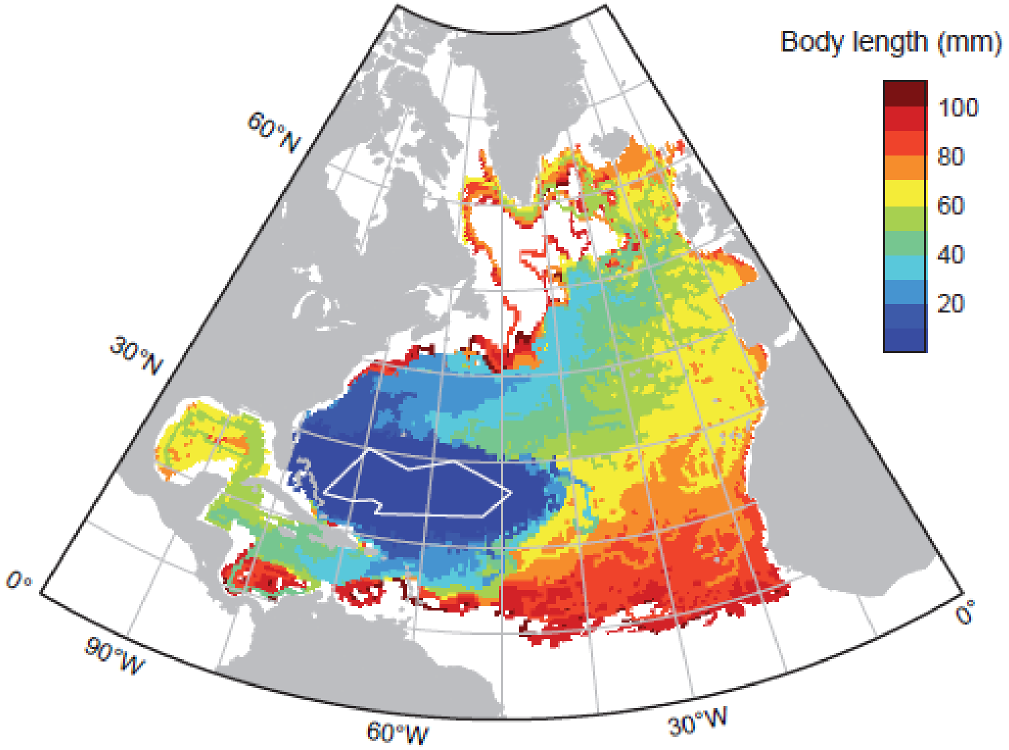

Figure 3.7 - Occurrence limits for European eel leptocephali of different body length, as obtained by simulation under reference scenario ③ (see text for details). The colour of each cell represents the maximum length of all leptocephali that passed through it during their migration. The polygon identified by McCleave et al. (1987) is marked in white

ones that fail in assimilating experimental data within a consistent conceptual framework. In the following, we discuss the most plausible conclusions that can be drawn from our simulation study, and contrast them with the current knowledge about the migration of eel leptocephali.

Body growth

A power function based on a 2.5-year migration hypothesis (PF-slow growth) fits Schmidt's (1923) data very closely. Figure 3.8 compares observed and simulated body length distributions at the three reference transects, as obtained by simulation under reference scenario ③. The curves derived under the hypothesis of a fast growth (PF/VB-fast growth) provide a slightly better fit of the body length distribution at the

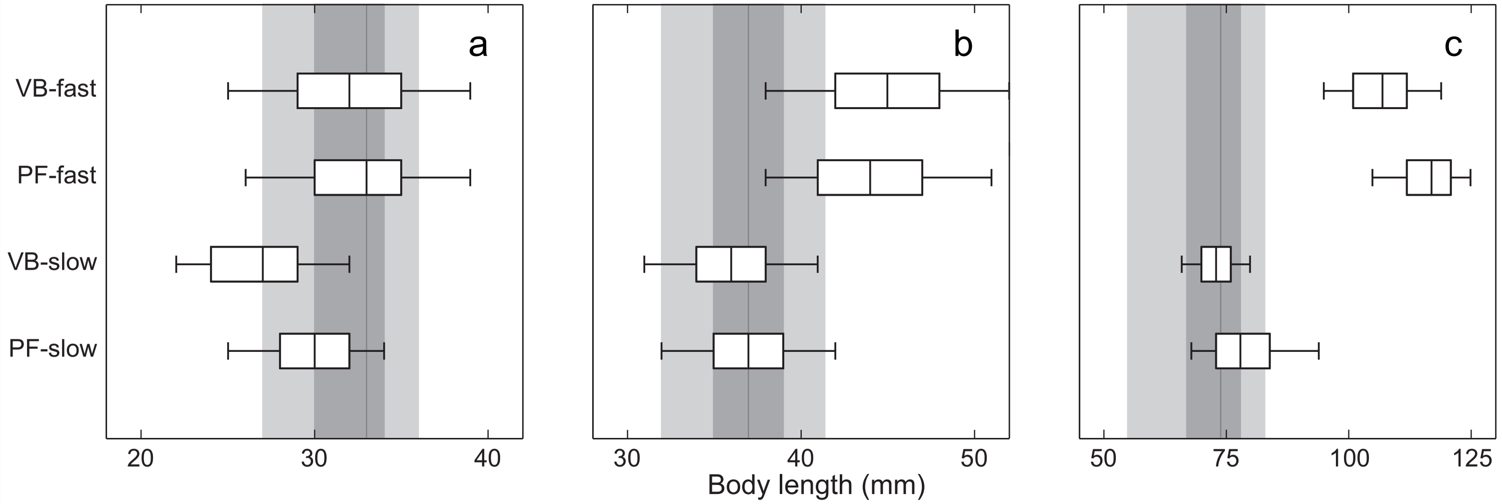

Figure 3.8 - Simulated body length distributions of European eel leptocephali at the three reference transects (a: Florida/Summer; b: Florida/Autumn; c: Iberian Basin), as obtained from 4 simulations with settings for mortality (high level) and locomotion (active, moderate speed) as in reference scenario ③ (see text for details), but differing with respect to body growth (see Figure 3.2). Boxes: interquartile range; vertical line: median; whiskers: 90% confidence intervals. Box-whisker plots are superimposed to a shaded area showing the body length distribution experimentally observed at each transect (straight line, darker shading and lighter shading indicate median, interquartile range and 90% CI, respectively). The same settings of high mortality and active locomotion with moderate swimming speed were used for all simulations (details in Table 3.1)

Florida/Summer transect compared with those derived by assuming a slower growth, consistent with Schmidt's original view. However, the former fail to reproduce the body length distribution at the Florida/Autumn transect. The error is even larger at the arrival line, because the shortest simulated migration duration (21 months) is still too long to be consistent with the fast growth hypothesis (1.5-yr migration). As a consequence, estimated body lengths at the IB transect under the fast growth hypothesis are unrealistically high (>100 mm) irrespective of the settings used for the mortality and locomotion sub-models. On the other hand, the VB-slow growth model is not able to accurately reproduce body growth patterns observed in the earliest developmental stages, while growth rates predicted by the power function are in good accordance with available information on early larval development of other eel species. In fact, the model predicts an average body growth rate of 0.32 mm day^{-1} for the first 50 days, and of 0.14 mm day^{-1} between the 50th and the 100th day of life, very close to the figures reported for laboratory grown leptocephali of *Anguilla japonica* (Tanaka et al. 2001, Tsukamoto et al. 2009). A similar growth rate (0.28 mm day^{-1}) was reported also for *A. rostrata* in the first five days after hatching (Oliveira & Hable 2010). Assessments of body growth rate in different eel species based on otolith microstructure analysis (e.g. Castonguay 1987, Kuroki et al. 2006, Shinoda et al. 2011) provided remarkably higher estimates, but might have been affected, as put forth by Zenimoto et al. (2011), by a reduced deposition of otolith increments at low temperatures.

Mortality

As anticipated above, simulated body length distributions at the reference transects are not markedly affected by the assumed mortality rate. Therefore, we could not draw from them any evidence about a likely range for this crucial parameter. In contrast, mortality has a pronounced effect on larval survival. Under the most favourable scenarios for body growth and locomotion (PF-slow growth and moderate swimming speed), migration success varied between 0.04% and 7% depending on the setting of the mortality sub-model. This wide range (spanning three orders of magnitude) encompasses the estimate (0.12%) obtained by Bonhommeau et al. (2009b) under a steady-state hypothesis of the European eel population. Under the mortality setting associated with reference scenario ③, migration success is 0.42%. A considerable proportion (>60%) of leptocephali dies during the first month of life. Interestingly, the combined effect of the variation in body size (increasing from 4 mm at birth to ca. 75 mm at the 15°W meridian) and water temperature (decreasing from ca. 21°C in the Sargasso Sea to ca. 14°C near European shelves) determines a steep decrease of mortality rate along the journey of leptocephali, from 0.14 days^{-1} at birth to 0.00042 days^{-1} (= 0.15 years^{-1}) at the end of the migration.

Despite the difficulty for identifying the most realistic mortality scenario in the absence of any data about larval survival, estimates of migration success can be used to derive a rough assessment of the global spawning stock. On the basis of a "Procrustean" estimate of 2 billion glass eels recruiting each year to European coasts (Dekker 2000), assuming a 20% hatching rate and a fecundity of 1.5 million eggs per female (Bonhommeau et al. 2009b), the spawning stock would range between 91,000 and 15 million spawning females depending upon the selected mortality scenario, with a "best" estimate of 1.6 million spawners.

Movement

Whether the oceanic migration of eel larvae is a purely passive process of long duration (2-3 years) or an (at least partially) active process of short duration (1 year or less) is the subject of long-standing debate (van Ginneken & Maes 2005, McCleave 2008). Our simulations suggest that active locomotion is important to determine the migration duration. The best performing scenarios are those assuming a swimming speed of 1 BL s^{-1}. Some scenarios at 0.5 BL s^{-1} are also good in terms of overall performances, but they are less satisfactory in reproducing the observed length distribution at the 15°W meridian (i.e. they overestimate body length). A swimming speed between 0.5 and 1 BL s^{-1} is consistent with estimates reported for migrating adults of different eel species (van Ginneken & Maes 2005). Compared with a passive drift scenario, swimming at 1 BL s^{-1} reduces the migration duration by 18–21%. Counter-intuitively, it is on migration success that the introduction of active locomotion has the most remarkable consequences. In fact, swimming at 1 BL s^{-1} guarantees in our simulations a 6 to 12-fold increase of migration success compared with analogous scenarios based on passive migration.

Some of the observed discrepancies between the results of previous simulations and ours may arise from the different modelling approach used to describe the movement of eel larvae. To assess the consequences of different assumptions about vertical movement, we compared the results obtained with our reference simulation scenario ③ with those of two additional scenarios sharing the same settings except that the diel vertical migration was described 1) with larvae maintaining the same depth throughout the migration route, as in Kettle & Haines (2006), and 2) with larvae switching between two fixed depths (50 m at night-time and 300 m at daytime), as in Bonhommeau et al. (2009a, b).. While migration duration and body length distribution at the reference transects were not appreciably affected by modifying vertical movement pattern, migration success was strongly affected. Success rate was remarkably higher (1.66% instead of 0.42%) for the single-depth scenario and lower (0.18%) for the two-depth one. This is in accordance with the findings of Bonhommeau et al. (2009a, 2010) and suggests that diel vertical migration might be aimed at maximizing migration success by minimizing mortality rather than minimizing migration duration.

Migration duration

The average migration duration to the 15°W meridian associated with the reference scenario is ~2.5 years. Considering the residual distance that leptocephali must cover to reach European shelves, the longitudinal component of the oceanic velocity field across that transect and the contribution of larval propulsion, it is possible to estimate 1–2 more months to complete the migration. This means that leptocephali would reach Europe in late autumn, metamorphose into glass eels in the subsequent 1–2 months (Arai et al. 2000) and recruit to continental waters after 2–3 more months (Wang & Tzeng 2000), between late winter and spring (Desaunay & Guérault 1997). This schedule fits perfectly with that sketched out, almost one century ago, by Schmidt (1923). It is also consistent with the estimated 3-year time lag between primary production in the Sargasso Sea and glass eel recruitment to European coasts (Bonhommeau et al. 2008) and with the view that otolith microstructure analysis provides a large underestimation of migration duration, as already argued by McCleave (2008). In fact, Zenimoto et al. (2011) showed that the discrepancy between age estimates resulting from cohort analysis and those derived through otolith microstructure analysis can be ascribed to the effect of temperature on the deposition rate of otolith increments. By using their approach to simulate temperature-dependent otolith deposition, we estimated an "apparent" age of ~19 months, which is more similar to the estimates obtained by the most recent otolith microstructure analyses (Wang & Tzeng 2000) than to the true age of particles reaching the arrival line. In contrast, Bonhommeau et al. (2009b) estimated a mean migration duration of 18 months only (to reach the 20°W meridian), to which they added 3 more months for leptocephali to reach Europe and metamorphose into glass eels. This implies a migration schedule longer than suggested by otolith microstructure analysis, but shorter than that resulting from cohort analysis and our Lagrangian simulation experiments. Besides the differences in the description of active movement, this discrepancy results also from the different spatio-temporal settings used for larval release. To verify it, we run two additional simulations with life history parameters set as in reference scenario ③ but different release settings. In the first simulation, releases were scheduled as in ③, but the initial position of larvae was uniformly distributed over a rectangle circumscribing McCleave et al.'s (1987) polygon, as in Kettle & Haines (2006). In the second simulation, the initial position was drawn from a trivariate Gaussian distribution as in ③, but releases were uniformly distributed throughout the year (as in Kettle & Haines 2006 and Bonhommeau et al. 2009a, b). As expected, both simulations showed poorer fitting performances than scenario ③.

Migration routes

Simulated migration trajectories are consistent with the body of knowledge deriving from both field surveys and simulation exercises. Leptocephali leave the Sargasso Sea, carried by the Antilles current, towards the Florida Current and then into the Gulf Stream that will carry them across the Atlantic Ocean. After the Gulf Stream branching, larvae scatter over the several meanders of the NE Atlantic circulation to reach Europe and North Africa. The area from which most successful Lagrangian particles originate (between 50–65°W in longitude and 25–30°N in latitude, see Figure 3.6) fits very well with the spawning area hand-drawn by Schmidt (1923, see his Figure 4) and with the distribution of the smallest leptocephali collected during the Sargasso Sea Eel Expedition 1979 (Figure 3 in Schoth & Tesch 1982). Noteworthy, none of the larvae released west of the 70°W meridian successfully reached the arrival line. This is in contrast with previous simulation studies (Kettle & Haines 2006, Bonhommeau et al. 2009a, b), which identified the “best” starting places in the western region (70–75°W) of the Sargasso Sea. However, that region falls outside the supposed reproductive range of the European eel and is most likely unsuitable for spawning, as it is directly influenced by the Antilles Current (Power & McCleave 1983).

The latitudinal distribution of arrivals obtained with the reference scenario is similar to those obtained by previous Lagrangian simulations. However, integrating the body growth model into the coupled physical-biological model allowed us not only to compare our results with those of previous simulations or with presence/absence data, but also to verify the agreement between our modelling work and observed body size patterns. Simulated occurrence limits for different body lengths (Figure 3.7) agree with those derived by Schmidt (1923, again his Figure 4). Note that our figure was obtained by letting Lagrangian particles move over the whole time horizon of the simulations (4 years), without removing them as soon as they crossed the arrival line (but removing those killed by natural mortality). As body growth was also not stopped, a few larvae attained unrealistically high body lengths (>90 mm).

Unfortunately, none of our simulations could replicate the increasing body length gradient (from South to North) observed in the proximity of European shelves (Bast & Strehlow 1990, McCleave et al. 1998). This gradient may result from the fact that some larvae take advantage of frontal jets in the Sargasso Sea (Miller & McCleave 1994, Munk et al. 2010) or from an active east-north-eastwards larval migration (Bast & Strehlow 1990). As regards the first hypothesis, our circulation model may not be able to provide an accurate description of small-scale circulation structures. However, Blanke et al. (2012) recently suggested that migration routes following the Gulf Stream and the North Atlantic Drift are likely to be shorter than those based on interior connections.

To test whether an oriented, active swimming may play a significant role in determining the body length gradient, we ran four additional simulations in which we introduced some speculative navigation mechanisms that might guide larval movement toward prescribed geographic directions. In these simulations, larval propulsion was in fact not oriented in the same direction as the oceanic current, but in a fixed direction (East, East-Northeast, Northeast, North-Northeast), with all other settings as in the reference simulation scenario ③. Figure 3.9 compares field data (from Bast & Strehlow 1990) with latitudinal body length

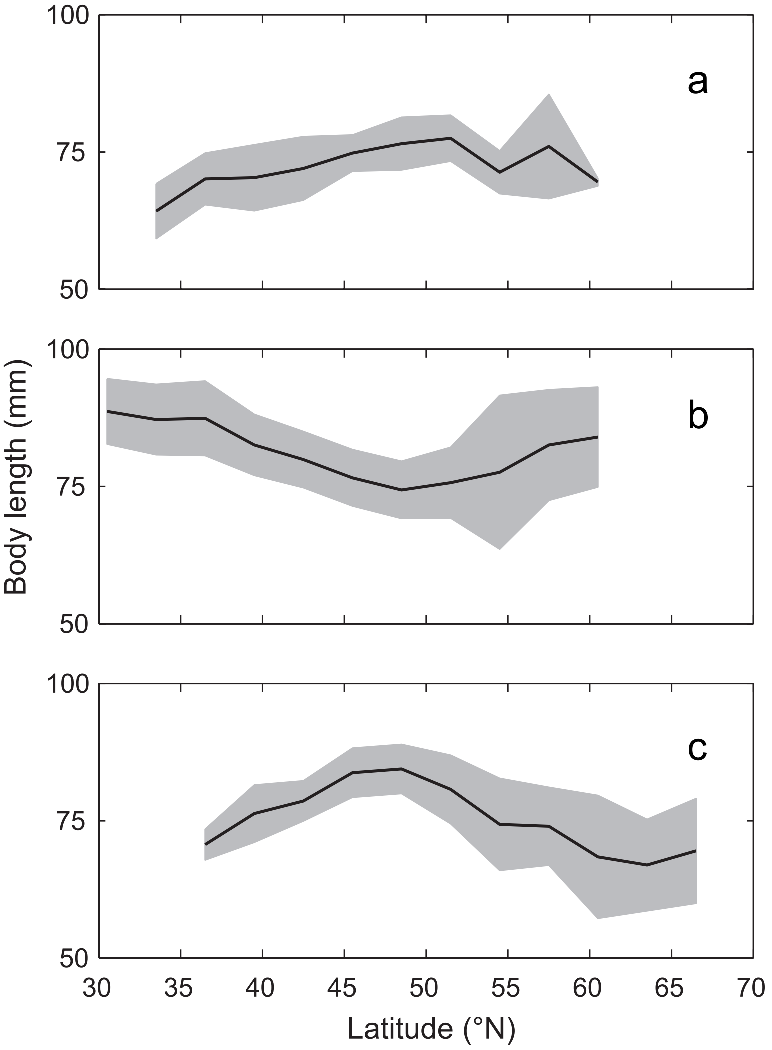

Figure 3.9 - (a) Latitudinal body size gradients of European eel leptocephali observed near European shelves (from Bast and Strehlow 1990, data referring to the range 11–15°W) compared with those obtained by simulation under reference scenario ③, with leptocephali (b) swimming in the direction of the current and (c) heading for Northeast (all other settings as in the reference scenario; see text for details). Solid lines and shaded areas indicate mean ± SD, respectively

patterns at the 15°W meridian obtained under scenario ③ and the Northeast-heading scenario. Although the Northeast-heading simulation generated the pattern qualitatively most similar to field data, none of the simulations was able to replicate it in full. Also, they all showed poorer performances than scenario ③ with respect to the two indicators d_{median}

and d_{iqr}. A further explanation of the observed gradient is that it might reflect a cline in body growth rate from warmer, yet less productive, southern waters to cooler, more productive northern waters. This hypothesis could be tested by incorporating data on primary production into the physical-biological model, and linking body growth to food availability or assuming that larval swimming is oriented towards increasing levels of food availability. Although it would be a very interesting extension of our model, it requires a deeper understanding of physiology, ecology and behaviour of eel larvae and is therefore outside the scope of the present work.

Final remarks

A fair appraisal of the actual scope of our simulation study requires some caveats. The first regards the spatial and temporal resolution of the ocean model used (1/2°). In fact, higher resolution (<1/10°) models can provide a description of small-scale structures, such as eddies and filaments, which might contribute to the formation of faster migration pathways (Blanke et al. 2012), perhaps allowing some larvae to carry out their migration faster than our simulations suggest. However, high-resolution ocean models are currently available only as hindcasts, i.e. they are not based on the assimilation of historical data. In contrast, the ocean re-analyses used in this work are created with the specific purpose of providing a more realistic description of the physical state of the ocean. Obtaining results that are as close as possible to empirical evidence was, in fact, the main goal of our study, and this is the main reason why we decided to use an ocean re-analysis, even if at a slightly coarser scale, rather to use a hindcast at a finer scale.

A second caveat is that candidate body growth curves are derived on the basis of a small number of data. In this respect, a comprehensive reanalysis of historical datasets, along with new experimental data, might provide useful information for a more rigorous assessment of body growth. Third, the estimates of survival across the migration derive from the extrapolation of a morphometric relationship referring to the continental phase of the species life cycle, which might not hold for leptocephali and might therefore impair a precise estimation of the actual mortality rate of leptocephali. However, we could not find any field data on body weight for European eel leptocephali, and using data from aquaculture experiments on other eel species (such as *Anguilla japonica*) might lead to even larger errors. Finally, the description of eel movement may still be too naive, as already pointed out in the previous section, and might be greatly enhanced by a deeper understanding of the behaviour of these larvae.

Although our analysis is not exempt from limitations, we believe it provides a promisingly plausible and consistent interpretation of most existing knowledge about the migration of European eel larvae. Further experimental effort to collect eel larvae at key places and times will hopefully allow filling up the existing knowledge gaps regarding the early life cycle of the European eel. Along with the availability in the near future of eddy-resolving ocean models able to assimilate all the ocean observations and give a more accurate estimate of the high-frequency ocean state, this is a fundamental step for the development of more realistic models. Integrating oceanographic, demographic and genetic data within coupled physical-biological models (similarly to what has been proposed in the multidisciplinary approach of Di Franco et al. 2012) can help decision makers to develop sustainable management strategies at a global level by identifying critical life history components and their responses to different environmental forces. In particular, the implementation of a realistic modelling framework of eel migration will provide a valuable tool to investigate possible long-term effects of physical and ecological changes occurring in the ocean on the viability of this mysterious fish.

References

Als TD, Hansen MM, Maes GE, Castonguay M, Riemann L, Aarestrup K, Munk P, Sparholt H, Hanel R & Bernatchez L (2011) All roads lead to home: panmixia of European eel in the Sargasso Sea. *Mol Ecol* **20**: 1333–1346

Andrello M, Bevacqua D, Maes GE & De Leo GA (2011) An integrated genetic- demographic model to unravel the origin of genetic structure in European eel (*Anguilla anguilla* L.). *Evol Appl* **4**:517–533

Arai T, Otake T & Tsukamoto K (2000) Timing of metamorphosis and larval segregation of the Atlantic eels *Anguilla rostrata* and *A. anguilla*, as revealed by otolith microstructure and microchemistry. *Mar Biol* **137**:39–45

Bast H-D & Strehlow B (1990) Length composition and abundance of eel larvae, *Anguilla anguilla* (Anguilliformes: Anguillidae), in the Iberian Basin (northeastern Atlantic) during July–September 1984. *Helgol Meeresunters* **44**:353–361

Bevacqua D, Melià P, Crivelli AJ, De Leo GA & Gatto M (2006) Timing and rate of sexual maturation of European eel in brackish and freshwater environments*. J Fish Biol* **69**(Suppl. C):200–208

Bevacqua D, Melià P, Crivelli AJ, De Leo GA & Gatto M (2009) Assessing Management Plans for the Recovery of the European Eel: A Need for Multi-Objective Analyses. In: Haro AJ et al. (eds) Challenges for Diadromous Fishes in a Dynamic Global Environment. *Am. Fish. Soc. Symp.* **69**:637–647

Bevacqua D, Melià P, De Leo GA & Gatto M (2011) Intra-specific scaling of natural mortality in fish: the paradigmatic case of the European eel. *Oecologia* **165**:333–339

Blanke B, Bonhommeau S, Grima N & Drillet Y (2012) Sensitivity of advective transfer times across the North Atlantic Ocean to the temporal and spatial resolution of model velocity data: Implication for European eel larval transport. *Dyn Atmos Oceans* **55**–56:22–44

Boëtius J & Harding EF (1985a) A re-examination of Johannes Schmidt's Atlantic eel investigations. *Dana* **4**:129–162

Boëtius J & Harding EF (1985b) List of Atlantic and Mediterranean *Anguilla* leptocephali: Danish material up to 1966. *Dana* **4**:163–249

Bonhommeau S, Chassot E & Rivot E (2008) Fluctuations in European eel (*Anguilla anguilla*) recruitment resulting from environmental changes in the Sargasso Sea. *Fish Oceanogr* **17**:32–44

Bonhommeau S, Blanke B, Tréguier A-M, Grima N, Rivot E, Vermard Y, Greiner E & Le Pape O (2009a) How fast can the European eel (*Anguilla anguilla*) larvae cross the Atlantic Ocean? *Fish Oceanogr* **18**:371–385

Bonhommeau S, Le Pape O, Gascuel D, Blanke B, Tréguier A-M, Grima N, Vermard Y, Castonguay M & Rivot E (2009b) Estimates of the mortality and the duration of the trans-Atlantic migration of European eel *Anguilla anguilla* leptocephali using a particle tracking model. *J Fish Biol* **74**:1891–1914

Bonhommeau S, Castonguay M, Rivot E, Sabatié R & Le Pape O (2010) The duration of migration of Atlantic *Anguilla* larvae. *Fish Fish* **11**:289–306

Brown JH, Gillooly JF, Allen AP, Savage VM & West GB (2004) Toward a metabolic theory of ecology. *Ecology* **85**:1771–1789

Castonguay M (1987) Growth of American and European eel leptocephali as revealed by otolith microstructure. *Can J Zool* **65**:875–878

Castonguay M & McCleave JD (1987) Vertical distributions, diel and ontogenetic vertical migrations and net avoidance of leptocephali of *Anguilla* and other common species in the Sargasso Sea. *J Plankton Res* **9**:195–214

Cowen RK & Sponaugle S (2009) Larval Dispersal and Marine Population Connectivity. *Annu Rev Marine Sci* **1**:443–466

De Leo GA & Gatto M (1995) A size and age-structured model of the Europeanzeel (*Anguilla anguilla* L.). *Can J Fish Aquat Sci* **52**:1351–1367

Di Franco A, Coppini G, Pujolar JM, De Leo GA, Gatto M, Lyubartsev V, Melià P, Zane L & Guidetti P (2012) Assessing dispersal patterns of fish propagules from an effective Mediterranean marine protected area. *Plos One* **7**:e52108.

Dekker W (2000) A Procrustean assessment of the European eel stock. ICES J *Mar Sci* **57**:938–947

Desaunay Y, Guérault D (1997) Seasonal and long-term changes in biometrics of eel larvae: a possible relationship between recruitment variation and North Atlantic ecosystem productivity. *J Fish Biol* **51**(Suppl. A):317–339

Fiksen Ø, Jørgensen C, Kristiansen T, Vikebø F & Huse G (2007) Linking behavioural ecology and oceanography: larval behaviour determines growth, mortality and dispersal. *Mar Ecol Prog Ser* **347**:195–205

Fukuda N, Kuroki M, Shinoda A, Yamada Y, Okamura A, Aoyama J & Tsukamoto K (2009) Influence of water temperature and feeding regime on otolith growth in *Anguilla japonica* glass eels and elvers: Does otolith growth cease at low temperatures? *J Fish Biol* **74**:1915–1933

Gallego A, North EW & Petitgas P (2007) Introduction: status and future of modelling physical–biological interactions during the early life of fishes. *Mar Ecol Prog Ser* 3**4**7:121–126

Halpern, B.S. et al. (2008) A global map of human impact on marine ecosystems. *Science* **319**:948–952

Hannah CG (2007) Future directions in modelling physical–biological interactions. *Mar Ecol Prog Ser* **347**:301–306

Harden Jones FR (1968) Fish Migration. London: Edward Arnold

Holyoak M, Casagrandi R, Nathan R, Revilla E & Spiegel O (2008) Trends and missing parts in the study of movement ecology. *PNAS* **105**:19060–19065

Hoyle SD & Jellyman DJ (2002) Longfin eels need reserves: modelling the effects of commercial harvest on stocks of New Zealand eels. *Mar Freshw Res* **53**:887–895

ICES (2010) Report of the 2010 session of the Joint EIFAC/ICES Working Group on Eels. ICES CM 2010/ACOM:18, 224 pp

Kelly JT & Klimley AP (2012) Relating the swimming movements of green sturgeon to the movement of water currents. *Environ Biol Fish* **2**:151–167

Kettle AJ, Haines K (2006) How does the European eel (*Anguilla anguilla*) retain its population structure during its larval migration across the North Atlantic Ocean? *Can J Fish Aquat Sci* **63**:90–106

Kettle AJ, Vøllestad LA, Wibig J (2011) Where once the eel and the elephant were together: decline of the European eel because of changing hydrology in southwest Europe and northwest Africa? *Fish Fish* **12**:380–411

Kirkpatrick M (1984) Demographic models based on size, not age, for organisms with indeterminate growth. *Ecology* **65**:1874–1884

Kuroki M, Aoyama J, Miller MJ, Wouthuyzen S, Arai T & Tsukamoto K (2006) Contrasting patterns of growth and migration of tropical anguillid leptocephali in the western Pacific and Indonesian Seas. *Mar Ecol Progr Ser* **309**:233–246

Lecomte-Finiger R (1992) Growth history and age at recruitment of European glass eels *Anguilla anguilla* as revealed by otolith microstructure. *Mar Biol* **114**:205–210

Masina S, Di Pietro P & Navarra A (2004) Interannual-to-decadal variability of the North Atlantic from an ocean data assimilation system. *Clim Dyn* **23**:531–546

McCleave JD (2008) Contrasts between spawning times of *Anguilla* species estimated from larval sampling at sea and from otolith analysis of recruiting glass eels. *Mar Bio*l **155**:249–262

McCleave JD & Kleckner RC (1987) Distribution of leptocephali of the catadromous *Anguilla* species in the western Sargasso Sea in relation to water circulation and migration. *Bull Mar Sci* **41**:789–806

McCleave JD, Kleckner RC & Castonguay M (1987) Reproductive simpatry of American and European eels and implications for migration and taxonomy. *Am Fish Soc Symp* **1**:286–297

McCleave JD, Brickley PJ, O'Brien KM, Kistner DA, Wong MW, Gallagher M & Watson SM (1998) Do leptocephali of the European eel swim to reach continental waters? Status of the question. *J Mar Biol Ass UK* **78**:285–306

Melià P, Bevacqua D, Crivelli AJ, De Leo GA, Panfili J & Gatto M (2006a) Age and growth of *Anguilla anguilla* in the Camargue lagoons. *J Fish Biol* **68**:876–890

Melià P, Bevacqua D, Crivelli AJ, Panfili J, De Leo GA & Gatto M (2006b) Sex differentiation of the European eel in brackish and freshwater environments: a comparative analysis. *J Fish Biol* **69**:1228–1235

Miller TJ (2007) Contribution of individual-based coupled physical–biological models to understanding recruitment in marine fish populations. *Mar Ecol Prog Ser* **347**:127–138

Miller MJ & McCleave FD (1994) Species assemblages of leptocephali in the Subtropical Convergence Zone of the Sargasso Sea. *J Mar Res* **52**:743–772

Montgomery JC, Baker CF & Carton AG (1997) The lateral line can mediate rheotaxis in fish. *Nature* **389**:960–963

Munk P, Hansen MM, Maes GE, Nielsen TG, Castonguay M, Riemann L, Sparholt H, Als TD, Aarestrup K, Andersen NG & Bachler M (2010) Oceanic fronts in the Sargasso Sea control the early life and drift of Atlantic eels. *Proc R Soc B* **277**:3593–3599

Nathan R, MG Wayne, Revilla E, Holyoak M, Kadmon R, Saltz D & Smouse

PE (2008) A movement ecology paradigm for unifying organismal movement research. *PNAS* **105**:19052–19059

Oliveira K & Hable E (2010) Artificial maturation, fertilization, and early development of the American eel (*Anguilla rostrata*). *Can J Zool* **11**:1121–1128

Olszewski J, Haehnel M, Taguchi M & Liao JC (2012) Zebrafish larvae exhibit rheotaxis and can escape a continuous suction source using their lateral line. *PLoS One* **7**:e36661

Peters RH (1983) The ecological implications of body size. Cambridge University Press

Power JH & McCleave JD (1983) Simulation of the North Atlantic Ocean drift of *Anguilla* leptocephali. *Fish Bull* **81**:483–500

Righton D, Aarestrup K, Jellyman D, Sébert P, van den Thillart G & Tsukamoto K (2012) The *Anguilla* spp. migration problem: 40 million years of evolution and two millennia of speculation*. J Fish Biol* **81**:365–386

Schmidt J (1923) The breeding places of the eels. *Philos Trans R Soc Lond B* **211**:179–208

Schoth M & Tesch F-W (1982) Spatial distribution of 0-group eel larvae (*Anguilla* sp.) in the Sargasso Sea. *Helgol Meeresunters* **35**:309–320

Shinoda A, Aoyama J, Miller MJ, Otake T, Mochioka N, Watanabe S, Minegishi Y, Kuroki M, et al. (2001) Production of leptocephali of Japanese eel (*Anguilla japonica*) in captivity. *Aquaculture* **201**:51–60

Tesch F-W (1980) Occurrence of eel *Anguilla anguilla* larvae west of the European continental shelf, 1971–1977. *Environ Biol Fish* **5**:185–190

Tesch F-W (2003) The eel. Oxford: Blackwell

Tsukamoto K, Yamada Y, Okamura A, Kaneko T, Tanaka H, Miller MJ, Horie N, Mikawa N, Utoh T & Tanaka S (2009) Positive buoyancy in eel leptocephali: an adaptation for life in the ocean surface layer. *Mar Biol* **156**:835–846

van Ginneken VJT, Maes GE (2005) The European eel (*Anguilla anguilla*, Linnaeus), its lifecycle, evolution and reproduction: a literature review. *Rev Fish Biol Fish* **15**:367–398

van Ginneken VJT, Antonissen E, Müller EK, Booms R, Eding E, Verreth J & van den Thillart G (2005) Eel migration to the Sargasso: remarkably high swimming efficiency and low energy costs. *J Exp Biol* **208**:1329–1335

Wang CH & Tzeng WN (2000) The timing of metamorphosis and growth rates of American and European eel leptocephali: A mechanism of larval segregative migration. *Fish Res* **46**:191–205

Yamada Y, Okamura A, Mikawa N, Utoh T, Horie N, Tanaka S, Miller MJ & Tsukamoto T (2009) Ontogenetic changes in phototactic behavior during metamorphosis of artificially reared Japanese eel Anguilla japonica larvae. *Mar Ecol Prog Ser* **379**:241–251

Zenimoto K, Sasai Y, Sasaki H & Kimura S (2011) Estimation of larval duration in *Anguilla* spp., based on cohort analysis, otolith microstructure, and Lagrangian simulations. *Mar Ecol Progr Ser* **438**:219–228

HAS THE OCEAN CONTRIBUTED TO THE DECLINE OF EUROPEAN EEL RECRUITMENT? RESULTS OF A 40-YEAR SIMULATION EXPERIMENT

Abstract

The European eel stock is declining since the late 70s. The causes of this decline are still debated, but most likely include habitat loss, water pollution, parasite impact, climate change and overfishing. In particular, climate change is deemed to have affected the larval migration of this catadromous fish from its reproductive area (the Sargasso Sea) to European coasts. Temperature changes might have changed the structure of the plankton community and decreased food availability, while changes in oceanic circulation might have affected migration routes and increased exposure to predation. So far, these (non mutually exclusive) hypotheses have been tested only through correlation analyses among aggregated indices of recruitment, oceanic circulation and environmental features. Attempts to describe eel migration by means of Lagrangian simulations with coupled physical-biological models have been limited to short-term analyses and did not provide any information on possible changes of recruitment success in the long run. In this work, we used a numerical model of the global ocean to simulate the North Atlantic circulation between 1958 and 2000 to assess if the probability of eel larvae to reach the continental shelf has significantly changed over the second half of the last century. Our main goal is to study the impact of climate change on the geographical distribution of eel larvae and their recruitment success.

Introduction

Understanding the processes that drive the population dynamics of endangered marine species is a preliminary step to devise effective strategies of conservation management. To this end, the analysis of the biophysical mechanisms determining the spatio-temporal variability of fish recruitment is a crucial source of information. The case of the European eel *Anguilla anguilla* is paradigmatic in this sense. The European eel is a panmictic species reproducing in the Sargasso Sea: eel larvae (also known as leptocephali) migrate across the North Atlantic Ocean following the Gulf Stream towards Europe and Africa, in a journey that lasts 2-3 years, before settling into continental waters. European eel recruitment underwent a dramatic decrease since the end of the 1970s (Kettle et al. 2011), and the species has recently been included in the IUCN Red List as critically endangered. In 2007, the European Council issued the European Regulation EC 1100/2007, aimed to recover the stock by limiting commercial eel fisheries and restoring habitat suitability.

However, assessing the effectiveness of these measures is difficult, because the triggers of the demographic collapse are still poorly understood. A range of human pressures (e.g. overfishing, habitat loss and pollution) have affected the stock directly (Feunteun 2002; Dekker 2003; Kettle et al. 2011), but there are other indirect factors that have likely played a significant role, such as the disease anguillicolosis caused by the invasive nematode worm Anguillicoloides crassus (Lefebvre et al 2005, 2013), and climate change (Knights 2003). Climate change might have affected the probability to successfully complete the journey of European larvae towards the European continent: changes in oceanic circulation might have prolonged migration routes and increased exposure to predation, while temperature changes might have changed the structure of the plankton community and decreased food availability.

In this work we use a coupled physical-biological model of the migration of European eel larvae (Melià et al. 2013) to study the impact of climate change on the geographical distribution of eel larvae and their recruitment success. The physical model is based on the Modular Ocean Model (Masina et al. 2004), which covers the period 1958-2000. The biological model takes into account the major biological processes and was tuned on the basis of the available knowledge on the vital traits of the species and of field data gathered during oceanic surveys. In particular, we investigate, through Lagrangian simulations, how migration duration, migration success, and latitudinal distribution of arrivals have changed during the second half of the last century.

Materials & Methods

A global ocean re-analysis of the period 1958-2000 (Masina et al. 2004) was used to simulate the thermohaline circulation of the Atlantic Ocean. Current velocity, temperature and salinity fields were obtained from an eddy-permitting version of the Modular Ocean Model covering a near-global domain (78°S-78°N) forced with an atmospheric re-analysis and constrained through data assimilation. The resolution of the model is constant (1/2°) in longitude, while it varies in latitude from 1/3° between 10°S and 10°N to 1/2° at the northern boundary of the domain.

Lagrangian simulations were performed by releasing a cohort of 5×106 particles, each one representing a single eel larva, every year from 1961 to 1997. Years from 1958 to 1960 were discarded because they are affected by the initial conditions of the ocean circulation model, which is set at rest at the beginning of the experiment. Particles were released daily within a time window encompassing the spawning season of the species (March to May) and distributed over time according to a Gaussian distribution with mean set to the 1st of April and SD = 20 days. The initial position of larvae was randomly drawn from a trivariate Gaussian distribution centred within the Sargasso Sea to match the available knowledge about the spawning region of the European eel (see chapter 3 for further details). Trajectories were stepped forward via an explicit Euler method with a 3-hour-step and tracked for 4 years.

The physical model describing the transport of eel larvae is coupled with a biological model describing the main biological features that characterize the larval stage of this species: body growth, natural mortality and movement. Vital rates are linked to body size, which, along with temperature, is a primary determinant of all biological processes of the European eel (Melià et al 2006b, Bevacqua et al 2006, Bevacqua et al. 2011). Parameter settings for each sub-model are defined according to the scenario that best reproduces observed field data (see chapter 3 for a full description of each biological component and of the model selection procedure).

Body growth is described by a power function linking body length L to age x ($L(x) = 77 - 73.05 \exp(-0.09x)$, with x in months and L in mm) that was fit to body length data collected at the beginning of the 20th century (Schmidt 1923). The model accounts for plasticity in body growth (De Leo & Gatto 1995) by describing inter-individual variability through an assignment-at-birth approach (Kirkpatrick 1984, see chapter 3 for details].

The mortality sub-model relies upon the metabolic theory of ecology (Brown et al. 2004) and is based on a model originally developed for the continental phase of European eel life cycle (Bevacqua et al. 2011) and adapted to the larval stage. Mortality rate μ is described as a function of body mass M (through an allometric term) and water temperature T (through a Boltzmann-Arrhenius factor), namely $\mu = a \exp(-E/kT) M^b$, where M is expressed in grams and T in Kelvin, E is the activation energy (= 1.23 eV, Bevacqua et al., 2011) and k the Boltzmann coefficient (= 8.62×10^{-5} eV K^{-1}), a is a proportionality coefficient (= 4.26×10^{20}, see chapter 3) and b is the allometric exponent (= -0.46 Bevacqua et al. 2011). Body mass M is calculated from body length L using the morphometric relationship $M = 2.24\times10^{-7} L^{3.37}$ (Melià et al. 2006a).

The movement sub-model describes the locomotion and navigation ability of eel larvae. Larval locomotion takes place along both the horizontal and vertical direction. Horizontal locomotion (propulsion) has a crucial role in determining the migration schedule and the migration success (see chapter 3). Eel larvae are supposed to swim with a speed proportional to their body length (one body length per second) and to orient their swimming along the direction of the current (see chapter 3). Besides their movement on the horizontal plane, eels larvae undergo a diel vertical migration (Castonguay & McCleave 1987) driven by a negative phototaxis, i.e. at daytime they swim at deeper depths than at night-time. Uncertainty associated to the vertical distribution of eel larvae is mimicked by randomly drawing the position of each larva from Gaussian distributions with different means at daytime and night-time. The parameters of the night-time distribution are kept constant (mean ± SD = 60 ± 25 m) along the whole journey, while the mean of the daytime distribution increases linearly with body length from 73.5 m at L = 5 mm to 470 m at L = 80 mm, with a constant SD of 25 m (see chapter 3).

The arrival of eel larvae to continental waters was monitored along the 15°W meridian. For each cohort, we recorded the number of successful arrivals, the median duration of the migration and the latitudinal distribution of arrivals. Then, we tested for possible changes in these metrics over the study period through a modified Mann-Kendall trend test (MKT) (Hamed & Rao 1998), which explicitly accounts for the effect of possible autocorrelation in time series.

Results

The results of the Lagrangian simulations show a high inter-annual variability of the metrics monitored along the 15°W meridian. The probability of success (Figure 4.1) is, in particular, subject to very wide fluctuations (spanning 3 orders of magnitude) and ranges between a minimum of 0.002% for the 1997 cohort and a maximum of 0.973% for the cohort released in 1982. The average (± SD) success rate over the whole study period was 0.132% ± 0.200%. The MKT test did not detect any significant trend in the series ($P > 0.05$). Therefore, we run a test for the presence of possible discontinuities in the series following the algorithm proposed by Zeileis et al. (2003) and found a discontinuity in the time series in 1972. Table 4.1 reports the basic statistics of migration success for the periods 1961-1972 and 1973-1997, showing a remarkable difference in the mean value and an increase in the standard deviation of migration success. A MKT performed separately on the two time series revealed significant trends in both periods ($P < 0.05$ for 1961-1972 and $P << 0.001$ for 1973-1997). Linear regression lines fitting the two sub-samples show a positive trend before 1972 and a negative trend in the second period.

Period	Mean ± S.D.	Median	I – III quartiles
1961-1972	0.043% ± 0.052%	0.022%	[0.014% - 0.038%]
1973-1997	0.175% ± 0.224%	0.089%	[0.026% - 0.226%]

Table 4.1 – Basic statistic of migration success for 1961-1972 and 1973-1997

Median migration duration (Figure 4.2) ranged between a minimum of 25.0 months for the 1987 cohort and a maximum of 45.3 months for the 1961 cohort, with an average (± SD) of 33.5 ± 5.6 months. The MKT test indicated a weakly significant trend in the series ($P < 0.05$). The regression of migration duration on time has a negative coefficient, indicating that the duration of the larval migration is decreasing, on

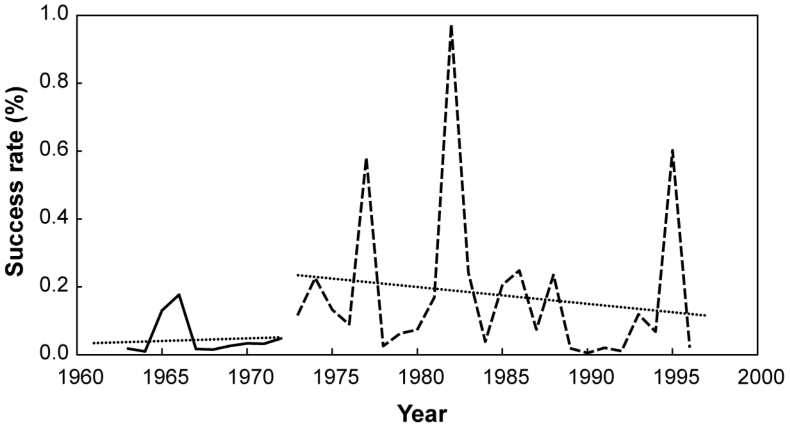

Figure 4.1 - Migration success recorded along the 15°W meridian between 1961-1972 (solid line) and 1973-1997 (dashed line). The year refers to the date in which the corresponding cohort was released from the Sargasso Sea. The dotted lines indicate the relevant regression lines (1961-1972: $y = 0.00002x + 0.0305$; 1973-1997: $y = -0.00005 + 0.1003$)

average, by about 6 days per year.

The average latitude of arrivals (Figure 4.3) ranged between 48.97°N in 1961 and 34.16°N in 1989, with a mean (± SD) of 42.06 ± 4.20°N. The MKT test revealed a strongly significant ($P << 0.001$) trend in this series, with the mean latitude of arrival that is moving southwards by ca. 1/4° per year.

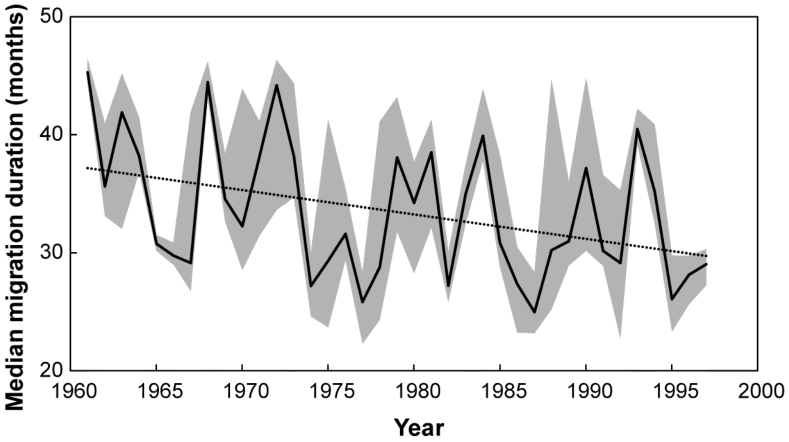

Figure 4.2 – Median (solid line) and interquartile range (gray area) of migration duration (from the Sargasso Sea to the 15°W meridian) for each cohort released between 1961-1997. The dotted line indicates the regression line (y = -0.2073x + 443.71)

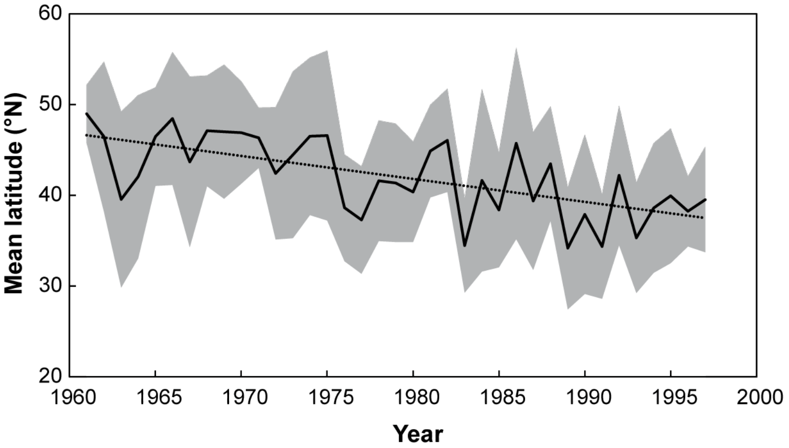

Figure 4.3 - Mean (solid line) ± standard deviation (gray area) of the latitude of arrival measured along the 15°W meridian for each cohort released between 1961-1997. The dotted line indicates the regression line (y = -0.2538x + 544.42)

Discussion

Our Lagrangian simulations have been performed on the basis of a number of hypotheses, some of which may not hold in the real world. For instance, Lagrangian particles have been released from a spatio-temporal distribution whose moments are kept constant year after year. Although little is known about the environmental cues followed by European eel spawners to reach their mating grounds, the most recent studies on the oceanic hydrography of the Sargasso Sea region and on the spatial distribution of European eel larvae suggest that the spawning area is delimited by two sharp fronts in the thermocline with a mixing zone in between, where the youngest larvae have been found (Munk et al. 2010). Such a structure could be the target of spawner migration and could enhance recruitment success acting as a nursery for eel larvae, offering a suitable habitat and superior feeding conditions (Munk et al. 2010). As inter-annual fluctuations in hydrodynamic features may slightly displace the actual spawning location from year to year, releasing larvae from the same location may have biased our results. A correct identification of this structure is crucial to generate realistic simulations and deserves additional investigation.

The results of analysing the time series of migration success suggests that a regime shift has occurred during the 1970s, causing a switch from a positive trend to a negative one. Detecting regime changes in time series is a challenging task, and our analysis provides only preliminary insights about the possible evolution of this metric over the study period. However, it is worth noting that previous work has already put forward the hypothesis that a regime shift (detected from the analysis of time series of glass eel recruitment) has occurred during the 1970s (Bonhommeau et al. 2008). Understanding the hydrodynamic mechanisms that might have caused this change undoubtedly requires further research effort, but if more comprehensive statistical analyses confirmed the existence of some form of discontinuity in oceanic features affecting the migration success of European eels this would provide an important contribution to the discussion about the causes of the collapse of the species.

Our results indicate also a decreasing, although weakly significant, trend of the migration duration, with a reduction of the median value of this metric of about 6 months in 40 years. If this trend were confirmed by evidence from the field, it might have severe implications for the recruitment schedule of eel leptocephali. Although the actual triggers for metamorphosis from the leptocephalus to the glass eel stage are poorly understood, physical signals such as temperature gradients are likely to have an important regulatory effect on this process (Kuroki et al. 2010), and a desynchronization between the periodic temperature fluctuations of the oceanic system and the schedule of the eel journey might have a dramatic impact of the viability of this endangered species. Also, a change of the season in which leptocephali reach European shelves might change the environmental conditions they encounter at their arrival. The high plasticity in vital traits of catadromous eels makes them likely able to buffer, at least to some degree, the intrinsic inter-annual variability of the oceanic circulation. However, a systematic shift in circulation features affecting their journey may be difficult to face even for a tolerant species such as the European eel. For instance, losing the synchronization between the arrival of leptocephali and the rainy season, when the freshwater lure calls eel larvae into the continental water system, might increase the time they have to wait in the open sea, exposing them to increased risk of predation and reducing their probability to successfully settle into inland waters.

We also identified a significant trend in the average latitude of arrivals. Arrivals of European eel larvae usually have a bimodal distribution, with a major peak in the Biscay bay (historically the region with the highest recruitment) and a minor peak close to the Strait of Gibraltar (Bonhommeau et al. 2009; see chapter 3). The observed change in mean (a shift of almost 10 latitude degrees southwards over four decades) suggests that the northernmost peak has reduced its weight while the southernmost one has increased its. Although this has no direct consequences on migration success, it could explain why recruitment time series from the Atlantic coasts (where the glass eel fishery was historically most important) are consistently declining, while the decline is less evident from the few time series available for the Mediterranean Sea (Alain Crivelli, pers. comm., Fabrizio Capoccioni, pers. comm.). A southward shift in the average latitude would displace a larger proportion of the stock towards a region characterized by highly productive coastal waters and higher temperatures, with the probable effect of shortening the duration of the continental phase of the eel's life cycle, but with final consequences on the viability of the species that are difficult to predict.

Our simulation exercise suggests that the ocean has an active role in determining the variability of eel recruitment to continental waters, but it is difficult to definitely confirm whether long-term changes in oceanic circulation have significantly contributed to the collapse of the stock. Further simulation effort and fieldwork are needed to improve our comprehension of the larval migration of the European eel. Although our work is not exempt from limitations, we believe that it provides interesting preliminary insights on how the ocean might have contributed to the observed decline of the recruitment of this mysterious fish.

References

Bevacqua D, Melià P, Crivelli AJ, De Leo GA & Gatto M (2006). Timing and rate of sexual maturation of European eel in brackish and freshwater environments, *J. Fish. Biol.* **69** (Suppl. C):200-208.

Bevacqua D, Melià P, De Leo GA & Gatto M (2011). Intra-specific scaling of natural mortality in fish: the paradigmatic case of the European eel, *Oecologia* **165:**333-339.

Bonhommeau S, Chassot E & Rivot E (2008). Fluctuations in European eel (*Anguilla anguilla*) recruitment resulting from environmental changes in the Sargasso Sea, *Fish. Oceanog.* **17**:32-44.

Bonhommeau S, Le Pape O, Gascuel D, Blanke B, Tréguier A-M, Grima N, Vermard Y, Castonguay M & Rivot E (2009). Estimates of the mortality and the duration of the trans-Atlantic migration of European eel *Anguilla anguilla* leptocephali using a particle tracking model, *J. Fish Biol.* **74**:1891–1914.

Brown JH, Gillooly JF, Allen AP, Savage VM & West GB (2004). Toward a metabolic theory of ecology, *Ecology* **85**:1771-1789.

Castonguay M & McCleave JD (1987). Vertical distributions, diel and ontogenetic vertical migrations and net avoidance of leptocephali of Anguilla and other common species in the Sargasso Sea, *J. Plankton Res.* **9**:195-214.

De Leo GA & Gatto M (1995). A size and age-structured model of the European eel (*Anguilla anguilla* L.), *Can. J. Fish. Aquat. Sci.* **52**:1351-1367.

Dekker W (2003). Did lack of spawners cause the collapse of the European eel, *Anguilla anguilla*?, *Fish. Manag. Ecol.* **10**:365-376.

Feunteun E (2002). Management and restoration of European eel population (*Anguilla anguilla*): an impossible bargain, *Ecol. Eng.* **18**:575-591.

Hamed KH, Rao AR (1998). A modified Mann-Kendall trend test for autocorrelated data, *J. Hydrol.* **204**:182-196.

Kettle AJ, Vøllestad LA & Wibig J (2011). Where once the eel and the elephant were together: decline of the European eel because of changing hydrology in southwest Europe and northwest Africa?, *Fish Fish.*, **12**:380-411.

Kirkpatrick M (1984). Demographic models based on size, not age, for organisms with indeterminate growth, *Ecology* **65**:1874-1884.

Knights B (2003). A review of the possible impacts of long-term oceanic and climate changes and fishing mortality on recruitment of anguillid eels of the Northern Hemisphere, *Sci. Total Environ.* **310**:237–244.

Kuroki M, Fukuda N, Yamada Y, Okamura A & Tsukamoto K (2010). Morphological changes and otolith growth during metamorphosis of Japanese eel leptocephali in captivity, *Coast. Mar. Sci.* **34**:31-38.

Lefebvre F & Crivelli A. (2005). Anguillicolosis: dynamics of the infection over two decades, Dis. Aquat Organ **62**(3):227-232.

Lefebvre F, Fazio G, Mounaix B & Crivelli AJ (2013). Is the continental life of the European eel *Anguilla anguilla* affected by the parasitic invader *Anguillicoloides crassus*?, *Proc. R. Soc. B* **280**

Masina S, Di Pietro P, Navarra A (2004). Interannual-to-decadal variability of the North Atlantic from an ocean data assimilation system, *Clim. Dynam.* **23**:531-546.

Melià P, Bevacqua D, Crivelli AJ, De Leo GA, Panfili J & Gatto M (2006a). Age and growth of Anguilla anguilla in the Camargue lagoons, *J. Fish Biol.* **68**:876-890.

Melià P, Bevacqua D, Crivelli AJ, Panfili J, De Leo GA & Gatto M (2006b). Sex differentiation of the European eel in brackish and freshwater environments: a comparative analysis, *J. Fish Biol.* **69**:1228-1235.

Melià P, Schiavina M, Gatto M, Bonaventura L, Masina S & Casagrandi R (2013). Integrating field data into individual-based models for the migration of European eel larvae, *Mar. Ecol. Progr. Ser.* in press.

Munk P, Hansen MM, Maes GE, Nielsen TG, Castonguay M, Riemann L, Sparholt H, Als TD, Aarestrup K, Andersen NG & Bachler M (2010). Oceanic fronts in the Sargasso Sea control the early life and drift of Atlantic eels, *Proc. R. Soc. B* **277**:3593–3599.

Schmidt J (1923). The breeding places of the eels, *Phil. Trans. R. Soc. B* **211**:179-208.

Zeileis A, Kleber C, Krämer W & Hornik K (2003). Testing and dating of structural changes in practice, *Comput. Stat. Data Anal.* **44**:109-123.

PART IV

CONCLUSIONS

Main results

In this thesis I have presented the study of larval dispersal processes in three case studies, namely the pelagic larval transport of two species in the Adriatic Sea and the European eel larval migration in the Atlantic Ocean. These processes obviously involve movement and, therefore, they were analysed following the Movement Ecology paradigm discussed in the introductory chapter. The movement process has been modelled, though, considering not just the physical transport generated by ocean currents, but integrating all available biological processes to represent motion and navigation capacities, and the possible interactions between individuals and the environment.

I began with two case studies in the Adriatic Sea selecting two ecologically important species as the European green crab and the white sea bream. The idea was to study the role of the ocean currents in determining, or not, a structure of the populations studying the level of connectivity among different sites. To determine the presence of such a structure, genetic marker analyses has been conducted on the two species, assessing the genetic divergence among samples of each location. I developed two species-specific individual-based models analysing the trajectories of dispersal in the Adriatic Sea and generating connectivity matrices among locations. The few biological information and field data of the species, limited the models to an explanatory approach (see introductory chapter), trying to explain the observed patterns with the mechanisms represented by the models. The objective was, in fact, to evaluate the consistency between the connectivity matrices generated by the modelling tools and the results of the genetic analyses. The consistency between the results could be an indication that the pelagic processes are driven by the ocean currents and determine the genetic structure of population.

The European green crab has been sampled and analysed in several sites all along the Italian Adriatic coast, revealing a genetic sub-division in three, weakly differentiated, groups: the north, the centre and the south Adriatic. The white sea bream has been sampled and analysed in a smaller area encompassing the Torre Guaceto Marine Protected Area and the surroundings. The results showed a very high connectivity of the TGMPA with all neighbouring areas indicating a continuous and stable gene flow among the sites. In both cases these results were corroborated by the Lagrangian simulations reflecting the three Adriatic sub-basins for the pelagic larval dispersal of the European green crab and the stable larval flow from north to south in the TGMPA region, connecting all sites in the analysis. The two results point out the active role of the ocean currents in clustering the populations in the Adriatic Sea (i.e. restraining larval dispersal in specific areas and generating a genetic divergence among them), and guaranteeing a stable flux of gene within sub-populations in the same area, even when high distances (>100 km) separate two locations. These two studies underlined the importance of a multidisciplinary approach, coupling the oceanography with genetics. The oceanographic and genetic results alone would have been not sufficient: dealing with such weak or none genetic differentiations could lead to misinterpretation of population structures due to the noise of sampling errors; on the other hand, the hydrodynamic used in the ICPBMs, even if it has a very high resolution, is not fully reliable on its boundary, not capturing the complex dynamics of coastal shallow waters, highly influenced by shoreline and bottom shapes and driven by tidal processes. However, as the two results are consistent with each other, this coupled approach strengthens the conclusions of the single approaches.

The modelling approach used to simulate the larval migration of the European eel is based on the many, but not exhaustive, information about this long-migrating phase of the species. It has been possible to calibrate four different body growth curves, on which all other biological processes depend, and develop an accurate ICPBM. This model, including the main biological features of the European eel larval phase, was used with an inferential approach (see introductory chapter) comparing alternative scenarios and parameters sets to determine which is more likely to occur. Field data gathered in literature allowed to discriminate among the body growth curves and to find the most reliable scenario (parameters set) of migration. On the basis of this scenario it was possible to characterize the migration analysing the duration, the routes and the arrival distribution on the European shelves. This model is finally used with an extended hydrodynamic dataset to investigate the role of the ocean changes in the recruitment drop experienced by the species after the 1980s.

The first numerical exercise found the "best" scenario able to assimilate the experimental data, selecting a body growth curve that is in good accordance with early-life-history of other eel species and pointing out the role and the importance of the active locomotion in speeding and boosting the migration success. Migration duration, which was one of the most discussed aspects in literature, fitted quite well with lot of previous studies as for the latitude of arrivals, coherent with data of recruitment distribution. The simulation result allows also a rough estimate of the spawning stock, that is one of the lacking information to model and understand the complete lifecycle of this species. Running the model, set as the "best" scenario, with the ocean hydrodynamic of the second half of last century it has been possible to produce and analyse the time series of migration success, duration and mean arrival latitude. The analyses pointed out a regime shift in the probability of migration success, from a positive to a negative trend, a significant reduction of migration duration, with a likely desynchronization effect on recruitment, and a southward movement of the mean arrival latitude, that could partially reflect the stronger recruitment drop recorded by northern countries. The statistical analyses conducted on these results allow to conclude that the ocean is responsible of the high variability of recruitment, but not to definitely confirm that it has directly contributed to the stock collapse without any further investigation. This exercise has generated some hypotheses about the long-term effect of the Gulf Stream changes on this species recruitment that could direct future research efforts for the understanding of the causes of the decline of European eel stock

With this thesis I pointed out the usefulness of ICPBMs approaches in explaining observed patterns, calibrating models parameters and generating hypotheses relative to a species life history. I underlined how this approach should, anyway, be conducted along with other disciplines to compare and corroborate results or to assimilate data in order to make a reliable representation of the movement process in the spatio-temporal scale.

Future improvements and directions

The works presented in chapters 1 and 2 are viable of lot of improvements on the biological side. As long as the research discovers more information about these two species they should be incorporated in these models to improve their ability to replicate the linkages between sites and, thus, their reliability. Moreover, the European green crab model should be integrated with more sites, mainly on the Dalmatian coast to effectively analyse the connectivity in the whole Adriatic basin.

A possible direction of the two works could be the inclusion of the population dynamics of the species, considering the settlement process and the habitat suitability in the post-larval survival, trying to study the evolution of dispersal in the Adriatic Sea. This study will be useful to detect those places capable of high retention and/or spill-over in order to help the selection of sites for new marine reserves and a better management of species fisheries.

Further developments of the European eel larval migration model regard the inclusion of an adaptive spawning area, modelling the environmental triggers of spawning, such as the thermocline front (as discussed in chapter 4) and the feeding process, affecting both the growth and mortality as the results of energy surplus or defect. Both features required high levels of details to be implemented and are not easy tasks to be reliable, requiring collaborations with oceanographer and biologists to identify the thermocline structure and the energetic mechanisms of growth and starvation. Moreover, in the next future, higher resolution data-assimilated oceanographic models will be available, allowing a more precise simulation of this larval migration by taking into account the small-scale eddies of the ocean currents.